UNIVERSIDADE ESTADUAL DE CAMPINAS
FACULDADE DE ENGENHARIA QUÍMICA

EMERSON PARAZZI LYRA

STRATEGIES FOR REDUCING CATALYST CONCENTRATION IN ATOM TRANSFER RADICAL POLYMERIZATION: A KINETIC STUDY APPROACH BY MATHEMATICAL MODELING AND SIMULATION

ESTRATÉGIAS PARA A REDUÇÃO DA CONCENTRAÇÃO DE CATALISADORES NA POLIMERIZAÇÃO RADICALAR POR TRANSFERÊNCIA DE ÁTOMO: UMA ABORDAGEM DE ESTUDO CINÉTICO POR MODELAGEM MATEMÁTICA E SIMULAÇÃO

CAMPINAS
2019

EMERSON PARAZZI LYRA

STRATEGIES FOR REDUCING CATALYST CONCENTRATION IN ATOM TRANSFER RADICAL POLYMERIZATION: A KINETIC STUDY APPROACH BY MATHEMATICAL MODELING AND SIMULATION

ESTRATÉGIAS PARA A REDUÇÃO DA CONCENTRAÇÃO DE CATALISADORES NA POLIMERIZAÇÃO RADICALAR POR TRANSFERÊNCIA DE ÁTOMO: UMA ABORDAGEM DE ESTUDO CINÉTICO POR MODELAGEM MATEMÁTICA E SIMULAÇÃO

DISSERTATION PRESENTED TO THE SCHOOL OF CHEMICAL ENGINEERING OF THE UNIVERSITY OF CAMPINAS IN PARTIAL FULFILLMENT OF THE REQUIREMENTS FOR DEGREE OF MASTER IN CHEMICAL ENGINEERING.

DISSERTAÇÃO APRESENTADA À FACULDADE DE ENGENHARIA QUÍMICA DA UNIVERSIDADE ESTADUAL DE CAMPINAS COMO PARTE DOS REQUISITOS EXIGIDOS PARA A OBTENÇÃO DO TÍTULO DE MESTRE EM ENGENHARIA QUÍMICA.

SUPERVISOR / ORIENTADOR: LILIANE MARIA FERRARESO LONA

ESTE EXEMPLAR CORRESPONDE À VERSÃO FINAL DA DISSERTAÇÃO DEFENDIDA PELO ALUNO EMERSON PARAZZI LYRA E ORIENTADA PELO PROFA. DRA. LILIANE MARIA FERRARESO LONA.

CAMPINAS
2019

Agência(s) de fomento e nº(s) de processo(s): CAPES, 1725186
ORCID: https://orcid.org/0000-0002-7969-3764

Ficha catalográfica
Universidade Estadual de Campinas
Biblioteca da Área de Engenharia e Arquitetura
Rose Meire da Silva - CRB 8/5974

L995s

Lyra, Emerson Parazzi, 1990-
Strategies for reducing catalyst concentration in atom transfer radical polymerization : a kinetic study approach by mathematical modeling and simulation / Emerson Parazzi Lyra. – Campinas, SP : [s.n.], 2019.

Orientador: Liliane Maria Ferrareso Lona.
Dissertação (mestrado) – Universidade Estadual de Campinas, Faculdade de Engenharia Química.

1. Polimerização radicalar. 2. Agentes redutores. 3. Cinética química. 4. Modelos matemáticos. 5. Simulação computacional. 6. Estudos de validação. I. Lona, Liliane Maria Ferrareso, 1966-. II. Universidade Estadual de Campinas. Faculdade de Engenharia Química. III. Título.

Informações para Biblioteca Digital

Título em outro idioma: Estratégias para a redução da concentração de catalisadores na polimerização radicalar por transferência de átomo : uma abordagem de estudo cinético por modelagem matemática e simulação
Palavras-chave em inglês:
Free-radical polymerization
Reducing agents
Chemical kinetics
Mathematical models
Computational simulation
Validation studies
Área de concentração: Engenharia Química
Titulação: Mestre em Engenharia Química
Banca examinadora:
Liliane Maria Ferrareso Lona [Orientador]
Luís Fernando Mercier Franco
Marcelo Alexandre de Farias
Data de defesa: 06-02-2019
Programa de Pós-Graduação: Engenharia Química

Folha de Aprovação da Dissertação de Mestrado defendida por Emerson Parazzi Lyra e aprovada em 06 de fevereiro de 2019 pela banca examinadora constituída pelos seguintes doutores:

Profa. Dra. Liliane Maria Ferrareso Lona

FEQ / UNICAMP

Prof. Dr. Luís Fernando Mercier Franco

FEQ / UNICAMP

Dr. Marcelo Alexandre de Farias

Laboratório Nacional de Nanotecnologia

LNNano

*A ATA da Defesa com as respectivas assinaturas dos membros encontra-se no SIGA/Sistema de Fluxo de Dissertação/Tese e na Secretaria do Programa da Unidade.

AGRADECIMENTOS

Quando o mundo diz "desista", Deus sussurra "tente mais uma vez". Primeiramente, agradeço a Deus por ter me mostrado ainda mais ao longo desses anos aquilo que realmente importa na vida de cada um de nós: a construção de um legado (isto é, sermos bons exemplos). A vida que temos não se resume meramente a conquistar e usufruirmos aquilo que obtivermos em benefício próprio, mas sim deixarmos ao próximo a experiência que construímos ao longo do tempo, para que as futuras gerações estejam sempre em constante evolução.

Agradeço aos meus pais por fazerem do meu sonho o deles também, pelo amor incondicional e também por terem me dado toda a educação para que eu tornasse um homem de valores nobres.

Agradeço aos meus familiares mais próximos que tenho contato pelo apoio e peço desculpas pela ausência ao longo desse tempo dedicado a pesquisa.

Tenho uma quantidade irrisória de amigos, mas estes poucos me fazem muito feliz. Agradeço aos irmãos que a vida me deu: Ícaro e Danilo. Vocês não sabem o quanto fizeram o caminho até aqui ser menos difícil (nunca diria mais fácil).

Esse trabalho tem um pouquinho do conhecimento de todos os professores da FEQ/UNICAMP que tive oportunidade de ser aluno e de alguns professores do IQ/UNICAMP que conheci ao longo dessa trajetória acadêmica, seria indelicadeza da minha parte e falta de consideração não lembrar dos mesmos e agradecê-los.

Agradeço aos funcionários da FEQ/UNICAMP, principalmente os da secretaria de Pós-Graduação pela paciência que tiveram em me ajudar (das incontáveis vezes que lhes fui "encher o saco" com dúvidas burocráticas).

Agradeço a professora Melissa Gurgel Adeodato Vieira da FEQ/UNICAMP, pela oportunidade de ter compartilhado um pouquinho de seu conhecimento comigo no Programa de Estágio Docente (PED). Foi uma experiência construtiva e desafiadora.

Agradeço ao professor Cesar Liberato Petzhold do IQ/UFRGS pelo conhecimento compartilhado na elaboração do meu primeiro artigo científico.

Por fim, mas não menos importante, agradeço a professora Liliane Maria Ferrareso Lona da FEQ/UNICAMP, orientadora deste trabalho. Tu certamente és a responsável pelo meu crescimento profissional ao longo desses anos (embora muito dos resultados ainda estejam por vir). Agradeço-a imensamente também pelos seus conselhos para me tornar alguém melhor pessoalmente (embora muito deles ainda não tenha conseguido colocar em prática), certamente

foi muito mais do que uma orientadora. A senhora me ensinou o significado literal da palavra paciência, algo muito importante não só na ciência, mas também na vida. Sou grato também pela confiança que me deu no Programa de Estágio Docente (PED), a experiência que tive ministrando algumas aulas para a graduação foi extremamente marcante para mim, tenho certeza que ao menos tentarei ser professor, pois foi algo gratificante e que me realizou profissionalmente.

Esse trabalho certamente não é o ponto final. Posso ainda não ter chegado aonde eu gostaria, mas estou mais perto do que ontem. Sei que poderia ter feito muito mais, mas viveria muito menos. O segredo é "ponderar" a vida.

Mesmo assim, dedico meu esforço e empenho para chegar até aqui e concluir esse trabalho simples e humilde a todos vocês que anteriormente mencionei. Meus sinceros agradecimentos.

O presente trabalho foi realizado com apoio da Coordenação de Aperfeiçoamento de Nível Superior – Brasil (CAPES) – Código de Financeamento 001.

"*Brothers, what we do in life... echoes in eternity*"
(General Máximus Décimus Meridius, *Gladiator*)

ABSTRACT

In the context of Reversible Deactivation Radical Polymerization (RDRP), the association of Activators Regenerated by Electron Transfer (ARGET) mechanism with the Atom Transfer Radical Polymerization (ATRP) has attracted attention in terms of research, mainly because it is an environmentally and economically more favorable polymerization method if compared to conventional ATRP, due to the catalyst concentration reduction verified in the process. By the scarcity of records in literature, this work has as main objective to provide mathematical tools to simulate the synthesis of polymers obtained by ARGET ATRP, with the originality of contribution focused on the comprehension of the reaction kinetics for the reducing agents. Through the experimental data found in the literature, two proposed mathematical models applied to the homopolymerization and random copolymerization processes via ARGET ATRP were validated. The mathematical modeling developed is based on the method of moments, being applied the method of pseudo-kinetic constants for the case equivalent to the random copolymerization process. In the model validation, kinetic constants, among those that have no records in the literature, were obtained by optimization algorithm. Results provided by the modeling indicate that the higher the initial concentrations of both deactivator and reducing agent, the monomer conversion, the higher the number-average molecular weight and the lower the dispersity. Simulations done also confirm that the initial concentration of deactivator is a critical parameter with higher sensitivity than the reducing agent in solution ARGET ATRP process.

Keywords: activators regenerated by electron transfer, reducing agent kinetics, model development.

RESUMO

No contexto da Polimerização Radicalar por Desativação Reversível (RDRP), a associação do mecanismo de Regeneração de Ativador por Transferência de Elétrons (ARGET) à Polimerização Radicalar por Transferência de Átomos (ATRP) tem atraído atenção em termos de pesquisa, principalmente por ser um método de polimerização ambientalmente e economicamente mais favorável se comparada a ATRP convencional, devido à redução da concentração de catalisador verificada no processo. Pela escassez de registros em literatura, este trabalho tem como objetivo principal prover ferramentas matemáticas para simular a síntese de polímeros obtidos via ARGET ATRP, com a originalidade de contribuição voltada para a compreensão da cinética de reação de agentes redutores. Através de dados experimentais encontrados na literatura, dois modelos matemáticos propostos aplicados aos processos de homopolimerização e copolimerização aleatória via ARGET ATRP foram validados. A modelagem matemática desenvolvida é baseada no Método dos Momentos, sendo aplicado o Método Pseudocinético para o caso equivalente a copolimerização aleatória. No processo de validação realizado, constantes cinéticas, dentre aquelas que não se tem registros na literatura, foram ajustadas aos modelos através de algoritmo de otimização. Resultados fornecidos pela modelagem indicam que quanto maiores as concentrações iniciais de tanto do desativador quanto do agente redutor, maior a conversão de monômero, maior o peso molecular médio e menor a dispersividade. Simulações feitas também confirmam que a concentração inicial de desativador é um parâmetro crítico com maior sensibilidade do que a de agente redutor no processo ARGET ATRP em solução.

Palavras-chave: regeneração de ativador por transferência de elétrons, cinética de agente redutor, desenvolvimento de modelo.

LIST OF FIGURES (i)

LIST OF FIGURES (ii)

LIST OF FIGURES (iii)

LIST OF FIGURES (iv)

LIST OF FIGURES (v)

LIST OF FIGURES (part vi)

LIST OF FIGURES (part vii)

LIST OF TABLES (i)

LIST OF TABLES (ii)

NOMENCLATURE (i)

Nomenclature	Description
A	Reducing agent
AN	Acrylonitrile
A_{oxi}	Oxidized reducing agent
ARGET	Activators Regenerated by Electron Transfer
asc^{*-}	Ascorbyl radical (unstable state of the H_2asc oxidized)
ATRP	Atom Transfer Radical Polymerization
BA	Butyl acrylate
BMA	Butyl methacrylate
$CuBr_2$	Copper(II) bromide
$CuCl_2$	Copper(II) chloride
$(Cu^{I}L)X$	Copper(I) catalyst or activator
$(Cu^{II}XL)X$	Copper(II) halide complex or deactivator
dha	Dehydroascorbic acid (stable state of the H_2asc oxidized)
eATRP	Electrochemically mediated Atom Transfer Radical Polymerization
EBiB	Ethyl 2-bromoisobutyrate
FRP	Free Radical Polymerization
GPC	Gel Permeation Chromatography
H^+	Proton dissociated of H_2asc or N_2H_4
H_2asc	Ascorbic acid

NOMENCLATURE (ii)

Nomenclature	Description
ICAR	Initiators for Continuous Activator Regeneration
M	Monomer
MA	Methyl acrylate
Me_6TREN	Tris[2-(dimethylamino)ethyl]amine
mechanoATRP	Mechanically mediated Atom Transfer Radical Polymerization
NMP	Nitroxide Mediated Polymerization
N_2H_2	Diimide or diazene
N_2H_3*	Hydrazil radical
N_2H_4	Hydrazine
PBA	Poly(butyl acrylate)
photoATRP	Photochemically mediated Atom Transfer Radical Polymerization
PMA	Poly(methyl acrylate)
P_i	Dead polymer chain with i (≥ 1) monomeric units long
PSt	Poly(styrene)
RAFT	Reversible Addition-Fragmentation chain Transfer
RDRP	Reversible-Deactivation Radical Polymerization
R_i	Living polymer chain with i (≥ 1) monomeric units long
R_iX	Dormant polymer chain with i (≥ 1) monomeric units long
R_0	Primary free radical

NOMENCLATURE (iii)

Nomenclature	Description
R_0X	Alkyl halide initiator
SARA	Supplemental Activator and Reducing Agent
$Sn^{II}(eh)_2$	Tin(II) 2-ethylhexanoate
$Sn^{III}(eh)_2X$	Tin(III)-based compound (unstable state of the $Sn^{II}(eh)_2$ oxidized)
$Sn^{IV}(eh)_2X_2$	Tin(IV)-based compound (stable state of the $Sn^{II}(eh)_2$ oxidized)
St	Styrene
TPMA	Tris[(2-pyridyl)methyl]amine
X^-	Halide anion
$\mu_{m,RX}$	m^{th} order moment for dormant chains
$\mu_{m,RX,i}$	m^{th} order moment for dormant chains ended by monomer i
$\mu_{m,R}$	m^{th} order moment for living chains
$\mu_{m,R,i}$	m^{th} order moment for living chains ended by monomer i
$\mu_{m,P}$	m^{th} order moment for dead chains

SYMBOLOGY (i)

Symbol	Description (Unit)
C_s	Solubility coefficient (-)
DP_n	Number-average chain length (-)
DP_w	Weight-average chain length (-)
F_i	Molar fraction of monomer *i* that reacted (-)
f_{Mi}	Molar fraction of monomer *i* (-)
f_{Di}	Molar fraction of dormant chains ended by monomer *i* (-)
f_{Ri}	Molar fraction of living chains ended by monomer *i* (-)
K	Mark–Houwink parameter (-)
k_a	Kinetic rate constant of activation ($L \cdot mol^{-1} \cdot s^{-1}$)
K_{ATRP}	ATRP equilibrium constant (-)
k_{da}	Kinetic rate constant of deactivation ($L \cdot mol^{-1} \cdot s^{-1}$)
k_p	Kinetic rate constant of propagation ($L \cdot mol^{-1} \cdot s^{-1}$)
k_r	Kinetic rate constant of reduction ($L \cdot mol^{-1} \cdot s^{-1}$)
k_r*	Intrinsic kinetic rate constant of reduction ($L \cdot mol^{-1} \cdot s^{-1}$)
k_{tc}	Kinetic rate constant of termination by combination ($L \cdot mol^{-1} \cdot s^{-1}$)
k_{td}	Kinetic rate constant of termination by disproportionation ($L \cdot mol^{-1} \cdot s^{-1}$)
M_M	Monomer molecular weight ($g \cdot mol^{-1}$)
M_n	Number-average molecular weight ($g \cdot mol^{-1}$)
M_w	Weight -average molecular weight ($g \cdot mol^{-1}$)

SYMBOLOGY (ii)

Symbol	Description (Unit)
r	Reactivity ratio (-)
t	Time (s, min or h)
T	Temperature (K)
$var_{exp.}$	set of experimental values of variable *var* available in a determined set of time (unit of *var*)
$var_{exp.(t)}$	experimental data of the variable *var* at the time *t* (unit of *var*)
$var_{sim.}$	set of values of variable *var* simulated in the times wherein the experimental data are available (unit of *var*)
$var_{sim.(t)}$	variable *var* simulated at the time *t* (unit of *var*)
α	Mark–Houwink parameter (-)
Đ	Dispersity (-)
$\delta_{var(t)}$	Normalized deviation between simulated and experimental data of the variable *var* at the time *t* (-)

CONTENTS

1. INTRODUCTION

1.1. Dissertation overview

This work presents a detailed mechanistic investigation of the use of some reducing agents to diminish the concentration of catalysts in Atom Transfer Radical Polymerization (ATRP) processes. The focus of the research extends to the study of the Activators Regenerated by Electron Transfer (ARGET) mechanism associated with the conventional ATRP, that still lacks full of understanding.

Based on the development of mathematical descriptive models and computational simulations, this research tries to elucidate how some ARGET ATRP systems work from the chemical kinetics point of view, aiming to obtain a better understanding of the experimental trends.

1.2. Dissertation outline

This dissertation follows an extended article style, where the main results and their conclusions are presented as if they were in the form of manuscripts prepared for publication.

Chapter 2 presents the research background, where aspects of scientific knowledge available in literature are discussed. The immersion into the research field of this work is given by the approach of fundamentals of the conventional ATRP. In a second moment, one of the most important limitations of this polymerization method and their implications is revealed, which is related to the high consumption of catalysts based on transition metals; and strategies reported in literature to overcome this problem are discussed. Finally, within the context previously described, the objectives of this work are highlighted, and aspects in what this research differs from existing approaches in literature are mentioned.

Chapter 3 reports the general methodology considered in this work. At this point the mathematical and computational approaches of this research are discussed. In the first moment, methods available in literature to model polymerization reactions are presented, as well as their application characteristics, being specified which will be the one considered in this work. Subsequently, information regarding the computational implementation to solve the proposed modeling is evidenced.

Chapter 4 presents in the form of an extended article some studies carried out in this work. This chapter is divided into Parts I and II, which deal with two complementary researches. Part I is a study to elucidate the kinetic mechanism of the use of some reducing agents (i.e., tin(II) 2-ethylhexanoate, ascorbic acid, and hydrazine) with copper-based catalysts as ARGET ATRP systems. Part II is a specific case study of the random copolymers synthesis via ARGET ATRP considering tin(II) 2-ethylhexanoate as a reducing agent and copper-based catalysts, being applied to the synthesis of poly[(styrene)-co-(acrylonitrile)]. The organization of this chapter comprises the following topics: (i) Abstract, which is a brief summary of the research performed; (ii) Highlights, which are short phrases that summarize the work done; (iii) Introduction, which discusses specific aspects of ARGET ATRP for the cases studied; (iv) Kinetic approach, which refers to the discussion of kinetic mechanisms; (v) Model development, where the mathematical approach and equations are provided; (vi) Kinetic modeling validation, where experiments found literature and considered in the model validation process are presented; (vii) Results and discussion, where it is discussed the representativeness of the modeling performed against experimental literature data and critical parameters of ARGET ATRP processes; and (viii) Conclusion, which summarizes the findings of the studies.

Chapter 5 highlights the contributions of this work and discuss the future perspectives of methods to reduce catalyst concentration in ATRP processes.

2. RESEARCH BACKGROUND

2.1. Contextualization of the scientific knowledge

2.1.1. Fundamentals of Atom Transfer Radical Polymerization

Concerning the production of large-scale polymeric materials, Free Radical Polymerization (FRP) deserves to be highlighted. FRP is based on the property of chemical compounds that have active unsaturations (i.e., monomers) to perform chain reactions to obtain macromolecules (i.e., polymers) [1].

Researches on FRP evolved allowing the control of molecular weight and functionality of the polymers by the generation of new techniques that increased the variety of synthesized materials [1].

In this context, in chronological order of discovery, three of them should be mentioned: Nitroxide Mediated Polymerization (NMP), Atom Transfer Radical Polymerization (ATRP), and Reversible Addition-Fragmentation Chain Transfer (RAFT) [1]. Such polymerization methods are inserted into the field of Reversible-Deactivation Radical Polymerization (RDRP) [1]. RDRP processes were earlier known as Controlled Radical Polymerization (CRP) or Living Radical Polymerization (LRP) [1].

Mechanistically, NMP, ATRP, and RAFT have in common the establishment of a dynamic equilibrium between active radicals and dormant species [1]. In order to extend the lifetime of the active radicals, the dormant species should be predominant regarding molar concentration, once they are unable to propagate or terminate; as a result of the persistent radical effect [1].

Although less environmentally friendly compared to NMP and also unable to generate molecules as large as those obtained via RAFT, ATRP allows a more effective control over the structure and molecular weight distribution of the polymer, which makes it the most promising among other RDRP methods [2].

ATRP was developed for the first time from independent studies of Mitsuo Sawamoto [3] and Krzysztof Matyjaszewski in 1995 [4], inspired in the Atom Transfer Radical Addition (ATRA) reactions [5]. Similarly to ATRA, in ATRP carbon-carbon bonds are formed with a transition metal catalyst (usually copper-based), a result of the reaction between intermittent radicals, originated by the reactivation of an alkyl halide adduct, and alkenes [2].

ATRP processes [2] are experimentally run with the following typical reactants: monomer, a chemical compound that have active(s) unsaturation(s); initiator, which generally comprehends an alkyl halide with the halogen(s) atom(s) easily transferable; transition metal salt, wherein the metal has two available oxidation states (usually copper-based); ligand, which combines with the transition metal salt through a covalent or ionic bond to form a catalytic complex; and solvent.

According to the Fig. 1, which illustrates a general scheme for the conventional ATRP mechanism [2] (which is governed by the equilibrium constant $K_{ATRP} = k_a/k_{da}$), copper(I) catalyst ($(Cu^{I}L)X$) provides the homolytic cleavage of a dormant (macro)alkyl halide (R_iX). As a result of the process, there is reversible oxidation of the transition metal because of the transfer of the halogen atom to the catalytic complex, deactivating the latter one and forming the copper(II) halide complex ($(Cu^{II}XL)X$). As reference, $(Cu^{I}L)X$ and $(Cu^{II}XL)X$ species are also designated as activator and deactivator, respectively.

The reversibly generated (macro)alkyl radical (R_i) can be deactivated by the $(Cu^{II}XL)X$ species, propagate (with a kinetic rate constant k_p) with a vinyl monomer (M), or even terminate (with a kinetic rate constant k_t) with another alkyl radical (R_j) to form the polymer itself (P_{i+j}, P_i and P_j species). The cycle of intermittent and repeated activation and deactivation process leads the polymer chains to grow.

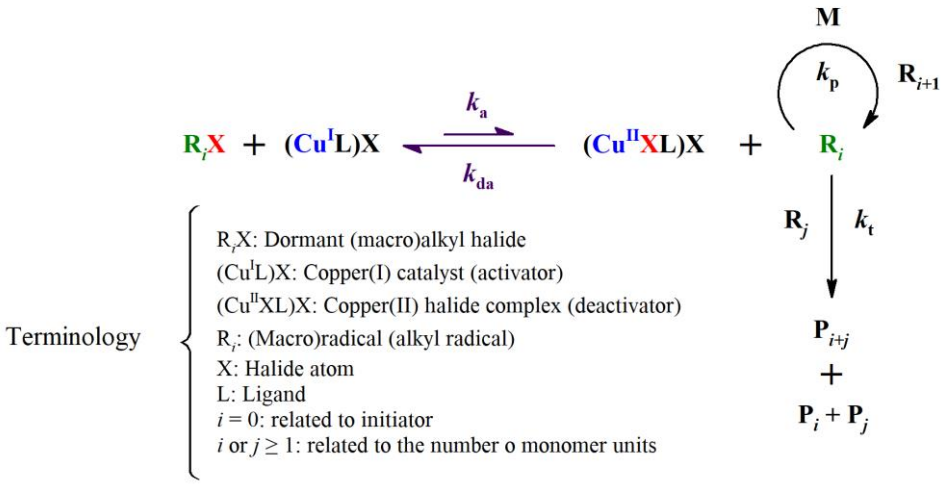

Fig. 1. The general scheme of the reaction mechanism of a polymerization process via ATRP. Adapted from [2].

Literature reports some studies of variables that influence K_{ATRP} [2]; they are temperature [6], pressure [7], and the chemical nature of alkyl halide [8–10], catalyst [10], and solvent [11, 12]. Theoretically, as depicted by Fig. 2, the ATRP equilibrium is composed of the four following contributing reactions [12]: (i) bond dissociation energy of the alkyl halide (K_{BD}); (ii) electron transfer between metal complexes (K_{ET}); (iii) electron affinity of the halogen (K_{EA}); and (iv) the heterolytic cleavage of the Cu^{II}–X bond (K_X), where the last one is also called the "halidophilicity" of the deactivator.

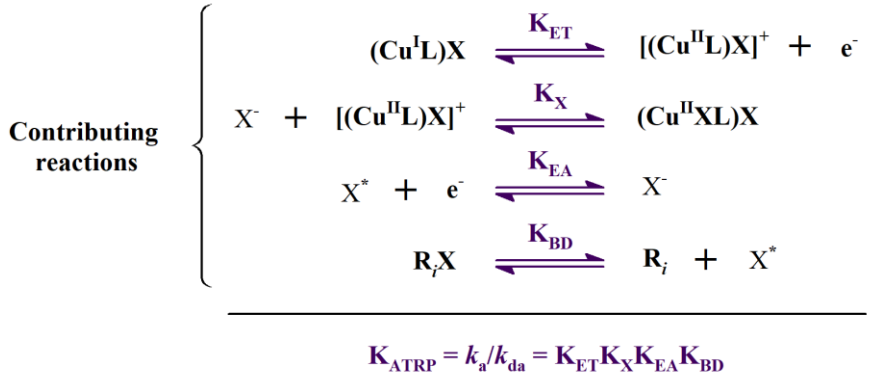

Fig. 2. ATRP equilibrium contributing reactions. Adapted from [12].

2.1.2 Diminishing catalyst concentration in atom transfer radical polymerization: an overview of strategies available in the literature

The large-scale production of polymeric materials meets some challenges. Increasing the production of polymers by conventional ATRP has limitations, mainly due to the high catalyst concentrations required in the process. In normal ATRP, literature reports an average concentration of the catalyst about 10–100 mM, or 1000–10000 ppm (expressed as the molar ratio of catalyst to monomer) [2].

Notoriously, economic and environmental benefits could be achieved if the amount of transition metal catalyst was reduced as much as possible without producing significant changes in reactivity and control of the reaction system.

Kinetically, the polymerization rate in ATRP (R_p) is represented by Eq. (1) [2]. To maintain a specific value of R_p, such an equation indicates that the $[Cu^I]/[Cu^{II}]$ ratio should remain constant. Thus, the catalyst concentration could be reduced if the original $[Cu^I]/[Cu^{II}]$ ratio and consequently R_p remains the same.

$$R_p = k_p[M][R_i] = k_p[M]\left(K_{ATRP}[R_iX]\frac{[(Cu^{I}L)X]}{[(Cu^{II}XL)X]}\right) \quad (1)^a$$

[a]R_p: rate of polymerization; M: monomer; R_i: (macro)alkyl radical (i.e., living polymer chains) with i (≥ 1) monomeric units long; R_iX: dormant (macro)alkyl halide (i.e., dormant polymer chains) with i (≥ 1) monomeric units long; $(Cu^{I}L)X$: copper(I) catalyst (activator); $(Cu^{II}XL)X$: copper(II) halide complex (deactivator).

Nevertheless, the direct reduction of the catalyst concentration is not a viable option. If the concentration of activator species (i.e., $(Cu^{I}L)X$) is significantly lower than that of the dormant (macro)alkyl halides (i.e., R_iX), nearly all activators would be converted irreversibly in the deactivator species (i.e., $(Cu^{II}XL)X$) stopping the polymerization process [2].

In this scenario, strategies to reduce the concentration of catalysts in ATRP systems have been studied and tested aiming to save reaction costs and simplify the purification process of the products.

To overcome such a bottleneck for run ATRP in the industrial-scale, the most common alternative reported in literature [2, 13] is to promote an additional redox cycle to convert $(Cu^{II}XL)X$ into $(Cu^{I}L)X$ species as depicted by Fig. 3. This kind of approach have allowed a significant reduction of the catalyst concentration (i.e., at parts per million levels) in the conventional ATRP.

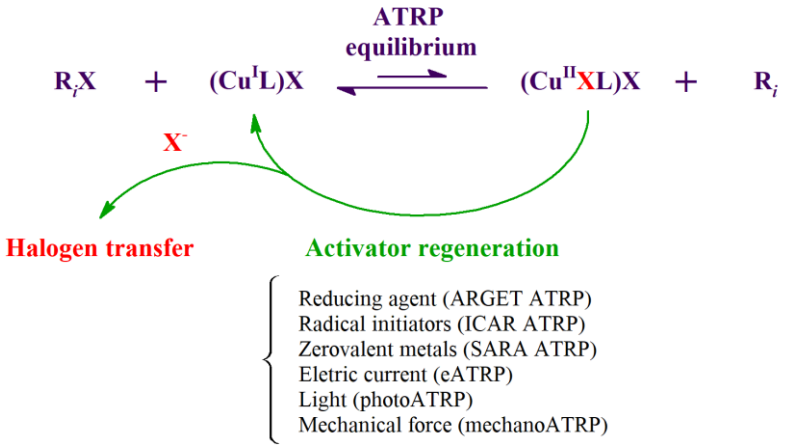

Fig. 3. Mechanism of various external regulations to conduct ATRP at low catalyst concentrations. Adapted from [2, 13].

Techniques developed [2, 13] are related to the use of chemical reducing agents in Activators Regenerated by Electron Transfer (ARGET) ATRP; radical initiators in Initiators for Continuous Activator Regeneration (ICAR) ATRP; zerovalent metals in Supplemental Activator and Reducing Agent (SARA) ATRP; electric current in electrochemically mediated ATRP (eATRP); light in photochemically mediated ATRP (photoATRP); and mechanical force in mechanically mediated ATRP (mechanoATRP).

Among the previously mentioned approaches, the most one developed and reported in the experimental field is ARGET ATRP. Thus, this research presents a more comprehensive understanding of the ARGET mechanism associated with conventional ATRP.

Throughout Chapter 4 of this work, the theoretical kinetic aspects of this polymerization technique will be discussed with more emphasis.

2.2. Research objectives

In the context of ARGET ATRP processes, the general objectives of this study are summarized below:

- To investigate the ARGET mechanism for some reducing agents reported in the literature (i.e., tin(II) 2-ethylhexanoate, ascorbic acid, and hydrazine), equating their reaction kinetics to reduce the concentration of (copper-based) catalysts in conventional ATRP;
- To develop more detailed mathematical models for both homopolymerization and random copolymerization via ARGET ATRP in relation to reaction kinetics than those available in literature up to now;
- To validate the mathematical models proposed for polymerizations via ARGET ATRP with experimental data provided in literature;
- To evaluate critical parameters for ARGET ATRP processes (i.e., ratio of the initial concentrations of monomer and deactivator, and ratio of the initial concentrations of deactivator and reducing agent), based on a parametric study by computational simulation of the validated proposed mathematical models.

Other specific and additional purposes to these previously reported will be described throughout Chapter 4, highlighting the differences of this work in relation to those available in the literature up to now.

3. GENERAL METHODOLOGY

3.1. Modeling polymerization reactions

3.1.1. Overview of polymerization modeling methods

Polymerization modeling methods are classified in two main classes: deterministic or kinetic-based (e.g., method of moments) and statistical or stochastic-based (e.g., Monte Carlo methods) [14].

The Monte Carlo methods consists of a statistical modeling, which involves the use of the probabilistic theory to reconstruct the problem modeled (i.e., stochastic-based) [14]. For a determined system, it generates states according to appropriate Boltzmann probabilities rather than trying to reproduce the system dynamics. Thus, such an approach is based on statistical mechanics of equilibrium rather than molecular dynamics [14]. Although this is a powerful method, it ignores the history of the reaction, which can result in significant discrepancies from reality [14].

On the other hand, the method of moments consists of a deterministic modeling, which is a kinetic-based approach [14, 15]. The kinetic modeling relies to a mathematical description of changes in properties of a determined system with respect to time [14, 15]. This method usually involves the derivation of mass balances of the reagents and products [14, 15]. Unlike the stochastic-based approach, this method takes into account the "memory" of the reaction history and, therefore, it is more appropriate for kinetic-controlled processes [14, 15]. Thus, the proposed mathematical models presented in this work were based on the method of moments.

3.1.2 Applying the method of moments in polymerization systems

Polymerization reactions are complex kinetic systems, the justification for the choice of the method of moments in the modeling lies in the difficulty to determine mathematically the molar concentration of the many existing chemical species.

Table 1 shows the three main types of polymer chains verified in normal ATRP (as well as in ARGET ATRP too): (i) dormant (i.e., the dormant (macro)alkyl halide), R_iX; (ii) living (i.e., the (macro)radical), R_i; and (iii) dead (i.e., the polymer itself), P_i, where i (with $i \geq 1$) is the number of monomeric units in each chain. Hence, it is necessary a mathematical construction for the populational balance of dormant, living, and dead polymer chains.

The m^{th} order moments for dormant ($\mu_{m,RX}$), living ($\mu_{m,R}$), and dead ($\mu_{m,P}$) polymer chains are presented in Table 1, where only zeroth and first-order moments have a direct meaning [15]. While the zeroth-order moment of a specific polymer chain type (i.e., dormant, living or dead chains) is related to its molar concentration, the first-order moment corresponds to its constituent monomer concentration [15].

Table 1. m^{th} order moments equations for dormant, living, and dead polymer chains.[a] Reprinted from [16].

m^{th} order moment	Equation	
Dormant chain	$\mu_{m,RX} = \sum_{i=1}^{\infty} i^m [R_iX]$	(2)
Living chain	$\mu_{m,R} = \sum_{i=1}^{\infty} i^m [R_i]$	(3)
Dead chain	$\mu_{m,P} = \sum_{i=1}^{\infty} i^m [P_i]$	(4)

[a] R_iX, R_i and P_i: dormant, living and dead polymer chains with i (≥ 1) monomeric units long, respectively; $\mu_{m,RX}$, $\mu_{m,R}$ and $\mu_{m,P}$: m^{th} order moments for dormant, living and dead chains, respectively.

By the zeroth, first, and second-order moments definitions, Table 2 shows examples of some polymerization parameters of engineering interest that can be obtained [15], which are the number-average chain length (DP_n), weight-average chain length (DP_w), number-average molecular weight (M_n), weight-average molecular weight (M_w), dispersity (Đ) and percentage of functionalized polymer chains (End functionality).

Table 2. Polymerization parameters of engineering interest obtained by the method of moments.[a] Reprinted from [16].

Parameter	Equation	
Number-average chain length	$\mathrm{DP_n} = \frac{\mu_{1,\mathrm{RX}} + \mu_{1,\mathrm{R}} + \mu_{1,\mathrm{P}}}{\mu_{0,\mathrm{RX}} + \mu_{0,\mathrm{R}} + \mu_{0,\mathrm{P}}}$	(5)
Weight-average chain length	$\mathrm{DP_w} = \frac{\mu_{2,\mathrm{RX}} + \mu_{2,\mathrm{R}} + \mu_{2,\mathrm{P}}}{\mu_{1,\mathrm{RX}} + \mu_{1,\mathrm{R}} + \mu_{1,\mathrm{P}}}$	(6)
Number-average molecular weight	$\mathrm{M_n} = \mathrm{M_M DP_n}$	(7)
Weight-average molecular weight	$\mathrm{M_w} = \mathrm{M_M DP_w}$	(8)
Dispersity	$Đ = \frac{\mathrm{DP_w}}{\mathrm{DP_n}}$	(9)
Percentage of functionalized polymer chains	$\text{End functionality (\%)} = \frac{\mu_{0,\mathrm{RX}}}{\mu_{0,\mathrm{RX}} + \mu_{0,\mathrm{R}} + \mu_{0,\mathrm{P}}} \times 100$	(10)

[a]$\mathrm{DP_n}$ and $\mathrm{DP_w}$: number-average and weight-average chain lengths, respectively; $\mathrm{M_n}$ and $\mathrm{M_w}$: number-average and weight-average molecular weights, respectively; $\mathrm{M_M}$: monomer molecular weight; Đ: dispersity; End functionality: percentage of functionalized polymer chains.

3.2. Computational approach

3.2.1. Stiff differential equations

Systems of differential equations with many equations describing kinetic models are good examples of stiff systems, like the ones observed in polymerization reactions. Stiff systems have the combination of dependent variables whose variations over time are orders of magnitude different from each other. As the mathematical resolution of such problems is only possible for tiny numerical integration steps, the employment of implicit methods is necessary. Hence, the proposed mathematical models presented in this work were solved by the Gear's method [17], which is adequate for stiff differential equations.

3.2.2. Fitting of kinetic parameters and optimization routine

The intrinsic kinetic rate constants for the polymerization reaction (i.e., propagation, termination, chain transfer, thermal initiation, backbiting, β-scission) can be easily found in the literature for usual monomers (e.g., styrene, methyl acrylate, butyl acrylate, methyl methacrylate).

However, the values of ATRP equilibrium kinetic rate constants (i.e, k_a and k_{da}) under polymerization conditions sometimes are challenging to be found, since they can vary with temperature, pressure, media/solvent, alkyl halide and both the chemical nature of ligand and halogen in transition metal catalysts, as previously evidenced by literature in Section 2.1.1.. The situation is even more restricted for the kinetic rate constants associated to the ARGET mechanism, since it has not explored well in the literature until now.

To validate the proposed mathematical models, aiming to obtain the kinetic rate constants unavailable in the literature for the experimental conditions used in this work, an optimization process is also necessary. Since the optimization is a nonlinear least-squares problem, the Levenberg–Marquardt algorithm [18, 19] was chosen to find the lacking kinetic rate constants that best fit the models to the experimental data considered in the validation process. Moreover, the strategy adopted in this work was based on the fitting of the natural logarithm of those lacking kinetic rate constants (i.e., ln(*k*)), aiming to put their values in the same order of magnitude to make each iteraction of the optimization process more accurate

The numerical solution of the models presented in this work was obtained in the software MATLAB (MATLAB R2018a, Natick, MA). In this software, there are preprogrammed implementations for the Gear's method (i.e., "*ode15s*" function) and the Levenberg-Marquardt optimization algorithm (i.e., "*lsqnonlin*" function), which were used in this work.

Additionally, to perform the optimization process to obtain the lacking kinetic rate constants, a complemental function referenced as "*objective*" was programmed. In the "*objective*" function, the normalized deviations between results from simulation and from experimental data of literature were calculated by Eq. (11).

Such an approach was necessary since experimental variables evaluated (i.e., monomer conversion, $\ln([M]_0/[M])$, number-average molecular weight and dispersity) have a very different orders of magnitude. Therefore, the optimization problem needed to be rescaled to make it work.

$$\delta_{var(t)} = \left(\frac{var_{sim.(t)} - var_{exp.(t)}}{\max\left\{\max\{var_{sim.}\}, \max\{var_{exp.}\}\right\}} \right) \quad (11)^{a,b}$$

[a] $\delta_{var(t)}$: normalized deviation between simulated and experimental data of the variable *var* at the time *t*; $var_{sim.(t)}$: variable *var* simulated at the time *t;* $var_{exp.(t)}$: experimental data of the variable *var* at the time *t*; $var_{sim.}$: set of values of variable *var* simulated in the times wherein the experimental data are available; $var_{exp.}$: set of experimental values of variable *var* available in a determined set of time; max: a function that returns the maximum value in a set of values. [b] Variable *var* can be monomer conversion, $\ln([M]_0/[M])$, number-average molecular weight or dispersity.

The termination criteria adopted for the optimization process were that the variation of the kinetic rate constants adjusted in the interactions or the sum of normalized deviations should be less than or equal to 10^{-3}. A schematic procedure representing the computational implementation of the optimization process is depicted by Fig. 4.

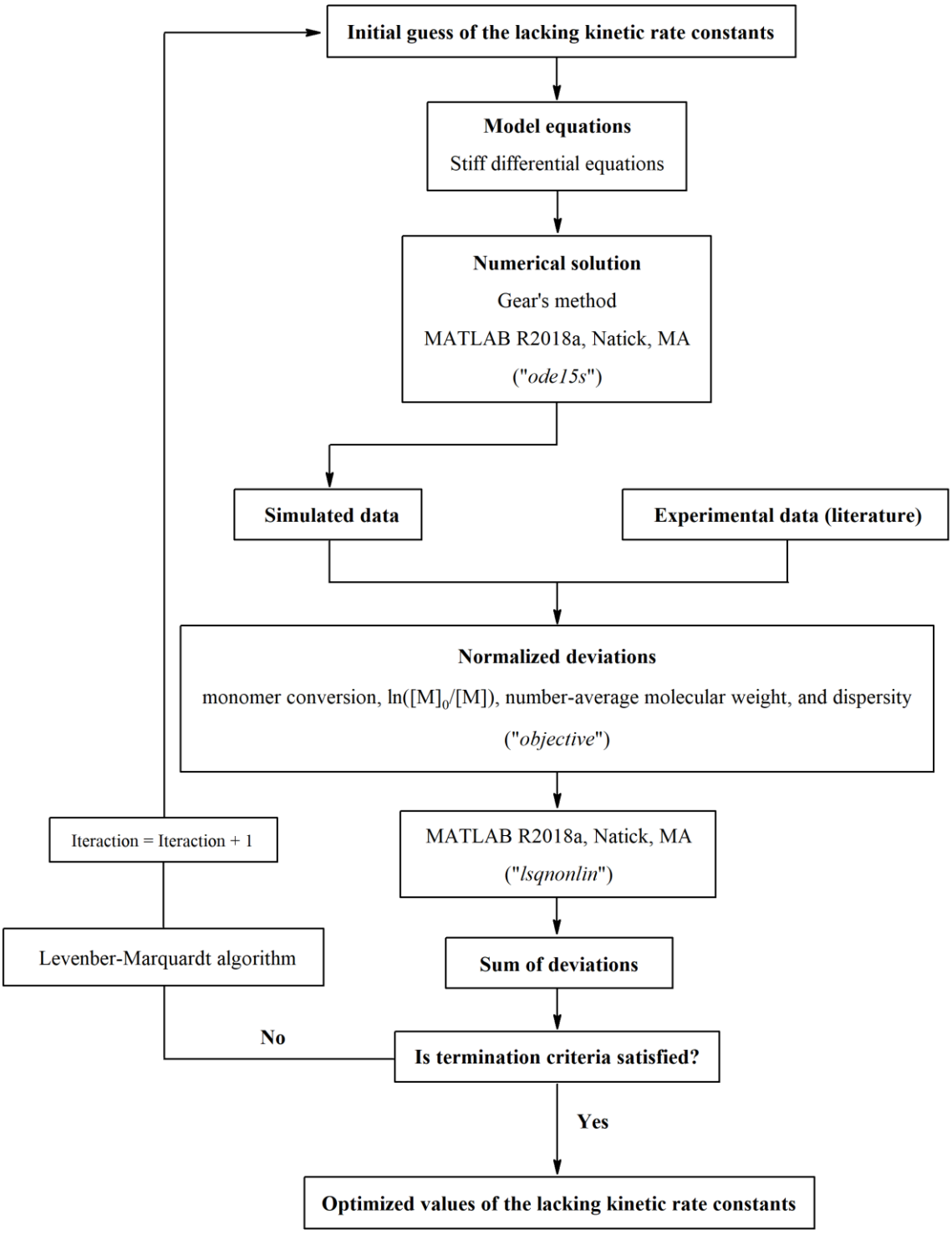

Fig. 4. Representative scheme for the process of obtaining the lacking kinetic rate constants in the literature for the ARGET ATRP systems studied in this work.

CHAPTER 4. ACTIVATORS REGENERATED BY ELECTRON TRANSFER FOR ATOM TRANSFER RADICAL POLYMERIZATION (ARGET ATRP)

Part of chapter 4 contents was published elsewhere [16].
Please, kindly check this reference:
[16] E. P. Lyra, C. L. Petzhold, L. M. F. Lona, Tin(II) 2-ethylhexanoate and ascorbic acid as reducing agents in solution ARGET ATRP: a kinetic study approach by mathematical modeling and simulation, Chemical Engineering Journal 364 (2019) 186–200.
DOI information: 10.1016/j.cej.2019.01.123

4.1. Part I. Tin(II) 2-ethylhexanoate, ascorbic acid and hydrazine as reducing agents in solution homopolymerization via ARGET ATRP: understanding the kinetic mechanisms and verifying experimental trends by simulation

4.1.1. Abstract (Part I)

In Section 4.1., a kinetic-based approach was considered to build a comprehensive mathematical model for solution homopolymerization via ARGET ATRP, in which the reducing agent consumption is detailed. Tin(II) 2-ethylhexanoate, ascorbic acid, and hydrazine were studied as reducing agents with copper(II) halide complex as a catalyst, and the ARGET mechanism for them was proposed and validated with experimental data available in the literature. Simulation results confirm that the higher the initial concentrations of both copper (II) halide complex and reducing agent, the higher the number-average molecular weight and the lower the dispersity. However, the initial concentration of copper(II) halide complex is a critical parameter with higher sensitivity than the reducing agent in solution ARGET ATRP process.

4.1.2. Highlights (Part I)

- A comprehensive mathematical model for solution ARGET ATRP is proposed and validated;
- Reaction kinetics for the reducing agent is considered in the model development;
- The use of tin(II) 2-ethylhexanoate, ascorbic acid, and hydrazine as reducing agents is investigated;
- The variation effect of kinetic parameters and reaction stoichiometry is studied in solution ARGET ATRP.

4.1.3. Introduction (Part I)

The mechanism called Activators Regenerated by Electron Transfer (ARGET) relies to the use of a reducing agent to continuously recover the transition metal catalyst in its lower oxidation state (active form), as schematically illustrated in Fig. 5. Such an approach is not only another way to initiate the conventional Atom Transfer Radical Polymerization (ATRP) by stable species (i.e., deactivator) and but also can be considered a “greener” procedure [20, 21].

The polymerization rate can be adjusted according to the reducing agent used and its amount in the reaction system. The reducing agent must be selected that it and its oxidized product do not interfere with the other ATRP reactants. This kind of precaution aims to avoid side reactions of reducing agent with ligand, monomer, or polymer; resulting in a poor polymerization control. Some reducing agents that have been successfully employed in the ARGET ATRP systems include tin(II)-based compounds [22], glucose [23], ascorbic acid [24], hydrazine [21]. Furthermore, some monomers and ligands (e.g., tertiary amines) [25] can be used as internal reducing agent.

Concerning the mathematical modeling works in ARGET ATRP, a brief literature review show that there are few publications in this area [26–34], wherein tin(II) 2-ethylhexanoate is the most studied reducing agent. Table 3 show the most relevant works found in the literature up to now, in which the model goal (i.e., predict the reaction kinetics or molecular weight distribution of the polymer obtained) and approach (i.e., kinetic or stochastic based), as well as the reducing agents investigated are highlighted.

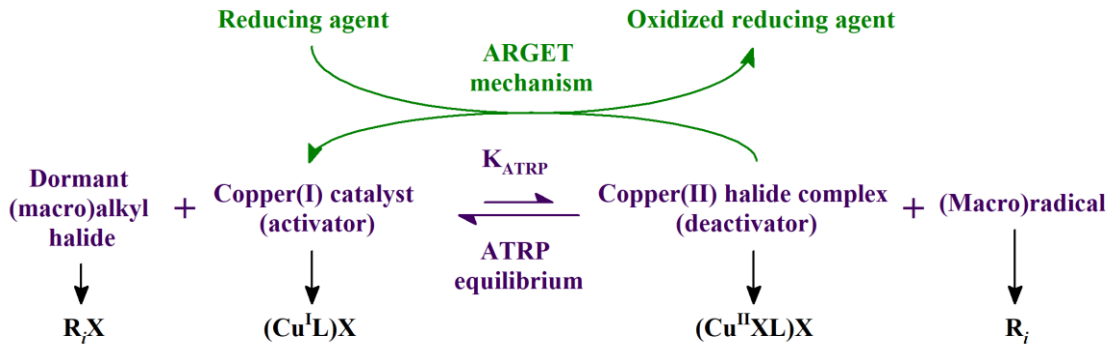

Fig. 5. The conceptual mechanism of ARGET ATRP technique. Reprinted from [16].

Although validated with experimental data, the works reported in Table 3 do not detail the reaction kinetics for the reducing agent (i.e., it is proposed empirical reaction kinetics for the activator regeneration), which is a significant contribution of this work. Thus, a deterministic approach based on chemical species experimentally verified is, then, proposed. Hence, this study provided in Section 4.1. aims at elucidating the ARGET mechanism focusing on the tin(II) 2-ethylhexanoate, ascorbic acid, and hydrazine, through the development of a comprehensive mathematical model to represent the ARGET ATRP processes for such reducing agents.

Table 3. ARGET ATRP models available in the literature, their goal, approach, and reducing agent investigated. Reprinted from [16].

Model goal	Model approach	Reducing agent	Reference
Reaction kinetics	Kinetic-based	Tin(II) 2-ethylhexanoate	[26–28]
		Sodium ascorbate Ascorbic acid	[29]
		Any	[30]
	Stochastic-based	Tin(II) 2-ethylhexanoate	[31, 32]
Molecular weight distribution	Kinetic-based	Tin(II) 2-ethylhexanoate	[33]
	Stochastic-based	Tin(II) 2-ethylhexanoate	[31, 32, 34]

Additionally, a better understanding of the ARGET ATRP technique is provided with the presentation of a detailed mapping of concentration profiles of the most important chemical species considered in the kinetic mechanism. The variation effect of kinetic parameters and reaction stoichiometry is also studied in solution ARGET ATRP, aiming to indicate the critical parameters and possible limitations of such polymerization process.

4.1.4. Kinetic approach (Part I)

The kinetic mechanism of the ARGET ATRP technique is based on the all elementary reactions verified in the conventional ATRP (see Table 4), such as initiation, propagation, termination, and the equilibrium between living (activated) and dormant (deactivated) chains. The latter one is also referred as ATRP equilibrium. As the initiator is generally an alkyl halide, the initiation step is also based on an ATRP equilibrium reaction. Furthermore, copper-based catalysts are considered, which are classical in ATRP systems.

Table 4 shows the three main types of polymer chains verified in ATRP: dormant (R_iX), living (R_i), and dead (P_i). The other chemical species also included in the kinetic mechanism are alkyl halide initiator, R_0X; copper(I) catalyst (activator), $(Cu^{I}L)X$; primary free radical generated by the alkyl halide initiator, R_0; copper(II) halide complex (deactivator), $(Cu^{II}XL)X$; and monomer, M.

Table 4. Steps of conventional ATRP and their respective elementary reactions.[a,b] Reprinted from [16].

Step	Mechanism	
Initiation (ATRP equilibrium)	$R_0X + (Cu^{I}L)X \xrightarrow{k_{a0}} R_0 + (Cu^{II}XL)X$	(12)
	$R_0 + (Cu^{II}XL)X \xrightarrow{k_{da0}} R_0X + (Cu^{I}L)X$	(13)
Propagation	$R_0 + M \xrightarrow{k_{p0}} R_1$	(14)
	$R_i + M \xrightarrow{k_p} R_{i+1}$	(15)
Termination (by combination)	$R_i + R_j \xrightarrow{k_{tc}} P_{i+j}$	(16)
Termination (by disproportionation)	$R_i + R_j \xrightarrow{k_{td}} P_i + P_j$	(17)
ATRP equilibrium	$R_iX + (Cu^{I}L)X \xrightarrow{k_a} R_i + (Cu^{II}XL)X$	(18)
	$R_i + (Cu^{II}XL)X \xrightarrow{k_{da}} R_iX + (Cu^{I}L)X$	(19)

[a] R_0X: alkyl halide initiator; $(Cu^{I}L)X$: copper(I) catalyst (activator); R_0: primary free radical (generated by the alkyl halide initiator); $(Cu^{II}XL)X$: copper(II) halide complex (deactivator); M: monomer; R_i, P_i and R_iX: living, dead and dormant polymer chains with i (≥ 1) monomeric units long, respectively; i or j: arbitrary numbers of monomeric units (≥ 1). [b] In this study it will be considered $k_{a0} = k_a$, $k_{da0} = k_{da}$ and $k_{p0} = k_p$, that is a usual approximation in polymerization engineering.

Besides the reactions presented in Table 4, the ARGET ATRP technique also accounts of the regeneration of the transition metal complex in its active form by the addition of an appropriate reducing agent. The reaction step previously described is designated as ARGET mechanism. In Sections 4.1.4.1, 4.1.4.2, and 4.1.4.3 it will be discussed the ARGET mechanisms of tin(II) 2-ethylhexanoate (Table 5), ascorbic acid (Table 6), and hydrazine (Table 7) as reducing agents, respectively, which are the ones considered in this study.

4.1.4.1. ARGET mechanism for tin(II) 2-ethylhexanoate as a reducing agent

Some experimental works with tin(II)-mediated solution ARGET ATRP can be found in the literature [22, 23, 35–40]. About the tin chemistry, the main existing stable species have the oxidation state +II or +IV, but unstable intermediates with oxidation state +III can also be obtained [41–48]. For the usage of a tin(II)-based compound as a reducing agent, such as tin(II) 2-ethylhexanoate ($Sn^{II}(eh)_2$), the reversible reactions represented by Eqs. (20) and (21) describe the oxidation kinetics to recover the catalytic complex in its inactive form, as depicted in Table 5.

Based on the tin(III)-based compounds instability (i.e., it is rapidly consumed) and the excess of the $Sn^{II}(eh)_2$ compared to copper(II) halide complex (i.e., the equilibriums are displaced towards the formation of the products), Eqs. (20) and (21) can be simplified as irreversible reactions, where the first one is the rate-determining step (i.e., the reaction represented Eq. (20) occurs deliberately slower than Eq. (21)). By those previous observations, an irreversible global reaction represented by Eq. (22) can represent the ARGET mechanism proposed for tin(II) 2-ethylhexanoate appropriately.

Table 5. Reaction mechanism proposed for tin(II) 2-ethylhexanoate as a reducing agent in ARGET ATRP systems.[a] Reprinted from [16].

Reaction	Mechanism		
Contributing	$Sn^{II}(eh)_2 + (Cu^{II}XL)X \rightleftharpoons Sn^{III}(eh)_2X + (Cu^{I}L)X$	→ slow	(20)
	$Sn^{III}(eh)_2X + (Cu^{II}XL)X \rightleftharpoons Sn^{IV}(eh)_2X_2 + (Cu^{I}L)X$	→ fast	(21)
Global	$Sn^{II}(eh)_2 + 2(Cu^{II}XL)X \xrightarrow{k_r} Sn^{IV}(eh)_2X_2 + 2(Cu^{I}L)X$		(22)

[a]$Sn^{II}(eh)_2$: tin(II) 2-ethylhexanoate; $Sn^{III}(eh)_2X$: tin(III)-based compound (unstable state of the $Sn^{II}(eh)_2$ oxidized); $Sn^{IV}(eh)_2X_2$: tin(IV)-based compound (stable state of the $Sn^{II}(eh)_2$ oxidized).

From all the references on ARGET ATRP system modeling shown in Table 3 that use the reducing tin(II) 2-ethylhexanoate, only Payne et al. [31, 32] adopted a similar mechanism assumed in this work (represented by Eqs. (20) and (21)), while the other authors proposed a generic approach (i.e., it is proposed empirical reaction kinetics for the activator regeneration), which did not explicitly consider the tin chemistry [26–28, 33, 34].

4.1.4.2. ARGET mechanism for ascorbic acid as a reducing agent

In addition to its importance in biochemical systems [49–50], the redox property of ascorbic acid is one of its most interesting chemical characteristics [51–52]. Thus, ascorbic acid has been applied as the reducing agent in ARGET ATRP systems [24, 53, 54].

The oxidation of ascorbic acid (H_2asc) does not only involve two electrons transfer as in tin(II) 2-ethylhexanoate, but two protons are also lost from its original structure, as evidenced by the reversible reactions represented by Eqs. (23) and (24) in Table 6. The final product of ascorbic acid oxidation is dehydroascorbic acid (dha), but some intermediate chemical species are verified in the process [51, 52, 55–57]. The main one is the ascorbyl radical (asc^{*-}), that results from the loss of two protons and one electron of the original ascorbic acid chemical structure, which has been experimentally verified [56]. Such approach differs from that of Keating et al. [30] in their ARGET ATRP modeling with ascorbic acid as a reducing agent, in which the specific chemistry of oxidation was not considered.

Although ascorbic acid may lead to the formation of complexes with metal ions, depending on the pH of the reaction medium, most of them are relatively unstable; therefore, they are not considered in the kinetic mechanism [51].

Considering that asc^{*-} is an unstable intermediate (i.e., it is rapidly consumed) [56] and the excess of H_2asc compared to copper(II) halide complex is also verified (i.e., the equilibrium are displaced towards the formation of the products), Eqs. (23) and (24) can be simplified as irreversible reactions, where the first one is the rate determining step (i.e., the reaction represented Eq. (23) occurs slower than Eq. (24)). Hence, the irreversible global reaction described by Eq. (25) can describe the ARGET mechanism for ascorbic acid adequately.

Table 6. Reaction mechanism proposed for ascorbic acid as a reducing agent in ARGET ATRP systems.[a] Reprinted from [16].

Reaction	Mechanism		
Contributing	$H_2asc + (Cu^{II}XL)X \rightleftharpoons 2H^+ + asc^{*-} + (Cu^{I}L)X + X^-$	→ slow	(23)
	$asc^{*-} + (Cu^{II}XL)X \rightleftharpoons dha + (Cu^{I}L)X + X^-$	→ fast	(24)
Global	$H_2asc + 2(Cu^{II}XL)X \xrightarrow{k_r} 2H^+ + dha + 2(Cu^{I}L)X + 2X^-$		(25)

[a]H_2asc: ascorbic acid; H^+: proton dissociated of ascorbic acid; asc^{*-}: ascorbyl radical (unstable state of the H_2asc oxidized); X^-: halide anion; dha: dehydroascorbic acid (stable state of the H_2asc oxidized).

In literature, the study of Cu^{II}/H_2asc oxidation occurs in aqueous solution with the presence of air [58–60]. Some works show a strong catalytic effect of halide anions (X^-), especially chlorides and acetates, which when in excess (compared to Cu^{II}) makes Eq. (25) an irreversible reaction [60].

In the outer sphere electron transfer process [61], it is known that dormant macro(radical) halide cleavage leads to the halide anions formation. As the halide anions are in excess compared to the transition metal catalyst in its lower oxidation state, the catalytic effect of the halide anions can also be verified in the polymerization systems.

4.1.4.3. ARGET mechanism for hydrazine as a reducing agent

Records of studies of hydrazines oxidation by transition-metal chemical compounds are long-standing [62–64], leading the first ones to be also tested as a reducing agent in ARGET ATRP systems [21]. Concerning the kinetics of the oxidation of hydrazine (N_2H_4) by a copper(II) halide complex, literature reports three main reactions [62–64] represented by Eqs. (26), (27) and (28) describe such process, as shown in Table 7.

Eq. (26) represents the formation of the hydrazyl radical (N_2H_3*), whereas the Eq. (27) refers to the formation of diimide (also called the diazene) (N_2H_2) and Eq. (28) is related to the decomposition of this last molecule for the formation of nitrogen (N_2) [62–64]. N_2H_3* and N_2H_2 species are unstable [62–64], thus, the reaction represented by Eq. (26) is the rate-determining step (i.e., the reaction represented Eq. (26) occurs slower than Eqs. (27) and (28)).

In addition to the experimental evidences previously mentioned, as the unstable species are rapidly consumed, and in ARGET ATRP systems the reducing agent (i.e., hydrazine) is in excess compared to copper(II) halide complex (i.e., the equilibrium is displaced towards the formation of the products), the irreversible global reaction described by Eq. (29) can be considered for describing the ARGET mechanism for hydrazine.

Table 7. Reaction mechanism proposed for hydrazine as a reducing agent in ARGET ATRP systems.[a]

Reaction	Mechanism		
Contributing	$N_2H_4 + (Cu^{II}XL)X \rightleftharpoons H^+ + N_2H_3{}^* + (Cu^{I}L)X + X^-$	→ slow	(26)
	$N_2H_3{}^* + (Cu^{II}XL)X \rightleftharpoons H^+ + N_2H_2 + (Cu^{I}L)X + X^-$	→ fast	(27)
	$N_2H_2 + 2(Cu^{II}XL)X \rightleftharpoons 2H^+ + N_2 + 2(Cu^{I}L)X + 2X^-$	→ fast	(28)
Global	$N_2H_4 + 4(Cu^{II}XL)X \xrightarrow{k_r} 4H^+ + N_2 + 4(Cu^{I}L)X + 4X^-$		(29)

[a]N_2H_4: hydrazine; H^+: proton dissociated of hydrazine; N_2H_3*: hydrazil radical (unstable state of the N_2H_4 oxidized); X^-: halide anion; N_2H_2: diimide/diazene (unstable state of the N_2H_4 oxidized); N_2: nitrogen (stable state of the N_2H_4 oxidized).

4.1.5. Model development (Part I)

4.1.5.1. General hypotheses (Part I)

The mathematical model development of solution homopolimerization via ARGET ATRP is fundamented on the following hypotheses: (i) the polymerization process occurs in isothermal batch reactors; (ii) constant volume; (iii) perfect mixing is assumed; (iv) side reactions are not considered in the kinetic mechanism (i.e., only initiation, propagation, termination, ATRP equilibrium, and ARGET mechanism are admitted); (v) monofunctional alkyl halides are the initiators; (vi) diffusional effects are not considered; (vii) both activator and deactivator are copper-based; (viii) it is assumed that copper salt is entirely complexed by ligand at the beginning of the polymerization; (ix) solvent is admited to be chemically inert; and (x) the halogen-exchange mechanism [65] is not considered (i.e., different halide anions observed in both initiator and catalyst do not lead to the observation of side reactions).

4.1.5.2. Molar balance of polymer chains (Part I)

The method of moments (see Table 1 and 2 in Section 3.1.1. for details) requires a derivation of the molar balance of polymer chains, represented by Eqs. (30)–(34) shown in Table 8.

Table 8. Molar balance for dormant, living, and dead chains in solution homopolimerization via ARGET ATRP in batch reactors. Reprinted from [16].

Chemical specie		**Equation**	
Dormant chain	for $i \geq 1$	$\frac{d[\mathrm{R}_i\mathrm{X}]}{dt} = -k_\mathrm{a}[\mathrm{R}_i\mathrm{X}][(\mathrm{Cu^I L})\mathrm{X}] + k_\mathrm{da}[\mathrm{R}_i][(\mathrm{Cu^{II}XL})\mathrm{X}]$	(30)
Living chain	for $i = 1$	$\frac{d[\mathrm{R}_1]}{dt} = k_{\mathrm{p0}}[\mathrm{R}_0][\mathrm{M}] - k_\mathrm{p}[\mathrm{R}_1][\mathrm{M}] - (k_\mathrm{tc} + k_\mathrm{td})[\mathrm{R}_1]\sum_{j=1}^{\infty}[\mathrm{R}_j] + k_\mathrm{a}[\mathrm{R}_1\mathrm{X}][(\mathrm{Cu^I L})\mathrm{X}] - k_\mathrm{da}[\mathrm{R}_1][(\mathrm{Cu^{II}XL})\mathrm{X}]$	(31)
	for $i \geq 2$	$\frac{d[\mathrm{R}_i]}{dt} = k_\mathrm{p}([\mathrm{R}_{i-1}] - [\mathrm{R}_i])[\mathrm{M}] - (k_\mathrm{tc} + k_\mathrm{td})[\mathrm{R}_i]\sum_{j=1}^{\infty}[\mathrm{R}_j] + k_\mathrm{a}[\mathrm{R}_i\mathrm{X}][(\mathrm{Cu^I L})\mathrm{X}] - k_\mathrm{da}[\mathrm{R}_i][(\mathrm{Cu^{II}XL})\mathrm{X}]$	(32)
Dead chain	for $i = 1$	$\frac{d[\mathrm{P}_1]}{dt} = k_\mathrm{td}[\mathrm{R}_1]\sum_{j=1}^{\infty}[\mathrm{R}_j]$	(33)
	for $i \geq 2$	$\frac{d[\mathrm{P}_i]}{dt} = \frac{k_\mathrm{tc}}{2}\sum_{j=1}^{i}[\mathrm{R}_j][\mathrm{R}_{i-j}] + k_\mathrm{td}[\mathrm{R}_i]\sum_{j=1}^{\infty}[\mathrm{R}_j]$	(34)

4.1.5.3. Model equations for solution homopolymerization via ARGET ATRP

Tables 9 and 10 show the model equations for polymerization via ARGET ATRP with tin(II) 2-ethylhexanoate, ascorbic acid or hydrazine as the reducing agent and copper-based catalysts. Table 9 consists of the zeroth, first, and second order moments definitions (see Table 1 in Section 3.1.1. for reference) applied to the set of equations presented in Table 8. Table 10 shows the molar balance for other relevant small chemical species; they are alkyl halide initiator, copper(II) halide complex, copper(I) catalyst, primary free radical, monomer, reducing agent (A), and oxidized reducing agent (A_{oxi}).

Table 9. Zeroth, first, and second order moments definitions for dormant, living, and dead chains molar balances.[a] Reprinted from [16].

Chemical specie	Moment order	Equation	
Dormant chain	Zeroth	$\frac{d\mu_{0,\mathrm{RX}}}{dt} = -k_{\mathrm{a}}\mu_{0,\mathrm{RX}}[(\mathrm{Cu^{I}L})\mathrm{X}] + k_{\mathrm{da}}\mu_{0,\mathrm{R}}[(\mathrm{Cu^{II}XL})\mathrm{X}]$	(35)
	First	$\frac{d\mu_{1,\mathrm{RX}}}{dt} = -k_{\mathrm{a}}\mu_{1,\mathrm{RX}}[(\mathrm{Cu^{I}L})\mathrm{X}] + k_{\mathrm{da}}\mu_{1,\mathrm{R}}[(\mathrm{Cu^{II}XL})\mathrm{X}]$	(36)
	Second	$\frac{d\mu_{2,\mathrm{RX}}}{dt} = -k_{\mathrm{a}}\mu_{2,\mathrm{RX}}[(\mathrm{Cu^{I}L})\mathrm{X}] + k_{\mathrm{da}}\mu_{2,\mathrm{R}}[(\mathrm{Cu^{II}XL})\mathrm{X}]$	(37)
Living chain	Zeroth	$\frac{d\mu_{0,\mathrm{R}}}{dt} = k_{\mathrm{p0}}[\mathrm{R}_0][\mathrm{M}] - (k_{\mathrm{tc}} + k_{\mathrm{td}})\mu_{0,\mathrm{R}}\mu_{0,\mathrm{R}} + k_{\mathrm{a}}\mu_{0,\mathrm{RX}}[(\mathrm{Cu^{I}L})\mathrm{X}] - k_{\mathrm{da}}\mu_{0,\mathrm{R}}[(\mathrm{Cu^{II}XL})\mathrm{X}]$	(38)
	First	$\frac{d\mu_{1,\mathrm{R}}}{dt} = k_{\mathrm{p0}}[\mathrm{R}_0][\mathrm{M}] + k_{\mathrm{p}}\mu_{0,\mathrm{R}}[\mathrm{M}] - (k_{\mathrm{tc}} + k_{\mathrm{td}})\mu_{1,\mathrm{R}}\mu_{0,\mathrm{R}} + k_{\mathrm{a}}\mu_{1,\mathrm{RX}}[(\mathrm{Cu^{I}L})\mathrm{X}] - k_{\mathrm{da}}\mu_{1,\mathrm{R}}[(\mathrm{Cu^{II}XL})\mathrm{X}]$	(39)
	Second	$\frac{d\mu_{2,\mathrm{R}}}{dt} = k_{\mathrm{p0}}[\mathrm{R}_0][\mathrm{M}] + k_{\mathrm{p}}(2\mu_{1,\mathrm{R}} + \mu_{0,\mathrm{R}})[\mathrm{M}] - (k_{\mathrm{tc}} + k_{\mathrm{td}})\mu_{2,\mathrm{R}}\mu_{0,\mathrm{R}} + k_{\mathrm{a}}\mu_{2,\mathrm{RX}}[(\mathrm{Cu^{I}L})\mathrm{X}] - k_{\mathrm{da}}\mu_{2,\mathrm{R}}[(\mathrm{Cu^{II}XL})\mathrm{X}]$	(40)
Dead chain	Zeroth	$\frac{d\mu_{0,\mathrm{P}}}{dt} = \left(\frac{k_{\mathrm{tc}}}{2} + k_{\mathrm{td}}\right)\mu_{0,\mathrm{R}}\mu_{0,\mathrm{R}}$	(41)
	First	$\frac{d\mu_{1,\mathrm{P}}}{dt} = (k_{\mathrm{tc}} + k_{\mathrm{td}})\mu_{1,\mathrm{R}}\mu_{0,\mathrm{R}}$	(42)
	Second	$\frac{d\mu_{2,\mathrm{P}}}{dt} = (k_{\mathrm{tc}} + k_{\mathrm{td}})\mu_{2,\mathrm{R}}\mu_{0,\mathrm{R}} + k_{\mathrm{tc}}\mu_{1,\mathrm{R}}\mu_{1,\mathrm{R}}$	(43)

[a] $\mu_{\mathrm{m,RX}}$, $\mu_{\mathrm{m,R}}$ and $\mu_{\mathrm{m,P}}$: $\mathrm{m^{th}}$ order moments for dormant, living and dead chains, respectively.

Eq. (49) is used to estimate the consumption of $\mathrm{Sn^{II}(eh)_2}$, $\mathrm{H_2asc}$, or $\mathrm{N_2H_4}$ while Eq. (50) is used to determine the formation of $\mathrm{Sn^{IV}(eh)_2X_2}$, dha, or $\mathrm{N_2}$ depending on the reducing agent considered. The ARGET mechanism proposed for all reducing agents studied have first-order kinetics to the copper(II) halide complex, as can be seen by Eqs. (47) and (48) (see Appendix A for details).

Table 10. Molar balance of other relevant small chemical species considered in the kinetic model of solution homopolymerization via ARGET ATRP.[a,b] Adapted from [16].

Chemical specie	Equation	
Alkyl halide initiator	$\frac{d[\mathrm{R_0X}]}{dt} = -k_{\mathrm{a0}}[\mathrm{R_0X}][(\mathrm{Cu^{I}L})\mathrm{X}] + k_{\mathrm{da0}}[\mathrm{R_0}][(\mathrm{Cu^{II}XL})\mathrm{X}]$	(44)
Primary free radical	$\frac{d[\mathrm{R_0}]}{dt} = k_{\mathrm{a0}}[\mathrm{R_0X}][(\mathrm{Cu^{I}L})\mathrm{X}] - k_{\mathrm{da0}}[\mathrm{R_0}][(\mathrm{Cu^{II}XL})\mathrm{X}] - k_{\mathrm{p0}}[\mathrm{R_0}][\mathrm{M}]$	(45)
Monomer	$\frac{d[\mathrm{M}]}{dt} = -k_{\mathrm{p0}}[\mathrm{M}][\mathrm{R_0}] - k_{\mathrm{p}}[\mathrm{M}]\mu_{0,\mathrm{R}}$	(46)
Copper(II) halide complex	$\frac{d[(\mathrm{Cu^{II}XL})\mathrm{X}]}{dt} = k_{\mathrm{a0}}[\mathrm{R_0X}][(\mathrm{Cu^{I}L})\mathrm{X}] + k_{\mathrm{a}}\mu_{0,\mathrm{RX}}[(\mathrm{Cu^{I}L})\mathrm{X}] - k_{\mathrm{da0}}[\mathrm{R_0}][(\mathrm{Cu^{II}XL})\mathrm{X}] - k_{\mathrm{da}}\mu_{0,\mathrm{R}}[(\mathrm{Cu^{II}XL})\mathrm{X}] - 2k_{\mathrm{r}}[\mathrm{A}][(\mathrm{Cu^{II}XL})\mathrm{X}]$	(47)[c]
	$\frac{d[(\mathrm{Cu^{II}XL})\mathrm{X}]}{dt} = k_{\mathrm{a0}}[\mathrm{R_0X}][(\mathrm{Cu^{I}L})\mathrm{X}] + k_{\mathrm{a}}\mu_{0,\mathrm{RX}}[(\mathrm{Cu^{I}L})\mathrm{X}] - k_{\mathrm{da0}}[\mathrm{R_0}][(\mathrm{Cu^{II}XL})\mathrm{X}] - k_{\mathrm{da}}\mu_{0,\mathrm{R}}[(\mathrm{Cu^{II}XL})\mathrm{X}] - 4k_{\mathrm{r}}[\mathrm{A}][(\mathrm{Cu^{II}XL})\mathrm{X}]$	(47)[d]
Copper(I) catalyst	$\frac{d[(\mathrm{Cu^{I}L})\mathrm{X}]}{dt} = -\frac{d[(\mathrm{Cu^{II}XL})\mathrm{X}]}{dt}$	(48)
Reducing agent	$\frac{d[\mathrm{A}]}{dt} = -k_{\mathrm{r}}[\mathrm{A}][(\mathrm{Cu^{II}XL})\mathrm{X}]$	(49)
Oxidized reducing agent	$\frac{d[\mathrm{A_{oxi}}]}{dt} = -\frac{d[\mathrm{A}]}{dt}$	(50)

[a]A: reducing agent (i.e., $Sn^{II}(eh)_2$, H_2asc and N_2H_4 when tin(II) 2-ethylhexanoate, ascorbic acid and hydrazine used, respectively); A_{oxi}: oxidized reducing agent (i.e., $Sn^{IV}(eh)_2X_2$, dha and N_2 when tin(II) 2-ethylhexanoate, ascorbic acid and hydrazine used, respectively). [b]The equations presented consist in a pseudo-homogeneous model when H_2asc and N_2H_4 are considered as reducing agent, once H_2asc generally have limited solubility in the reaction media [53] and N_2 is gaseous. [c]Equation valid for both $Sn^{II}(eh)_2$ and H_2asc as reducing agent. [d]Equation valid when N_2H_4 as reducing agent.

4.1.6. Kinetic modeling validation (Part I)

The proposed model was validated using the experimental data of solution ARGET ATRP of styrene (St) at 110 °C published by Aitchison et al. [40] when $Sn^{II}(eh)_2$ is employed as the reducing agent (Table 11, entry 1), solution ARGET ATRP of methyl acrylate (MA) at 60 °C published by Min et al. [53] when H_2asc is considered (Table 11, entry 2), and solution ARGET ATRP of butyl acrylate (BA) at 60°C published by Matyjaszewski et al. [21] for N_2H_4 (Table 11, entry 3).

Concerning entries 1, 2 and 3, ethyl 2-bromoisobutyrate (EBiB) was used as alkyl halide initiator and anisole as the solvent. For the entries 1 and 2 copper(II) bromide/tris[2-(dimethylamino)ethyl]amine ($CuBr_2/Me_6TREN$) was considered as copper(II) halide complex (activator), while for entry 3 copper(II) chloride/tris(2-pyridylmethyl)amine ($CuCl_2$/TPMA) was used in the experiments. The initial stoichiometry ratios of the concentrations used in the simulations for the cases validated are depicted in Table 11.

Table 11. Initial stoichiometry ratios of the concentrations used in the simulations for solution homopolymerizations via ARGET ATRP. Adapted from [16].

Entry	$[M]_0:[R_0X]_0:[(Cu^{II}XL)X]_0:[A]_0$	Reference
1[a]	300:1:0.015:0.15	[40]
2[b]	400:1:0.01:0.1	[53]
3[c]	200:1.28:0.01:0.1	[21]

[a]$[M]_0:[R_0X]_0:[(Cu^{II}XL)X]_0:[A]_0$ = $[St]_0:[EBiB]_0:[CuBr_2/Me_6TREN]_0:[Sn^{II}(eh)_2]_0$, with $[St]_0$ = 5.80 mol·L^{-1}. [b]$[M]_0:[R_0X]_0:[(Cu^{II}XL)X]_0:[A]_0$ = $[MA]_0:[EBiB]_0:[CuBr_2/Me_6TREN]_0:[H_2asc]_0$, with $[MA]_0$ = 7.00 mol·L^{-1}. [c]$[M]_0:[R_0X]_0:[(Cu^{II}XL)X]_0:[A]_0$ = $[BA]_0:[EBiB]_0:[CuCl_2/TPMA]_0:[N_2H_4]_0$, with $[BA]_0$ = 5.88 mol·L^{-1}.

In the developed kinetic model, the transition metal salt is assumed to be completely complexed with the ligand at the beginning of the reaction. Consequently, the deactivator initial concentration is considered equal to the one adopted for the transition metal salt in the experimental data validated (i.e., transition metal salt is the limiting reactant). The mechanism associated with the complexation process is not discussed in this study (i.e., ligands are not directly involved in the developed kinetic model). Another additional point is that the solvent is assumed to be chemically inert.

Table 12 shows the kinetic rate constants for propagation and termination applied to the polymerizations of St, MA and BA; monomers used when $Sn^{II}(eh)_2$, H_2asc and N_2H_4 are considered as reducing agents in solution ARGET ATRP, respectively.

By the case studies considered in the model validation, there are no suitable values for ATRP equilibrium constant in the literature under polymerization conditions used in our work. For the ARGET mechanism, the situation is even more restricted, since new reaction kinetics (Eqs. (20), (23) and (27)) are being proposed in this research. Therefore, the kinetic rate constants for such reaction steps are new and were obtained via nonlinear regression by Levenberg–Marquardt algorithm, as previously discussed in Section 3.2.2..

Table 12. Kinetic rate constants applied to the solution polymerizations of St, MA, and BA via ARGET ATRP.[a] Adapted from [16].

Monomer	Kinetic rate constant (L·mol^{-1}·s^{-1})		Reference
St	$k_p = 10^{7.630} \cdot \exp(-3908/T)$		[66]
	$k_t = \begin{cases} DP_n^{-0,51} \cdot [\exp(23.7 - 1117/T)], & DP_n \leq 30 \\ 0.3041 \cdot DP_n^{-0,16} \cdot [\exp(23.7 - 1117/T)], & DP_n > 30 \end{cases}$		[67][b]
	$k_{tc} = k_t$		[68]
	$k_{td} = 0$		[68]
MA	$k_p = \exp(16.46 - 2080/T)$		[69]
	$k_t = 10^{(9.48-454/T)}$		[70]
	$k_{tc} = 0.9 \cdot k_t$		[71]
	$k_{td} = 0.1 \cdot k_t$		[71]
BA	$k_p = 2.24 \times 10^7 \exp(-2151/T)$		[72]
	$k_t = \begin{cases} DP_n^{-0,85} \cdot [1.3 \times 10^{10} \cdot \exp(-1010/T)], & DP_n \leq 30 \\ 0.1173 \cdot DP_n^{-0,22} \cdot [1.3 \times 10^{10} \cdot \exp(-1010/T)], & DP_n > 30 \end{cases}$		[73][b]
	$k_{tc} = 0.9 \cdot k_t$		[71]
	$k_{td} = 0.1 \cdot k_t$		[71]

[a]T: Temperature (K). [b]The dependence of the chain length in k_t was adapted and, in this study, it is based on the number-average chain length (DP_n) for St and BA.

4.1.7. Results and discussion (Part I)

4.1.7.1. Model validation (Part I)

As shown in Figs. 6, 7 and 8, the model agrees well with the experimental data of the entries 1, 2 and 3 (see Table 11 for reference details), respectively. The experimental data error bars were not represented since the values were extracted digitally with the WebPlotDigitizer software, where the uncertainty of the measurement can be neglected.

The profiles of predicted values and percent deviation (Eq. (51)) vs. experimental values were obtained for the following parameters: (i) monomer conversion, (ii) $\ln[M]_0/[M]$, (iii) number-average molecular weight (M_n), and (iv) dispersity (Đ).

$$\text{Percent deviation (\%)} = \left(\frac{var_{sim.(t)} - var_{exp.(t)}}{var_{exp.(t)}}\right) \times 100 \quad (51)^a$$

[a]Percent deviation (%): percentual deviation between simulated and experimental data of the variable *var* at the time *t*.

In order to quantify the effectiveness of the fitting, a linear regression was performed to correlate both predicted and experimental values (i.e., the values were adjusted to the linear model "y = a·x + b", wherein "y" and "x" correspond to the predicted and experimental values, respectively). By the entries 1, 2 and 3 results (c.f., Figs. 6c, 6d, 6e, 6f, 7c, 7d, 7e, 7f, 8c, 8d, 8e, and 8f), it is possible to note that the coefficient of determination values (i.e., R^2) for all parameters are close to 1, what implies that there is a strong relationship between the predicted and experimental values.

Furthermore, R^2 values presented in Figs. 6f, 7f, and 8f also indicate an observed standard, where the weakest relationship between the predicted and experimental values are related to the dispersity variable. Figs. 6f, 7f, and 8f show that, in great part of reaction time, dispersity experimental data remains practically constant. However, such a trend is not verified in the predicted data, which varies. Thus, such a deviation in the behavior of these two data sources could explain a weaker relationship for dispersity than other analyzed variables, although it has been obtained the smallest percent deviation values.

The estimated values of $\ln(k_r)$, $\ln(k_a)$, and $\ln(k_{da})$ (see Table 4 footnotes for details) obtained via nonlinear regression for the entries studied are presented in Table 13, considering 95% confidence level.

Table 13. Estimated natural logarithm of the kinetic rate constants for experimental cases validated of solution homopolymerization via ARGET ATRP.[a,b] Adapted from [16].

Step	Parameter	Estimated values		
		Entry 1[c]	Entry 2[d]	Entry 3[e]
		Mean ± error	Mean ± error	Mean ± error
ARGET mechanism	$\ln(k_r)$ ($L \cdot mol^{-1} \cdot s^{-1}$)	-3.23 ± 0.84	-5.58 ± 0.21	-7.23 ± 0.12
ATRP equilibrium	$\ln(k_a)$ ($L \cdot mol^{-1} \cdot s^{-1}$)	4.41 ± 3.49	8.81 ± 8.42	8.54 ± 0.56
	$\ln(k_{da})$ ($L \cdot mol^{-1} \cdot s^{-1}$)	16.60 ± 1.04	17.46 ± 0.52	18.08 ± 0.37

[a]It was considered $k_a = k_{a0} = k_{a1}$ and $k_{da} = k_{da0} = k_{da1}$ in the model validation. [b]The values presented lie within the estimated 95% confidence interval. [c]Solution ARGET ATRP of St with $CuBr_2$/Me_6TREN and $Sn^{II}(eh)_2$ carried out at 110 °C (Table 11, entry 1). [d]Solution ARGET ATRP of MA with $CuBr_2$/Me_6TREN and H_2asc carried out at 60 °C (Table 11, entry 2). [e]Solution ARGET ATRP of BA with $CuCl_2$/TPMA and N_2H_4 carried out at 60 °C (Table 11, entry 3).

According to Table 13, the best fit for the St/EBiB/$CuBr_2$/Me_6TREN/$Sn^{II}(eh)_2$ system at 110°C was $k_r = 0.04$ $L \cdot mol^{-1} \cdot s^{-1}$, $k_a = 82.2$ $L \cdot mol^{-1} \cdot s^{-1}$ and $k_{da} = 1.6 \times 10^7$ $L \cdot mol^{-1} \cdot s^{-1}$, wherein $K_{ATRP} = k_a/k_{da} = 5 \times 10^{-6}$. In addition, for the MA/EBiB/$CuBr_2$/Me_6TREN/H_2asc system at 60°C best results were obtained when employed $k_r = 0.0038$ $L \cdot mol^{-1} \cdot s^{-1}$, $k_a = 6700.9$ $L \cdot mol^{-1} \cdot s^{-1}$ and $k_{da} = 3.8 \times 10^7$ $L \cdot mol^{-1} \cdot s^{-1}$, wherein $K_{ATRP} = k_a/k_{da} = 1.8 \times 10^{-4}$. The parameters adjusted to experimental data for the the BA/EBiB/$CuCl_2$/TPMA/N_2H_4 system at 60°C were $k_r = 0.00072$ $L \cdot mol^{-1} \cdot s^{-1}$, $k_a = 5115.3$ $L \cdot mol^{-1} \cdot s^{-1}$ and $k_{da} = 7.1 \times 10^7$ $L \cdot mol^{-1} \cdot s^{-1}$, wherein $K_{ATRP} = k_a/k_{da} = 7.2 \times 10^{-5}$.

From the Table 13, at 95% confidence level, the errors of $\ln(k_a)$ are more significant than the ones obtained for $\ln(k_r)$ and $\ln(k_{da})$, a trend highlighted for the entries 1 and 2; which implies that k_a is a less sensitive (i.e., more robust) kinetic parameter than the others analyzed (more details when Figs. 16, 17 and 18 were discussed in the Section 4.1.7.3.1.). A lower confidence interval of such kinetic rate constants could be achieved if a larger sample of experimental data were available and information about their variability also were known.

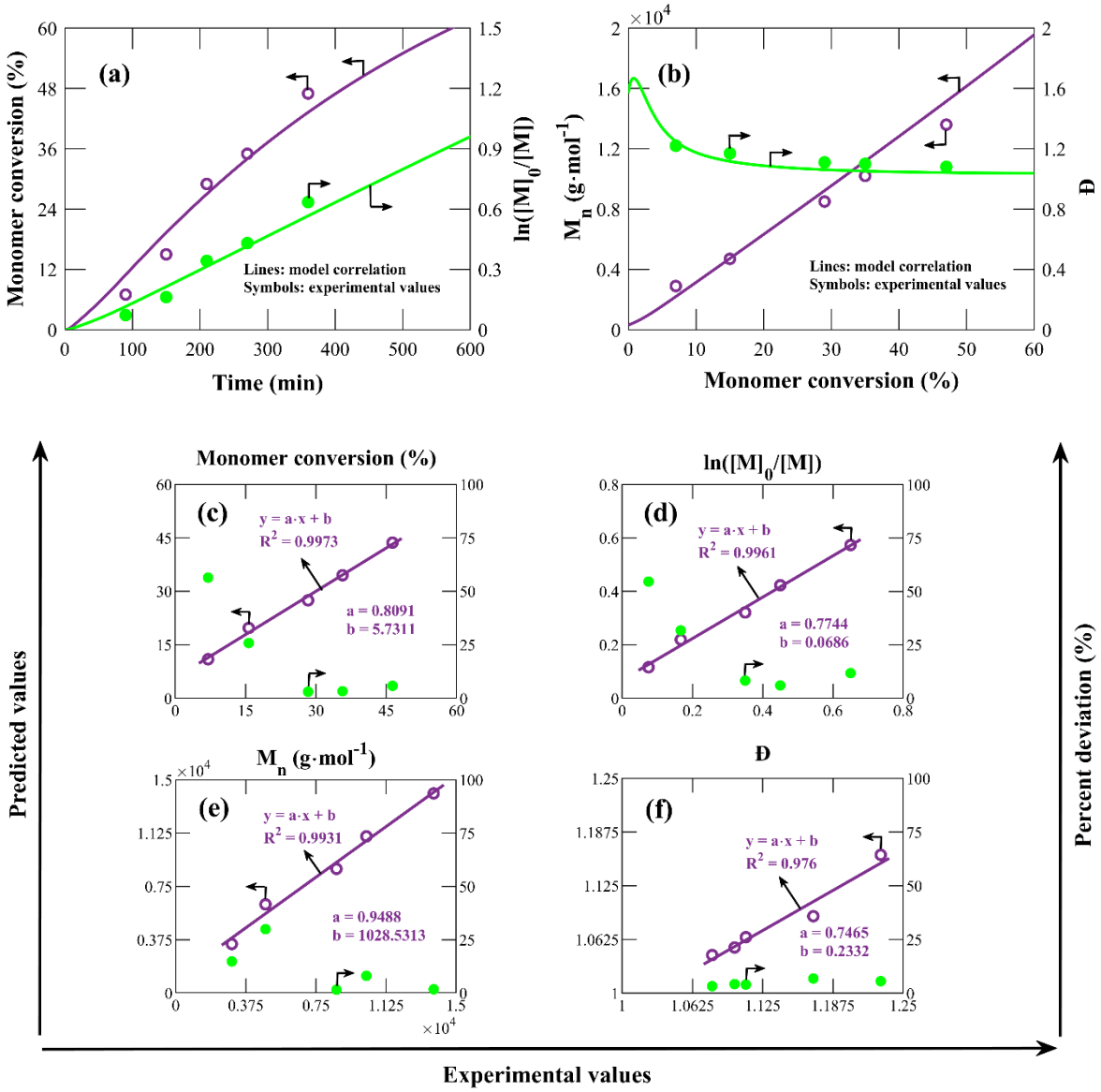

Fig. 6. Model validation for solution ARGET ATRP of St with $CuBr_2$/Me_6TREN and $Sn^{II}(eh)_2$ (Table 11, entry 1). (a) Monomer conversion (left) and $\ln[M]_0/[M]$ (right) vs. reaction time, (b) number-average molecular weight (M_n) (left) and dispersity (Đ) (right) vs. monomer conversion. Predicted values (left) and percent deviation (right) vs. experimental values of (c) monomer conversion, (d) $\ln[M]_0/[M]$, (e) number-average molecular weight (M_n), and (f) dispersity (Đ). Simulation at T = 110 °C, $[St]_0$ = 5.80 mol·L^{-1}, $[St]_0$:$[EBiB]_0$:$[CuBr_2/Me_6TREN]_0$:$[Sn^{II}(eh)_2]_0$ = 300:1:0.015:0.15, based on kinetic parameters from Tables 12 and 13. Experimental values of reference [40]. Adapted from [16].

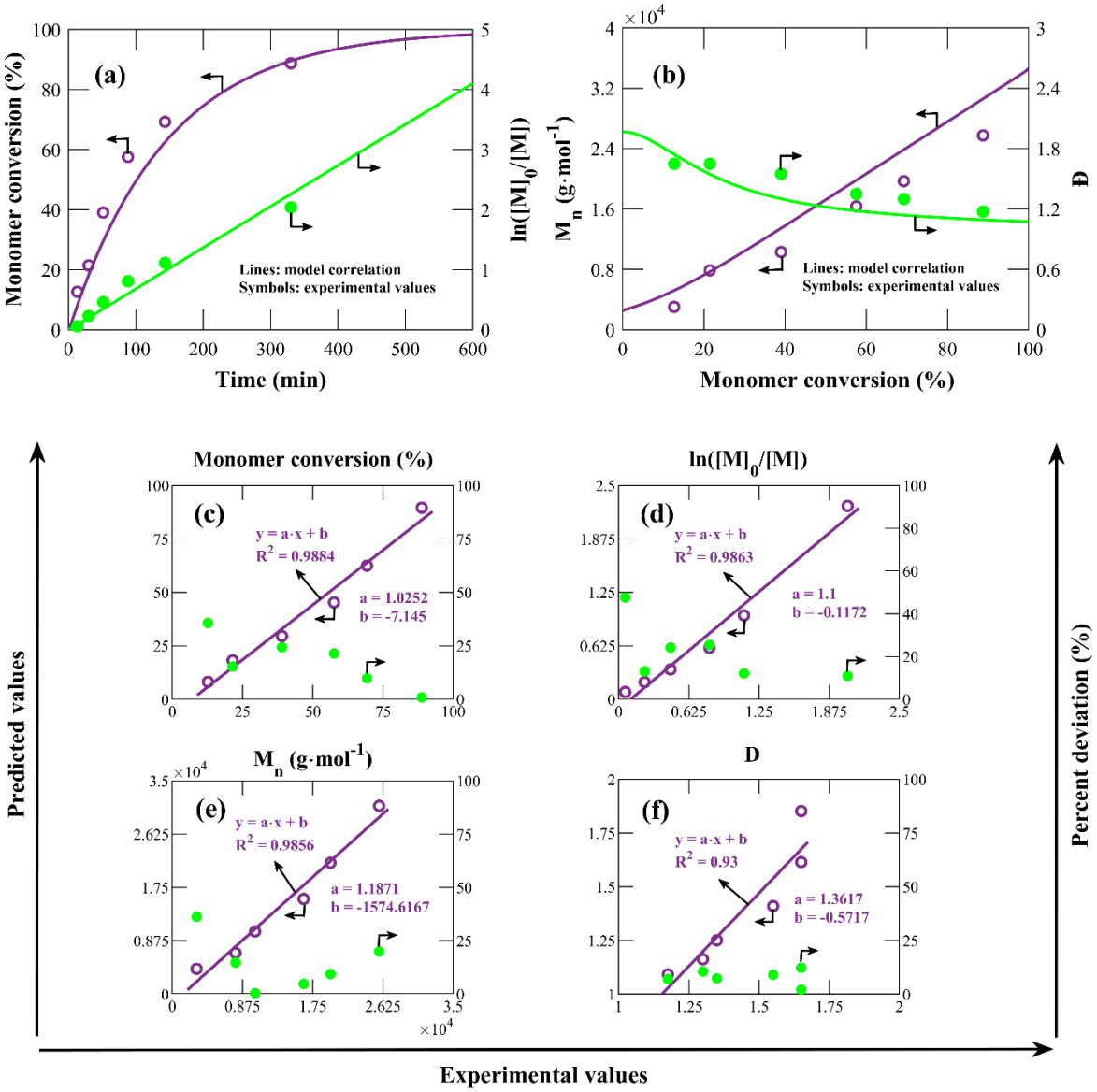

Fig. 7. Model validation for solution ARGET ATRP of MA with $CuBr_2$/Me_6TREN and H_2asc (Table 11, entry 2). (a) Monomer conversion (left) and $\ln[M]_0/[M]$ (right) vs. reaction time, (b) number-average molecular weight (M_n) (left) and dispersity (Đ) (right) vs. monomer conversion. Predicted values (left) and percent deviation (right) vs. experimental values of (c) monomer conversion, (d) $\ln[M]_0/[M]$, (e) number-average molecular weight (M_n), and (f) dispersity (Đ). Simulation at T = 60 °C, $[MA]_0$ = 7.00 mol·L^{-1}, $[MA]_0$:$[EBiB]_0$:$[CuBr_2/Me_6TREN]_0$:$[H_2asc]_0$ = 400:1:0.01:0.1, based on kinetic parameters from Tables 12 and 13. Experimental values of reference [53]. Adapted from [16].

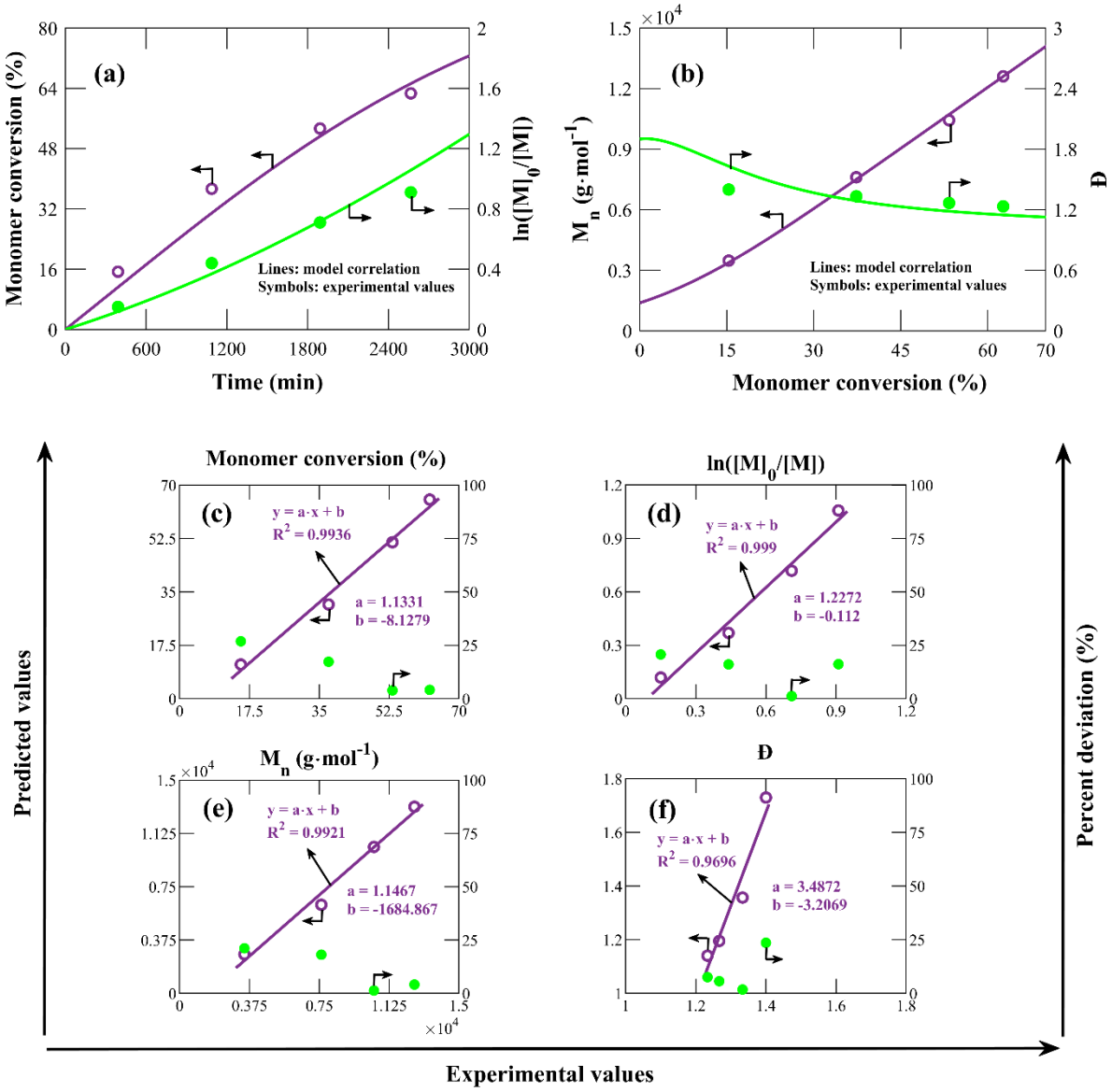

Fig. 8. Model validation for solution ARGET ATRP of BA with $CuCl_2$/TPMA and N_2H_4 (Table 11, entry 3). (a) Monomer conversion (left) and $\ln[M]_0/[M]$ (right) vs. reaction time, (b) number-average molecular weight (M_n) (left) and dispersity (Đ) (right) vs. monomer conversion. Predicted values (left) and percent deviation (right) vs. experimental values of (c) monomer conversion, (d) $\ln[M]_0/[M]$, (e) number-average molecular weight (M_n), and (f) dispersity (Đ). Simulation at T = 60 °C, $[BA]_0$ = 5.88 mol·L^{-1}, $[BA]_0$:$[EBiB]_0$:$[CuCl_2/TPMA]_0$:$[N_2H_4]_0$ = 200:1.28:0.01:0.1, based on kinetic parameters from Tables 12 and 13. Experimental values of reference [21].

Considering comparable ARGET mechanisms in the literature, Payne et al. [31, 32] studied the BMA/EBiB/$CuBr_2$/TPMA/$Sn^{II}(eh)_2$ system at 70°C, wherein BMA refers to butyl methacrylate. By kinetic modeling and simulation, these authors obtained k_r = 0.3 and 1 $L \cdot mol^{-1} \cdot s^{-1}$ for the reactions represented by Eqs. (19) and (20) respectively, when $Sn^{II}(eh)_2$ is used as a reducing agent (herein represented by k_{r1} = 0.3 $L \cdot mol^{-1} \cdot s^{-1}$ and k_{r2} = 1 $L \cdot mol^{-1} \cdot s^{-1}$, respectively). Since the tin(III)-based compounds are unstable and Eq. (19) is the rate-determining step as discussed, thus, the ratio k_{r2}/k_{r1} should be higher than the one reported. Nonetheless, it would be also expected that k_{r1} would be lower than the value of k_r obtained in this work (i.e., k_r = 0.04 $L \cdot mol^{-1} \cdot s^{-1}$), because a higher reaction temperature is considered in this work (i.e., 110 °C).

Ascorbic acid, H_2asc; has limited solubility in the reaction medium under polymerization conditions, as reported by Min et al. [53]. Thus, the kinetic rate constants adjusted in this work are not intrinsic to the global reaction assumed for ascorbic acid oxidation as manifested in Eq. (25), since the reaction system is heterogeneous and the developed model is applied to homogeneous systems. Therefore, in the optimization process, what is determined is the product of the solubility coefficient of ascorbic acid under the polymerization conditions (C_s) and the kinetic rate constant intrinsic of the reaction considered (k_r*) (i.e., $k_r = C_s \cdot k_r$*). A similar discussion can be done for the BA/EBiB/$CuCl_2$/TPMA/N_2H_4 system, since the oxidized reducing agent is N_2, which is gaseous.

In the literature, Tang et al. [10] experimentally obtained k_a = 227.8 $L \cdot mol^{-1} \cdot s^{-1}$ (22 °C) and $K_{ATRP} = k_a/k_{da} = 1.5 \times 10^{-4}$ (35 °C) for the ATRP system of EBiB/Cu^I/Me_6TREN and acetonitrile as a solvent. For the ATRP system of EBiB/Cu^I/TPMA in acetonitrile, Tang et al. [10] also reported k_a = 31.2 $L \cdot mol^{-1} \cdot s^{-1}$ (22 °C) and $K_{ATRP} = k_a/k_{da} = 9.6 \times 10^{-6}$ (35 °C).

Neglecting effects of solvent, note that both k_a and K_{ATRP} obtained for entries 2 and 3 agree with the experimental trends reported by Tang et al. [10], since the higher reaction temperature verified (i.e., 60 °C), the higher values for such kinetic parameters should be expected. However, such a trend previously highlighted is not verified for the entry 1 at 110 °C.

In RDRP processes, the profile of $\ln([M]_0/[M])$ vs. time is typically a straight line (see Figs. 6a, 7a and 8a). For entry 1, the experimental data show some delay (i.e., an induction time is observed), as pointed out by Aitchison et al. [40]. According to these authors, the delay can be an indication of oxygen impurities present in the reaction system, oxidizing Cu^I to Cu^{II} (see Fig. 6a). Hence, the deviations not expected for k_a and K_{ATRP} values for entry 1 could be

related with this experimental observation, since such kinetic parameters influence the rate of polymerization (more details when Figs. 16, 17 and 18 were discussed in the Section 4.1.7.3.1.).

However, note that for entry 3 the model deviates from the expected trend. According to Matyjaszewski et al. [2], such a behavior obtained can be associated with a slow initiation of the polymerization process. Hence, the deviation in the profile of $\ln([M]_0/[M])$ vs. time for the entry 3 could be associated with some side reactions between Cu^{II}-based catalysts and N_2H_4 neglected in the kinetic model [62–64].

The chemical nature of the alkyl halide (and, consequently, of the monomer too) influences the K_{ATRP} value [8]. According to the literature, under comparable conditions (i.e., same temperature, pressure, media/solvent, and catalyst), K_{ATRP} should be dependent only on the bond dissociation energy of the alkyl halide, as mentioned in Section 2.1.1. Even at a lower temperature, the best fit leads to higher values for K_{ATRP} in the entries 2 and 3. Such an observation is explained by a higher bond dissociation energy observed for MA and BA [8].

The number-average molecular weight data considered in the model validation of the entries 1, 2 and 3 were obtained by gel permeation chromatography (GPC) using poly(styrene) standards. The inherent deviations between the model and experimental data (see Figs. 6b, 7b and 8b) can be associated with the different Mark-Houwink parameters (K and α) observed for poly(styrene) (PSt), poly(methyl acrylate) (PMA) and poly(butyl acrylate) (PBA).

Based on the empirical Mark-Houwink-Kuhn-Sakurada equation, it is possible to obtain the relation between of a specific molecular weight of "Polymer 2" ($M_{n,Polymer\ 2}$) which elutes at the same time that a determined molecular weight of "Polymer 1" ($M_{n,Polymer\ 1}$), represented by Eq. (52) [75].

$$\log\left(M_{n,Polymer\ 2}\right) = \frac{\log\left(\frac{K_{Polymer\ 1}}{K_{Polymer\ 2}}\right)}{1+\alpha_{Polymer\ 2}} + \frac{1+\alpha_{Polymer\ 1}}{1+\alpha_{Polymer\ 2}} \cdot \log\left(M_{n,Polymer\ 1}\right) \quad (52)^a$$

[a] $M_{n,Polymer\ 1}$: number-average molecular weight of polymer 1 that elutes in a determined time t; $M_{n,Polymer\ 2}$: number-average molecular weight of polymer 2 that elutes at same time t that a determined molecular weight of polymer 1; $K_{Polymer\ 1}$ and $\alpha_{Polymer\ 1}$: Mark-Houwink parameters for polymer 1; $K_{Polymer\ 2}$ and $\alpha_{Polymer\ 2}$: Mark-Houwink parameters for polymer 2.

Considering Mark-Houwink parameters available in the literature and obtained under comparable conditions (i.e., at the same temperature and solvent) for PSt (K_{PSt} = 16.2×10^{-3} dm^3·kg^{-1} and α_{PSt} = 0.71) [75], PMA (K_{PMA} = 7.88×10^{-3} dm^3·kg^{-1} and α_{PMA} = 0.885) [76] and PBA (K_{PBA} = 8.57×10^{-3} dm^3·kg^{-1} and α_{PBA} = 0.865) [76], an estimative of the deviation found in the experimental data of PMA and PBA, based on Eq. (50), is depicted in Fig. 9.

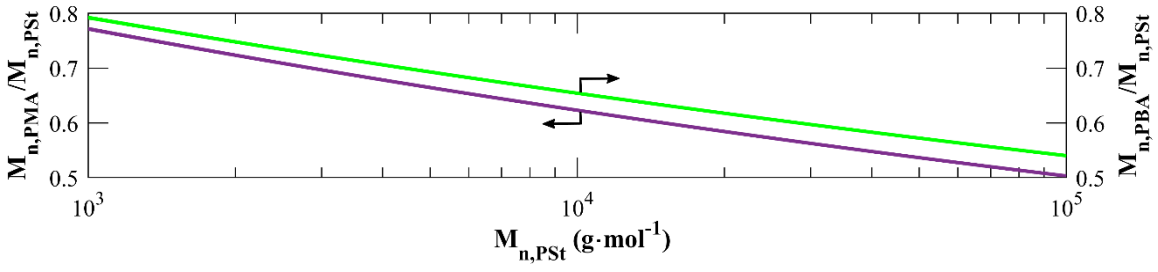

Fig. 9. Dependence of the ratio of the molecular weight of the PMA and PBA to the molecular weight of PSt at constant retention time on the molecular weight of PSt.

From the profile presented in Fig. 9, the molecular weights obtained via GPC should be higher than the ones considered in the model validation for PMA and PBA. This trend could be enough to explaining the better fit for PSt compared to PMA (see Fig. 6b and 7b). However, such a trend also expected when compared PSt with PBA molecular weights was not observed (see Fig. 6b and 8b). Since the Mark-Houwink parameters were obtained at 298 K with tetrahydrofuran for both PMA and PBA, which is the same condition of GPC analysis to obtain the molecular weights for such polymers, the adjustment for PBA should be worse than the one obtained.

4.1.7.2. Model prediction (Part I)

After the model validation process, the concentration profiles of the leading chemical species considered in the kinetic model can be obtained for the experimental cases studied. Figs. 10, 11 and 12 present the reactants consumption and products formation (other than polymer chains) throughout the polymerization for the entries 1, 2 and 3, respectively.

Since H_2asc oxidation is limited by diffusion because of its low solubility in the reaction medium, its concentration exhibits slower decay than that of $Sn^{II}(eh)_2$ and N_2H_4 (c.f., A and A_{oxi} profiles in Figs. 10, 11 and 12). Another experimental observation that reinforces this trend is the presence of oxygen impurities in the solution ARGET ATRP of St with $CuBr_2$/Me_6TREN and $Sn^{II}(eh)_2$. A more significant amount of $Sn^{II}(eh)_2$ needs to be consumed to produce Cu^I species, which participates as a reactant in both ATRP equilibrium and undesirable side reaction.

The reducing agent consumption is based on the adjusted k_r values (i.e., k_r = 0.04 L·mol^{-1}·s^{-1} for entry 1, k_r = 0.0038 L·mol^{-1}·s^{-1} for entry 2 and k_r = 0.00072 L·mol^{-1}·s^{-1} for entry 3). In addition to a lower temperature of polymerization, the abovementioned observations justify the lower values of k_r obtained for entries 2 and 3.

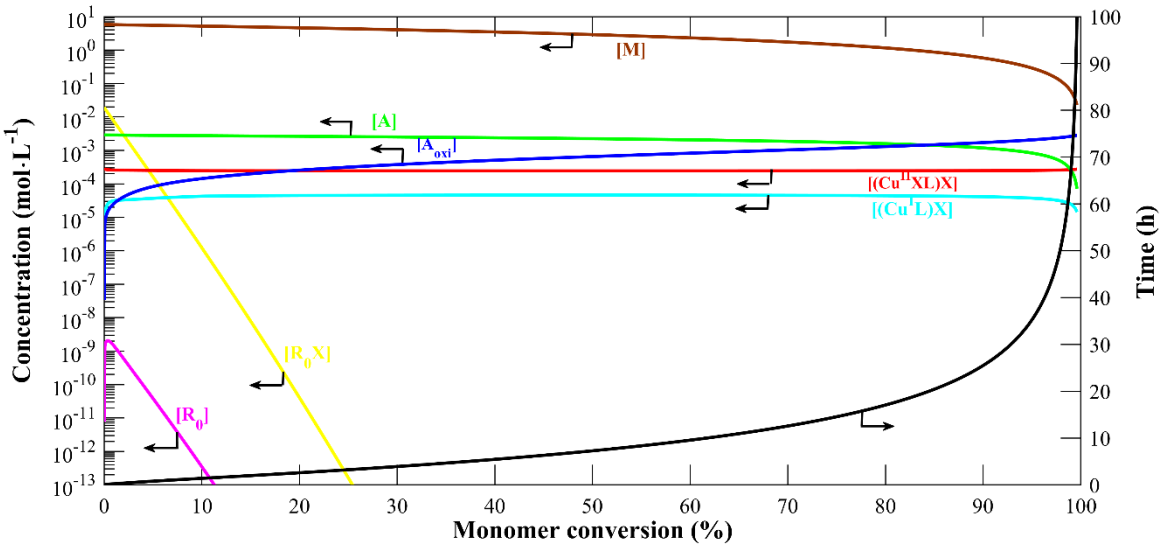

Fig. 10. Concentration profiles of the main chemical species considered in the kinetic model (other than polymer chains) (left) and reaction time (right) vs. monomer conversion for solution ARGET ATRP of St with $CuBr_2$/Me_6TREN and $Sn^{II}(eh)_2$ (Table 11, entry 1). Simulation at T = 110 °C, $[St]_0$ = 5.80 mol·L^{-1}, $[St]_0$:$[EBiB]_0$:$[CuBr_2/Me_6TREN]_0$:$[Sn^{II}(eh)_2]_0$ = 300:1:0.015:0.15, based on kinetic parameters from Tables 12 and 13. Reprinted from [16].

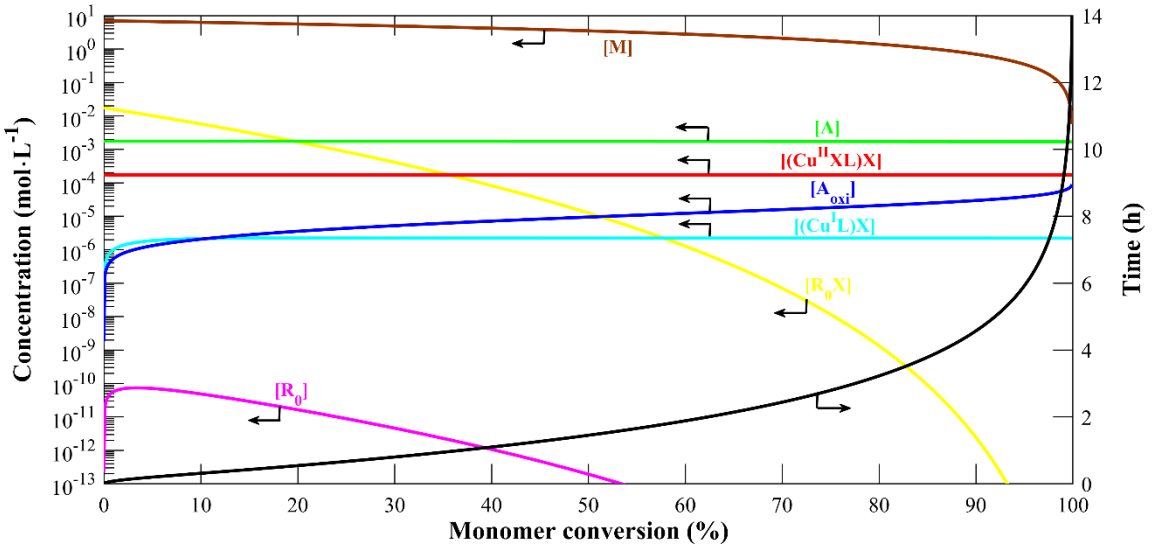

Fig. 11. Concentration profiles of the main chemical species considered in the kinetic model (other than polymer chains) (left) and reaction time (right) vs. monomer conversion for solution ARGET ATRP of MA with $CuBr_2$/Me_6TREN and H_2asc (Table 11, entry 2). Simulation at T = 60 °C, $[MA]_0$ = 7.00 mol·L^{-1}, $[MA]_0$:$[EBiB]_0$:$[CuBr_2/Me_6TREN]_0$:[H_2asc]$_0$ = 400:1:0.01:0.1, based on kinetic parameters from Tables 12 and 13. Reprinted from [16].

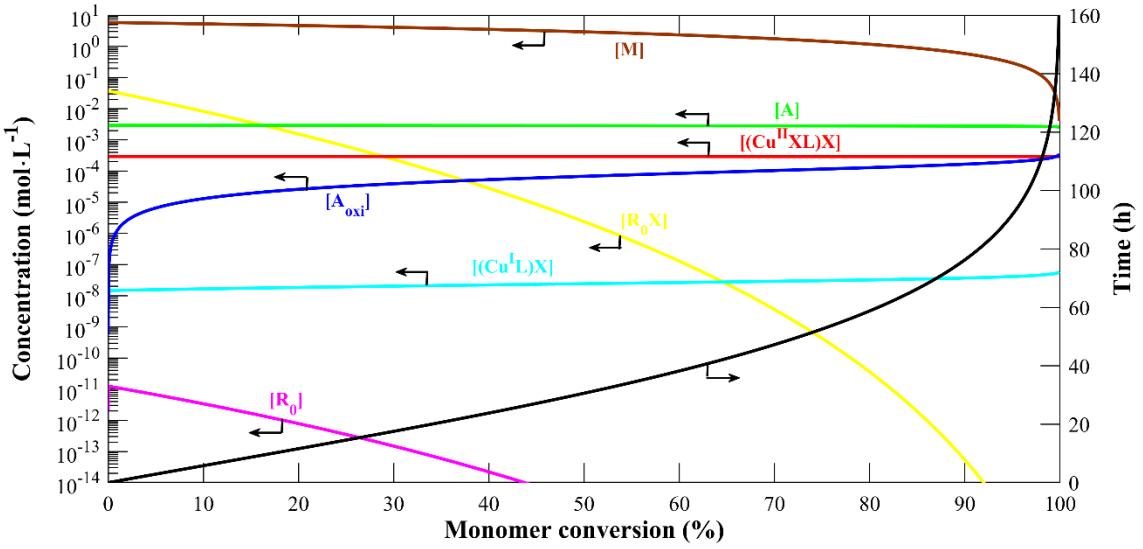

Fig. 12. Concentration profiles of the main chemical species considered in the kinetic model (other than polymer chains) (left) and reaction time (right) vs. monomer conversion for solution ARGET ATRP of BA with $CuCl_2$/TPMA and N_2H_4 (Table 11, entry 3). Simulation at T = 60 °C, $[BA]_0$ = 5.88 mol·L^{-1}, $[BA]_0$:$[EBiB]_0$:$[CuCl_2/TPMA]_0$:$[N_2H_4]_0$ = 200:1.28:0.01:0.1, based on kinetic parameters from Tables 12 and 13.

The EBiB consumption rate is faster for the entry 1 (c.f., R_0X profile in Figs. 10, 11 and 12). Likewise, $Cu^{II}Br_2$/ME_6TREN and $Cu^{II}Cl_2$/TPMA depict a similar behavior (c.f., $(Cu^{II}XL)X$ and $(Cu^{I}L)X$ profiles in Figs. 10, 11 and 12). Both observations can be related to the K_{ATRP} values adjustments (i.e., $K_{ATRP} = 5\times10^{-6}$ for entry 1, $K_{ATRP} = 1.8\times10^{-4}$ for entry 2 and $K_{ATRP} = 7.2\times10^{-5}$ for entry 3).

The zeroth-order moment of a compound corresponds to its molar concentration. Considering the whole extension of the monomer consumption, the concentration of dormant species is higher than those of radical and dead polymer chains (c.f., $\mu_{0,RX}$ with $\mu_{0,R}$ and $\mu_{0,P}$ curves in Figs. 13, 14 and 15 for entries 1, 2 and 3). Such a comparison can also be emphasized by the high percentage of functionalized polymer chains, which guarantees the control of the systems studied.

Furthermore, the first-order moment of a polymer corresponds with its constituent monomer concentration. By the model prediction for both cases studied in this work, the amounts of monomers in dead chains increase in a faster rate if compared to dormant and living chains (c.f., $\mu_{1,P}$ with $\mu_{1,RX}$ and $\mu_{1,R}$ curves in Figs. 13, 14 and 15 for entries 1, 2 and 3).

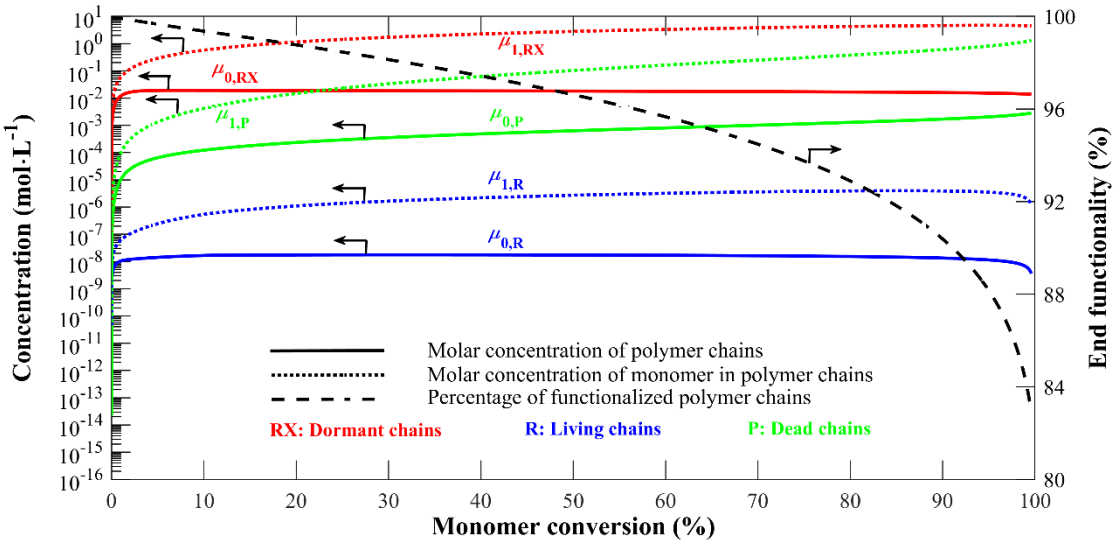

Fig. 13. Prediction of zeroth and first-order moments for dormant, living, and dead chains (left) and percentage of functionalized polymer chains (right) vs. monomer conversion for solution ARGET ATRP of St with $CuBr_2$/Me_6TREN and $Sn^{II}(eh)_2$ (Table 11, entry 1). Simulation at T = 110 °C, $[St]_0$ = 5.80 mol·L^{-1}, $[St]_0$:$[EBiB]_0$:$[CuBr_2/Me_6TREN]_0$:$[Sn^{II}(eh)_2]_0$ = 300:1:0.015:0.15, based on kinetic parameters from Tables 12 and 13. Reprinted from [16].

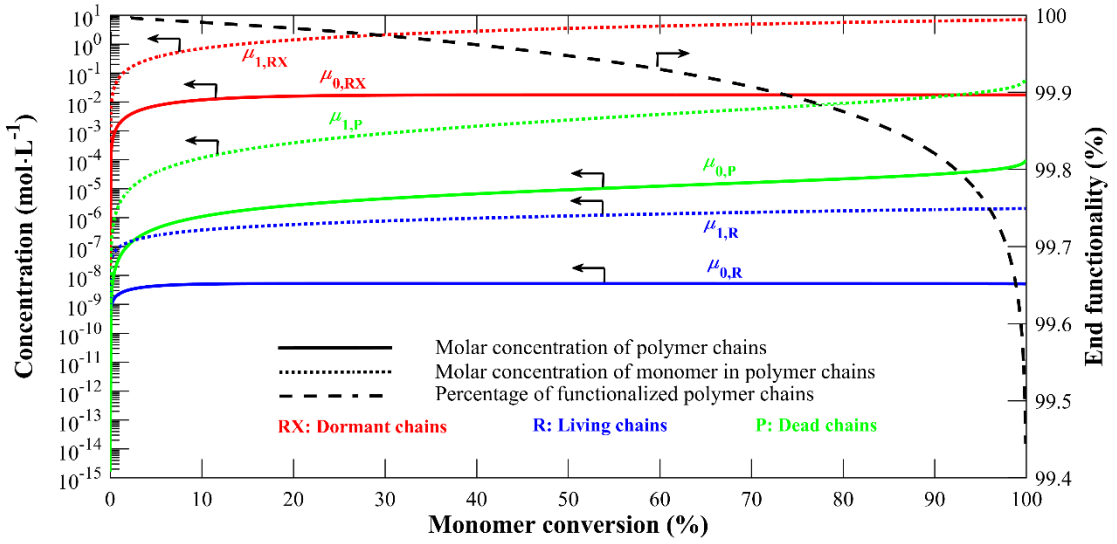

Fig. 14. Prediction of zeroth and first-order moments for dormant, living, and dead chains (left) and percentage of functionalized polymer chains (right) vs. monomer conversion for solution ARGET ATRP of MA with $CuBr_2$/Me_6TREN and H_2asc (Table 11, entry 2). Simulation at T = 60 °C, $[MA]_0$ = 7.00 mol·L^{-1}, $[MA]_0$:$[EBiB]_0$:$[CuBr_2/Me_6TREN]_0$:$[H_2asc]_0$ = 400:1:0.01:0.1, based on kinetic parameters from Tables 12 and 13. Reprinted from [16].

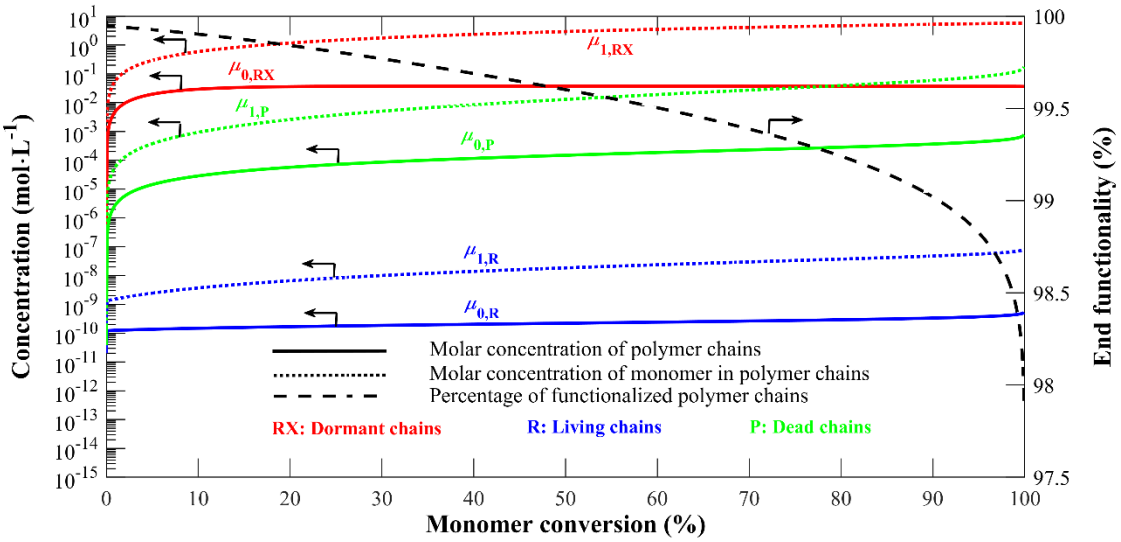

Fig. 15. Prediction of zeroth and first-order moments for dormant, living, and dead chains (left) and percentage of functionalized polymer chains (right) vs. monomer conversion for solution ARGET ATRP of BA with $CuCl_2$/TPMA and N_2H_4 (Table 11, entry 3). Simulation at T = 60 °C, $[BA]_0$ = 5.88 mol·L^{-1}, $[BA]_0$:$[EBiB]_0$:$[CuCl_2/TPMA]_0$:$[N_2H_4]_0$ = 200:1.28:0.01:0.1, based on kinetic parameters from Tables 12 and 13.

As can be seen in Figs. 10, 11, 12, 13, 14 and 15, the order of magnitude of the concentration values are significantly different. This trend previously noted justifies the choice of the Gear's Method to solve the model equations, emphasizing the stiffness of the system.

4.1.7.3. Analysis of critical parameters for solution ARGET ATRP (Part I)

4.1.7.3.1. Effects of k_r, k_a, and k_{da} kinetic rate constants in solution homopolymerization via ARGET ATRP

A parametric analysis was done varying k_r, k_a, and k_{da} values to evaluate the sensitivity of the kinetic parameters on the model prediction for experimental cases validated in solution homopolymerization via ARGET ATRP. As methodology employed, each kinetic constant was modified one at a time from 0.1 to 10 times relative to the values referenced in Table 11. The effects of those kinetic parameters were verified on the monomer conversion, number-average molecular weight, and dispersity (Figs. 16, 17 and 18 for entries 1, 2 and 3, respectively).

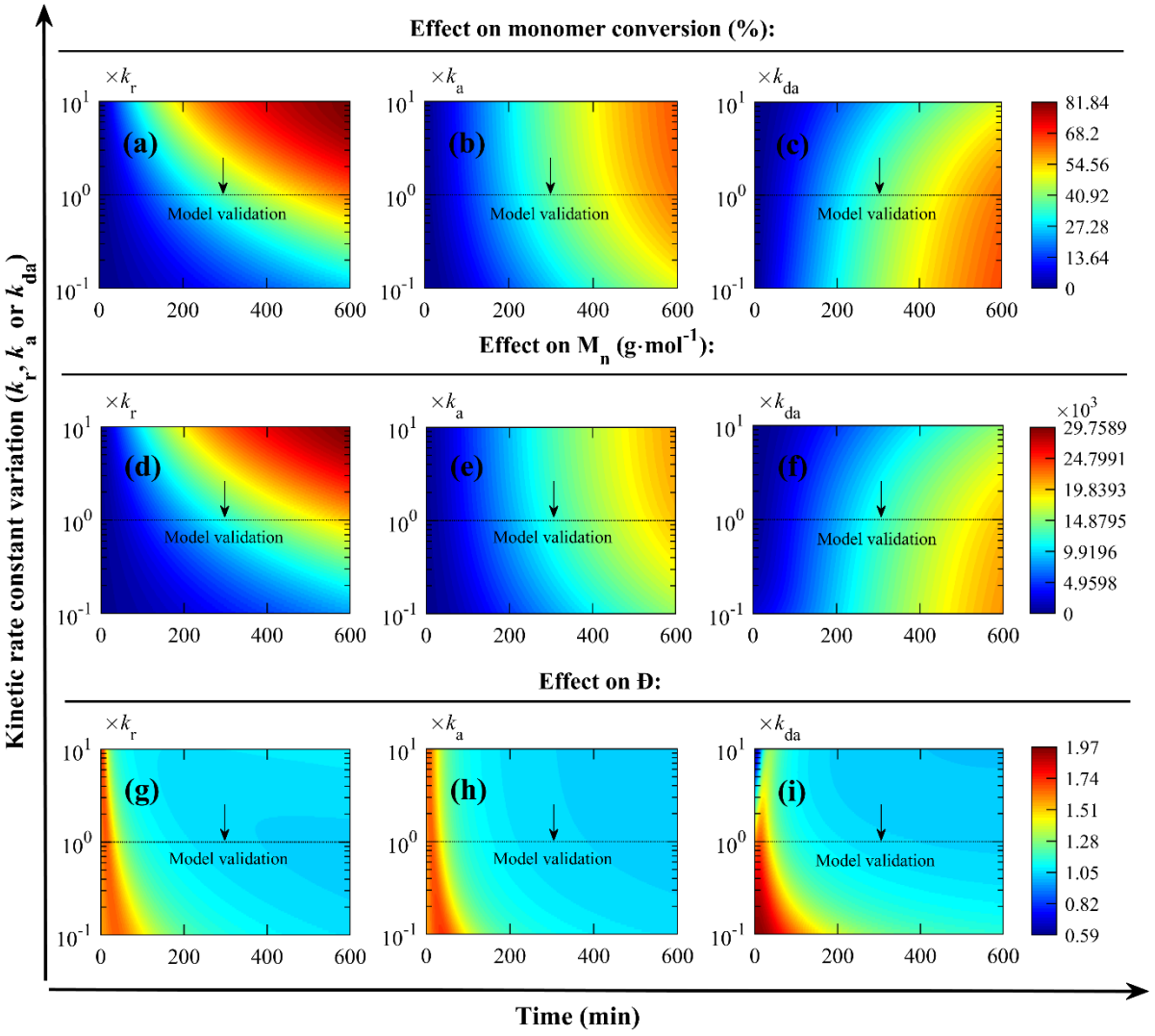

Fig. 16. Influence of k_r, k_a, and k_{da} kinetic rate constants on the model prediction in solution ARGET ATRP of St with $CuBr_2$/Me_6TREN and $Sn^{II}(eh)_2$ (Table 11, entry 1). Effects of (a) k_r, (b) k_a, and (c) k_{da} values on the profile monomer conversion vs. reaction time. Effects of (d) k_r, (e) k_a, and (f) k_{da} values on the profile number-average molecular weight (M_n) vs. reaction time. Effects of (g) k_r, (h) k_a, and (i) k_{da} values on the profile dispersity (Đ) vs. reaction time. Simulation at T = 110 °C, $[St]_0$ = 5.80 mol·L^{-1}, $[St]_0$:$[EBiB]_0$:$[CuBr_2/Me_6TREN]_0$:$[Sn^{II}(eh)_2]_0$ = 300:1:0.015:0.15, based on kinetic parameters from Tables 12 and 13. Adapted from [16].

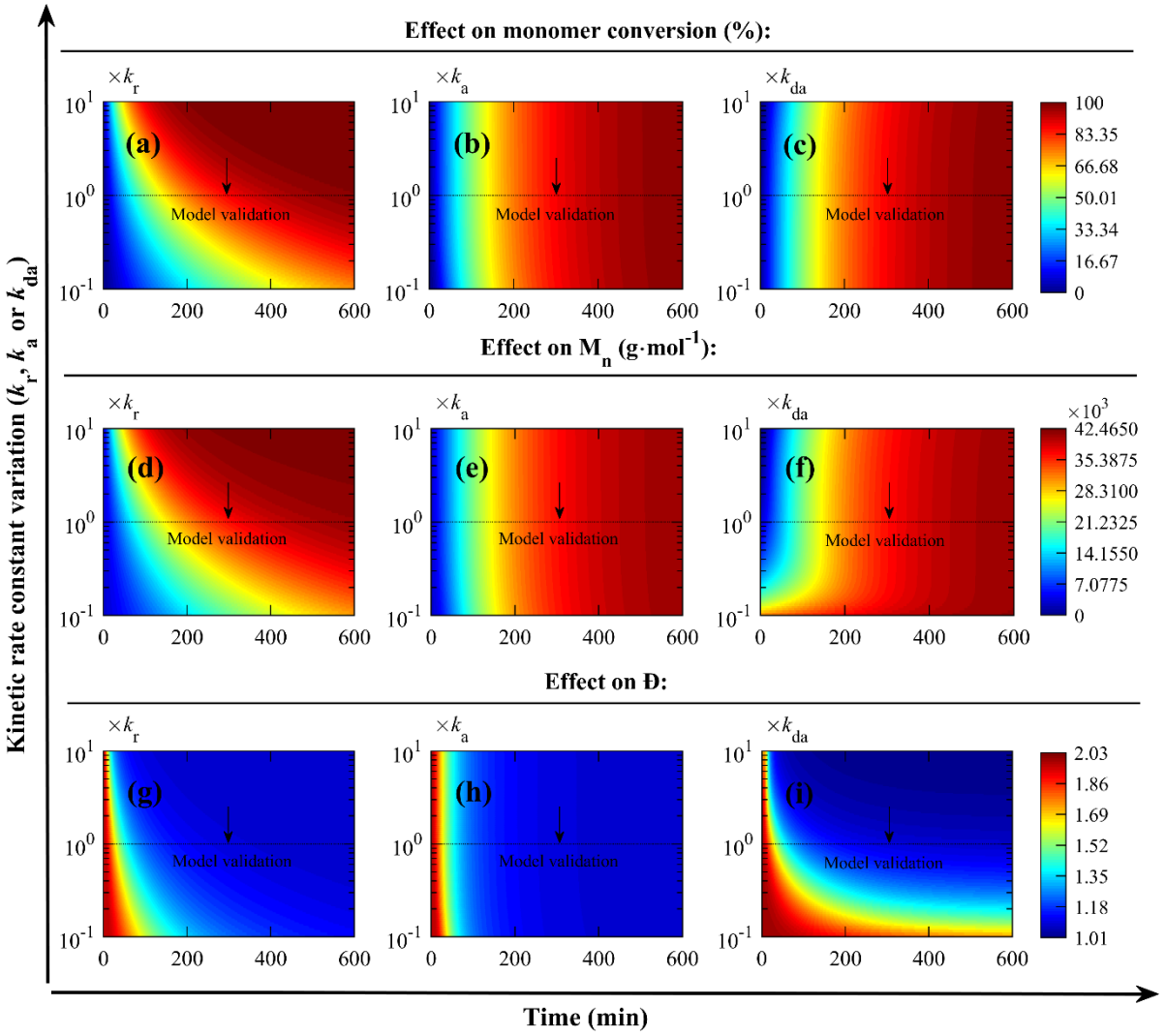

Fig. 17. Influence of k_r, k_a, and k_{da} kinetic rate constants on the model prediction in solution ARGET ATRP of MA with $CuBr_2$/Me_6TREN and H_2asc (Table 11, entry 2). Effects of (a) k_r, (b) k_a, and (c) k_{da} values on the profile monomer conversion vs. reaction time. Effects of (d) k_r, (e) k_a, and (f) k_{da} values on the profile number-average molecular weight (M_n) vs. reaction time. Effects of (g) k_r, (h) k_a, and (i) k_{da} values on the profile dispersity (Đ) vs. reaction time. Simulation at T = 60 °C, $[MA]_0$ = 7.00 mol·L^{-1}, $[MA]_0$:$[EBiB]_0$:$[CuBr_2/Me_6TREN]_0$:$[H_2asc]_0$ = 400:1:0.01:0.1, based on kinetic parameters from Tables 12 and 13. Adapted from [16].

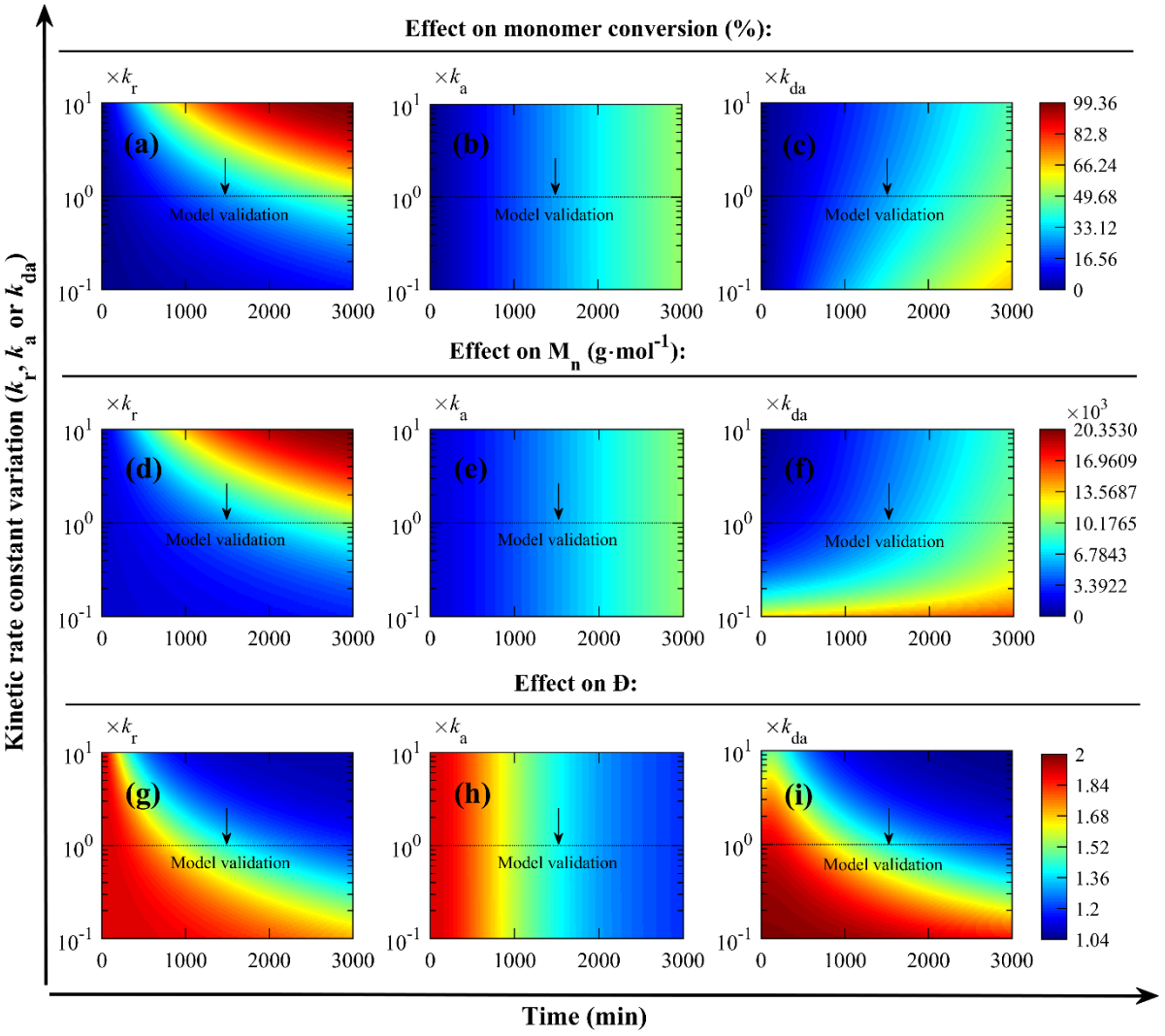

Fig. 18. Influence of k_r, k_a, and k_{da} kinetic rate constants on the model prediction in solution ARGET ATRP of BA with $CuCl_2$/TPMA and N_2H_4 (Table 11, entry 3). Effects of (a) k_r, (b) k_a, and (c) k_{da} values on the profile monomer conversion vs. reaction time. Effects of (d) k_r, (e) k_a, and (f) k_{da} values on the profile number-average molecular weight (M_n) vs. reaction time. Effects of (g) k_r, (h) k_a, and (i) k_{da} values on the profile dispersity (Đ) vs. reaction time. Simulation at T = 60 °C, $[BA]_0$ = 5.88 mol·L^{-1}, $[BA]_0$:$[EBiB]_0$:$[CuCl_2/TPMA]_0$:$[N_2H_4]_0$ = 200:1.28:0.01:0.1, based on kinetic parameters from Tables 12 and 13.

Simulations allow to infer that an increase of k_r or K_{ATRP} values also leads to an increase in the rate of polymerization (see Figs. 16a, 16b, 16c, 17a, 17b, 17c, 18a, 18b and 18c) and in the number-average molecular weight at the end of the reaction (see Figs. 16d, 16e, 16f, 17d, 17e, 17f, 18d, 18e and 18f). An opposite response is observed for dispersity, that reduces over the time (see Figs. 16g, 16h, 16i, 17g, 17h, 17i, 18g, 18h, and 18i).

In relation to the kinetic rate constants of the ATRP equilibrium (i.e., k_a and k_{da}), an inversely proportional behavior in the prediction of the rate of polymerization and number-average molecular weight was observed, as expected. However, the dispersity seems to have a near equivalent trend for both k_a and k_{da}, being the parameter more sensitive for the second kinetic rate constant according to the model prediction, which justifies the higher confidence intervals obtained for $\ln(k_a)$ presented in Table 13 and previously evidenced in Section 4.1.7.1..

In the reaction time very near zero for entry 1 (see Fig. 16i), dispersity values lower than one are obtained in the calculations. Very close to time zero the system is chaotic; therefore, such fluctuations are attributed to numerical noises, without physical meaning.

4.1.7.3.2. Effects of $[R_0X]_0/[(Cu^{II}XL)X]_0$ and $[(Cu^{II}XL)X]_0/[A]_0$ ratios in solution homopolymerization via ARGET ATRP

The effects of $[R_0X]_0/[(Cu^{II}XL)X]_0$ and $[(Cu^{II}XL)X]_0/[A]_0$ ratios on the model prediction in solution homopolymerization via ARGET ATRP are also studied in this work for the validated experimental cases. As a first step, the $[R_0X]_0$ values shown in Table 11 were kept constant, while $[R_0X]_0/[(Cu^{II}XL)X]_0$ ratios were varied from 10 to 1000. In a second moment, the $[(Cu^{II}XL)X]_0$ values of Table 11 were fixed and $[(Cu^{II}XL)X]_0/[A]_0$ ratios were modified from 0.01 to 1. The effects of $[R_0X]_0/[(Cu^{II}XL)X]_0$ and $[(Cu^{II}XL)X]_0/[A]_0$ ratios were evaluated on the monomer conversion, number-average molecular weight and dispersity (Figs. 19, 20 and 21 for entries 1, 2 and 3, respectively).

According to the model prediction, a reduction of the $[R_0X]_0/[(Cu^{II}XL)X]_0$ or $[(Cu^{II}XL)X]_0/[A]_0$ ratio increases the rate of polymerization (see Figs. 19a, 19b, 20a, 20b, 21a, and 21b) as well as the number-average molecular weight at the end of the simulated reaction time (see Figs. 19c, 19d, 20c, 20d, 21c, and 21d). Contrarily, the dispersity tends to reduce (see Figs. 19e, 19f, 20e, 20f, 21e and 21f). Again, dispersity values lower than one are observed for case 1 in the reaction time very near zero (see Fig. 18e), as a result of fluctuations attributed to numerical noises as previously discussed in Section 4.1.7.3.1..

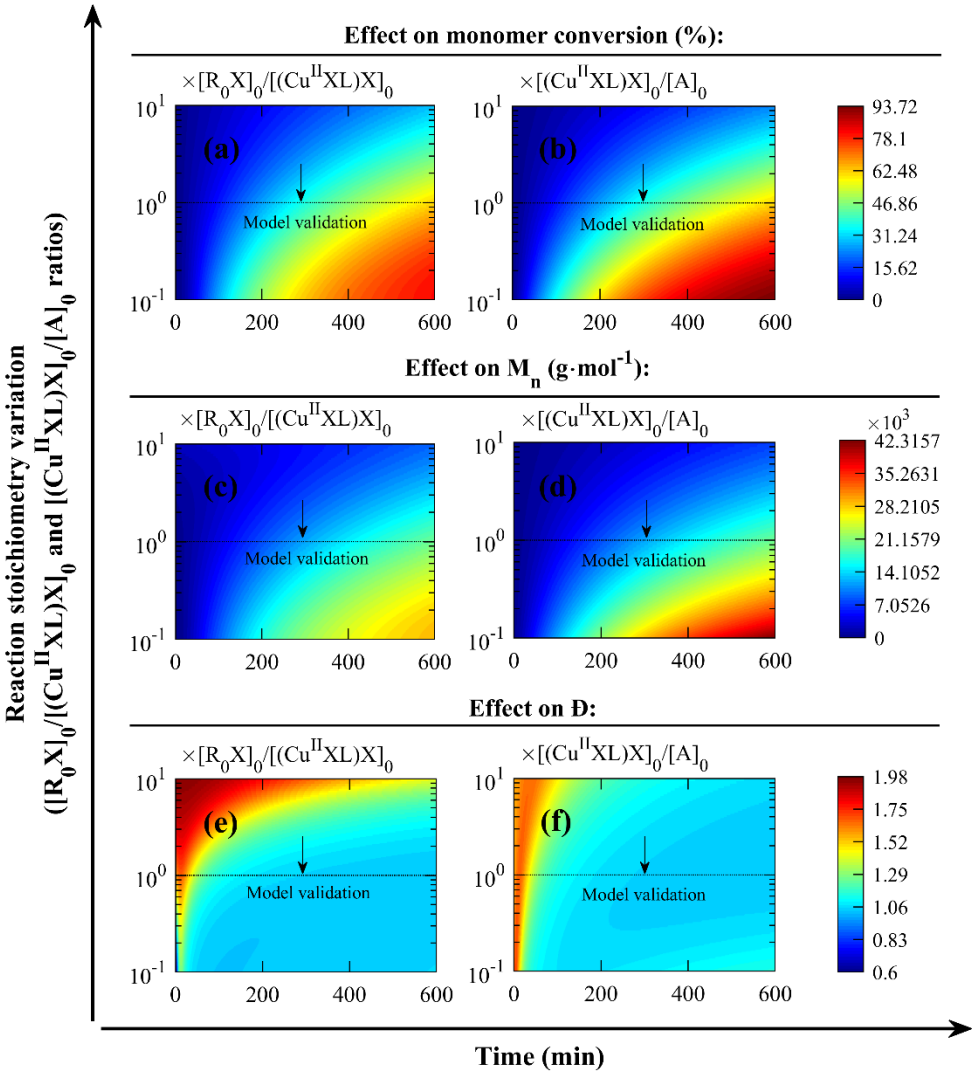

Fig. 19. Influence of $[R_0X]_0/[(Cu^{II}XL)X]_0$ and $[(Cu^{II}XL)X]_0/[A]_0$ ratios on the model prediction in solution ARGET ATRP of St with $CuBr_2/Me_6TREN$ and $Sn^{II}(eh)_2$ (Table 11, entry 1). Effects of (a) $[R_0X]_0/[(Cu^{II}XL)X]_0$ and (b) $[(Cu^{II}XL)X]_0/[A]_0$ ratios values on the profile monomer conversion vs. reaction time. Effects of (c) $[R_0X]_0/[(Cu^{II}XL)X]_0$ and (d) $[(Cu^{II}XL)X]_0/[A]_0$ ratios values on the profile number-average molecular weight (M_n) vs. reaction time. Effects of (e) $[R_0X]_0/[(Cu^{II}XL)X]_0$ and (f) $[(Cu^{II}XL)X]_0/[A]_0$ ratios values on the profile dispersity (Đ) vs. reaction time. Simulation at T = 110 °C, $[St]_0$ = 5.80 mol·L^{-1}, $[St]_0$:$[EBiB]_0$:$[CuBr_2/Me_6TREN]_0$:$[Sn^{II}(eh)_2]_0$ = 300:1:0.015:0.15, based on kinetic parameters from Tables 9 and 10. Adapted from [16].

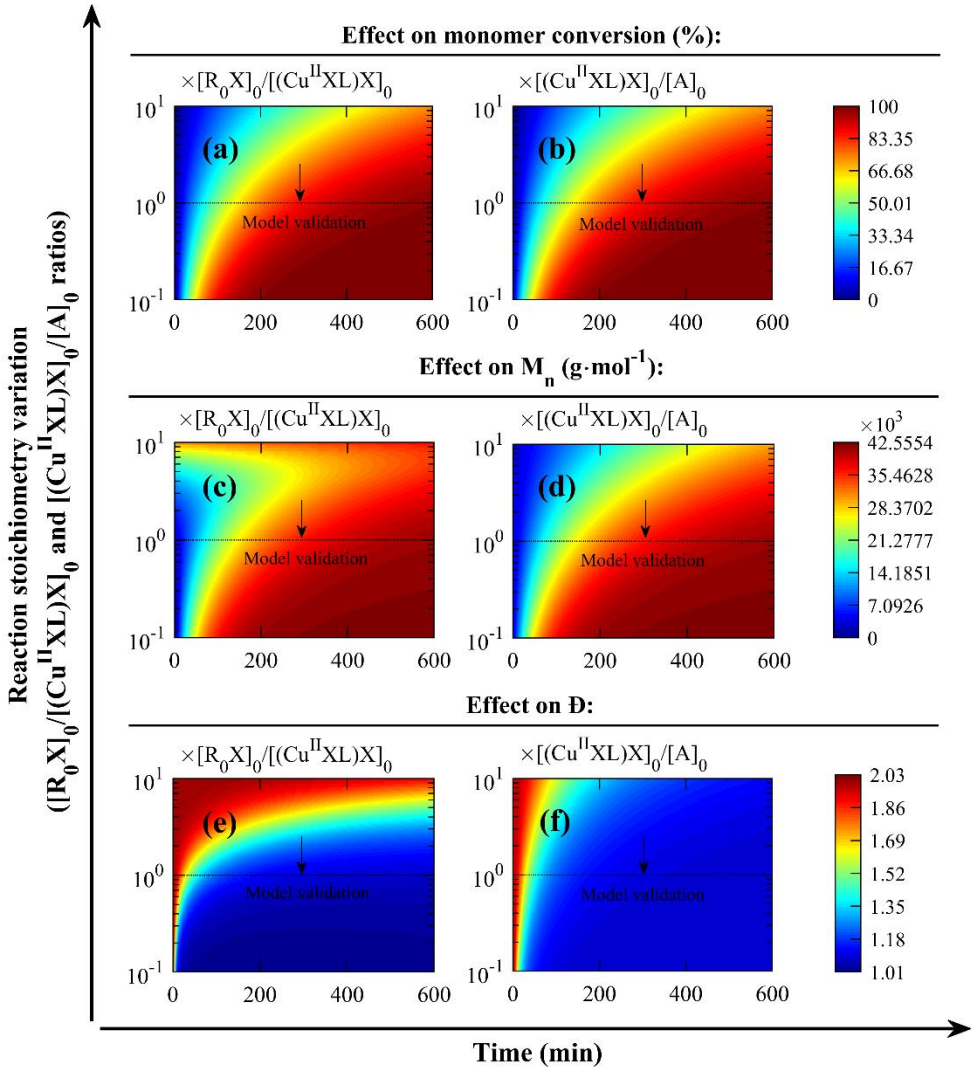

Fig. 20. Influence of $[R_0X]_0/[(Cu^{II}XL)X]_0$ and $[(Cu^{II}XL)X]_0/[A]_0$ ratios on the model prediction in solution ARGET ATRP of MA with $CuBr_2$/Me_6TREN and H_2asc (Table 11, entry 2). Effects of (a) $[R_0X]_0/[(Cu^{II}XL)X]_0$ and (b) $[(Cu^{II}XL)X]_0/[A]_0$ ratios values on the profile monomer conversion vs. reaction time. Effects of (c) $[R_0X]_0/[(Cu^{II}XL)X]_0$ and (d) $[(Cu^{II}XL)X]_0/[A]_0$ ratios values on the profile number-average molecular weight (M_n) vs. reaction time. Effects of (e) $[R_0X]_0/[(Cu^{II}XL)X]_0$ and (f) $[(Cu^{II}XL)X]_0/[A]_0$ ratios values on the profile dispersity (Đ) vs. reaction time. Simulation at T = 60 °C, $[MA]_0$ = 7.00 mol·L^{-1}, $[MA]_0$:$[EBiB]_0$:$[CuBr_2/Me_6TREN]_0$:$[H_2asc]_0$ = 400:1:0.01:0.1, based on kinetic parameters from Tables 12 and 13. Adapted from [16].

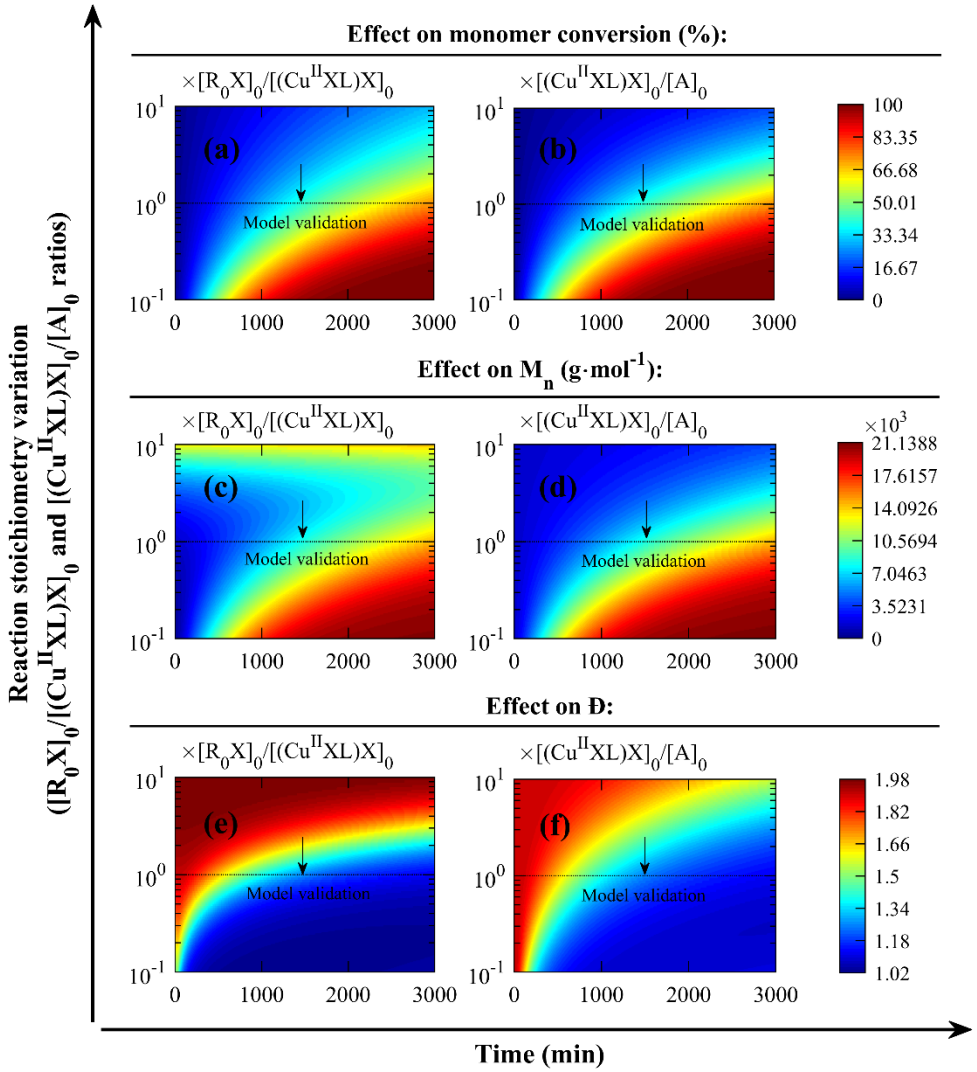

Fig. 21. Influence of $[R_0X]_0/[(Cu^{II}XL)X]_0$ and $[(Cu^{II}XL)X]_0/[A]_0$ ratios on the model prediction in solution ARGET ATRP of BA with $CuCl_2$/TPMA and N_2H_4 (Table 11, entry 3). Effects of (a) $[R_0X]_0/[(Cu^{II}XL)X]_0$ and (b) $[(Cu^{II}XL)X]_0/[A]_0$ ratios values on the profile monomer conversion vs. reaction time. Effects of (c) $[R_0X]_0/[(Cu^{II}XL)X]_0$ and (d) $[(Cu^{II}XL)X]_0/[A]_0$ ratios values on the profile number-average molecular weight (M_n) vs. reaction time. Effects of (e) $[R_0X]_0/[(Cu^{II}XL)X]_0$ and (f) $[(Cu^{II}XL)X]_0/[A]_0$ ratios values on the profile dispersity (Đ) vs. reaction time. Simulation at T = 60 °C, $[BA]_0$ = 5.88 mol·L^{-1}, $[BA]_0$:$[EBiB]_0$:$[CuCl_2/TPMA]_0$:$[N_2H_4]_0$ = 200:1.28:0.01:0.1, based on kinetic parameters from Tables 12 and 13.

Analyzing separately the effects of $[R_0X]_0/[(Cu^{II}XL)X]_0$ and $[(Cu^{II}XL)X]_0/[A]_0$ ratios, the model seems to be more sensitive to the first one. A more significant variation of the results is observed mainly in the dispersity prediction. This kind of behavior emphasizes that the $[(Cu^{II}XL)X]_0$ is a critical parameter with higher sensitivity than $[A]_0$ according to the simulation predictions.

4.1.8. Conclusion (Part I)

A comprehensive mathematical model for the solution homopolymerization via ARGET ATRP processes was proposed aiming to study the kinetic mechanism of three reducing agents to recover copper-based catalysts: tin(II) 2-ethylhexanoate, ascorbic acid, and hydrazine. To detail the reaction kinetics, differently from the literature, an approach based on chemical species experimentally verified was considered.

The ARGET mechanisms were successfully validated with three sources of experimental data available in literature: solution polymerizations of styrene at 110 °C for tin(II) 2-ethylhexanoate, methyl acrylate at 60 °C for ascorbic acid and butyl acrylate at 60 °C for hydrazine. For all the case studies, ethyl 2-bromoisobutyrate was used as alkyl halide initiator and anisole as a solvent. Furthermore, copper(II) bromide/tris[2-(dimethylamino)ethyl]amine was considered as deactivator for the systems of tin(II) 2-ethylhexanoate and ascorbic acid, while copper(II) chloride/tris(2-pyridylmethyl)amine for the system which consider hydrazine.

The ARGET mechanism kinetic rate constants for tin(II) 2-ethylhexanoate (k_r = 0.04 $L \cdot mol^{-1} \cdot s^{-1}$), ascorbic acid ($k_r$ = 0.0038 $L \cdot mol^{-1} \cdot s^{-1}$) and hydrazine ($k_r$ = 0.00072 $L \cdot mol^{-1} \cdot s^{-1}$) were obtained by optimization, and they are compatible with the experimental conditions of the case studies validated. Even at a lower temperature, the K_{ATRP} values for solution ARGET ATRP of methyl acrylate and butyl acrylate are almost 36 and 15 times higher than that obtained for solution ARGET ATRP of styrene, respectively; confirming the higher energy bond dissociation for the two first monomers.

A parametric analysis allowed to verify that an increase of k_r or K_{ATRP} values has a favorable impact on the rate of polymerization, leading to higher number-average molecular weight and lower dispersity. The effects of alkyl halide initiator-to-copper(II) halide complex and copper(II) halide complex-to-reducing agent ratios in solution homopolymerization via ARGET ATRP were also evaluated after the model validation. In this case, copper(II) halide

complex (i.e., deactivator) initial concentration is a critical parameter with higher sensitivity than reducing agent according to the predictions obtained by simulation.

4.2. Part II. Mathematical modeling and simulation of the synthesis of random poly(styrene-co-acrylonitrile) via ARGET ATRP with tin(II) 2-ethylhexanoate as reducing agent and copper-based catalysts.

4.2.1. Abstract (Part I)

In Section 4.2., it was studied the synthesis of random poly[(styrene)-co-(acrylonitrile)] via ARGET ATRP with tin(II) 2-ethylhexanoate as reducing agent and copper-based catalysts by mathematical modeling and simulation. The kinetic approach for describing the random copolymerization of two monomers was based on the terminal model. The adopted mathematical description derives from the pseudo-kinetic rate constant method, and it consists of an adaptation of the model equations for the homopolymerization process via ARGET ATRP proposed in Section 4.1. of this work. The kinetic rate constant of reduction (k_r) for tin(II) 2-ethylhexanoate was obtained by an optimization algorithm, and the molecular weights and dispersity were predicted using the method of moments. Sensitivity analyses were performed varying kinetic parameters, both k_r and ATRP equilibrium constants (i.e., k_a and k_{da}); as well as stoichiometric relations (i.e., initial concentrations of reducing agent and deactivator). Simulations results allow to infer that the increase k_r, and initial concentrations of both deactivator and reducing agent have significant impact on the increase of the polymerization rate of the random copolymerization of styrene and acrylonitrile via ARGET ATRP with tin(II) 2-ethylhexanoate as reducing agent and copper-based catalysts.

4.2.2. Highlights (Part II)

- A mathematical model for solution random copolymerization via ARGET ATRP of two monomers is proposed and validated;
- Reaction kinetics is based on the terminal model and on the mathematical description of the pseudo-kinetic rate constant method;
- Tin(II) 2-ethylhexanoate is studied as reducing agent with copper-based catalysts;
- An analysis of critical parameters for solution ARGET ATRP is done.

4.2.3. Introduction (Part II)

To increase the commercial value attached to the polymeric materials, copolymerization processes are conducted to incorporate attractive properties of two or more monomers into a single polymer chain. As a result, polymer properties, such as rheology, glass transition temperature, and melting point, can be tunned by the incorporation of functional groups or changing the degree of branching.

The potential of Atom Transfer Radical Polymerization (ATRP) for production of copolymers deserves to be mentioned. In addition to obtaining random (statistical) copolymers, ATRP also allows the synthesis of controlled composition such as alternating, gradient, block, graft, brush, and star structures [2].

In general, copolymers are often more expensive than homopolymers due to their more complex synthesis processes. To make copolymers more widely used, the reduction of their price would be interesting. In this context, some classes of copolymers previously described have also been obtained via Activators Regenerated by Electron Transfer (ARGET) ATRP [23, 32, 35, 36, 38, 40], aiming to save costs due to the reduction of catalyst consumption compared to the conventional ATRP.

Concerning the mathematical modeling works in ARGET ATRP for copolymerization processes, literature accounts for limited references. Payne et al. [31] realized a study of the synthesis of the random poly[(butyl methacrylate)-co-(butyl acrylate)] via ARGET ATRP considering tin(II) 2-ethylhexanoate as reducing agent and copper-based catalysts, such a modeling was developed based on the kinetic Monte Carlo methods. Hernández-Ortiz et al. [29] opted to develop a kinetic-based mathematical model for generic random copolymerization processes by ARGET ATRP based on the method of moments,

however, in their work the reducing agent is not specified (i.e., a generic kinetic mechanism is presented) and there is no model validation with experimental data.

Due to the few available publications in the literature, this study has as its significant contribution to present and validate a kinetic-based model for the random solution copolymerization of two monomers via ARGET ATRP. Thus, this research accounts as a case study the kinetic modeling of the synthesis of random poly[(styrene)-co-(acrylonitrile)] with tin(II) 2-ethylhexanoate as reducing agent and copper-based catalysts.

Furthermore, differently from the existing references in the literature, a more detailed mapping of concentration profiles of the chemical species considered in the kinetic mechanism is done, allowing a better understanding of the ARGET ATRP process under random copolymerization. An extensive parametric analysis around the kinetic parameters and the reaction stoichiometry is also provided in this research, aiming to understand their natural effects on the model prediction of the rate of polymerization, molecular weight, and dispersity.

4.2.4. Kinetic approach (Part II)

Table 14 depicts the main reactions for the random copolymerization of two monomers via ARGET ATRP, including initiation (ATRP equilibrium), propagation, termination, ATRP equilibrium, and ARGET mechanism. The kinetics of ARGET mechanism for tin(II) 2-ethylhexanoate ($Sn^{II}(eh)_2$) as a reducing agent with copper-based catalysts was discussed appropriately in Section 4.1.4.1..

By simplification, the kinetic approach considered is described for a terminal model, wherein only the last monomeric unit added to the molecular structure of the living, and dormant polymer chains play an essential role in the copolymerization reactions [77].

According to the Table 14, the polymer chains considered in the kinetic mechanism are $R_{i,1}X$ and $R_{i,2}X$ (dormant chains ended by monomers 1 and 2, respectively), $R_{i,1}$ and $R_{i,2}$ (living chains ended by monomers 1 and 2, respectively), and P_i (dead chains), where i (≥ 1) is the number of monomeric units in each chain.

The other chemical species also included in the kinetic mechanism are R_0X (alkyl halide initiator), $(Cu^{I}L)X$ (copper(I) catalyst, also designated by activator), R_0 (primary free radical generated by the alkyl halide initiator), $(Cu^{II}XL)X$ (copper(II) halide complex, also designated by deactivator), M_1 (monomer 1) and M_2 (monomer 2).

Table 14. Steps of the random copolymerization of two monomers via ARGET ATRP and their respective elementary reactions.[a,b]

Step	Mechanism	
Initiation (ATRP equilibrium):	$R_0X + (Cu^{I}L)X \xrightarrow{k_{a0}} R_0 + (Cu^{II}XL)X$	(53)
	$R_0 + (Cu^{II}XL)X \xrightarrow{k_{da0}} R_0X + (Cu^{I}L)X$	(54)
Propagation:	$R_0 + M_1 \xrightarrow{k_{p01}} R_{1,1}$	(55)
	$R_0 + M_2 \xrightarrow{k_{p02}} R_{1,2}$	(56)
	$R_{i,1} + M_1 \xrightarrow{k_{p11}} R_{i+1,1}$	(57)
	$R_{i,1} + M_2 \xrightarrow{k_{p12}} R_{i+1,2}$	(58)
	$R_{i,2} + M_1 \xrightarrow{k_{p21}} R_{i+1,1}$	(59)
	$R_{i,2} + M_2 \xrightarrow{k_{p22}} R_{i+1,2}$	(60)
Termination (by combination):	$R_{i,1} + R_{j,1} \xrightarrow{k_{tc11}} P_{i+j}$	(61)
	$R_{i,1} + R_{j,2} \xrightarrow{k_{tc12}} P_{i+j}$	(62)
	$R_{i,2} + R_{j,1} \xrightarrow{k_{tc21}} P_{i+j}$	(63)
	$R_{i,2} + R_{j,2} \xrightarrow{k_{tc22}} P_{i+j}$	(64)
Termination (by disproportionation):	$R_{i,1} + R_{j,1} \xrightarrow{k_{td11}} P_i + P_j$	(65)
	$R_{i,1} + R_{j,2} \xrightarrow{k_{td12}} P_i + P_j$	(66)
	$R_{i,2} + R_{j,1} \xrightarrow{k_{td21}} P_i + P_j$	(67)
	$R_{i,2} + R_{j,2} \xrightarrow{k_{td22}} P_i + P_j$	(68)
ATRP equilibrium:	$R_{i,1}X + (Cu^{I}L)X \xrightarrow{k_{a1}} R_{i,1} + (Cu^{II}XL)X$	(69)
	$R_{i,2}X + (Cu^{I}L)X \xrightarrow{k_{a2}} R_{i,2} + (Cu^{II}XL)X$	(70)
	$R_{i,1} + (Cu^{II}XL)X \xrightarrow{k_{da1}} R_{i,1}X + (Cu^{I}L)X$	(71)
	$R_{i,2} + (Cu^{II}XL)X \xrightarrow{k_{da2}} R_{i,2}X + (Cu^{I}L)X$	(72)
ARGET mechanism	$Sn^{II}(eh)_2 + 2(Cu^{II}XL)X \xrightarrow{k_r} Sn^{IV}(eh)_2X_2 + 2(Cu^{I}L)X$	(73)[c]

[a] R_0X: alkyl halide initiator; $(Cu^{I}L)X$: copper(I) catalyst (activator); R_0: primary free radical (generated by the alkyl halide initiator); $(Cu^{II}XL)X$: copper(II) halide complex (deactivator); M: monomer; $R_{i,1}$ and $R_{i,2}$, living polymer chains with i (≥ 1) monomeric units long ended by monomer 1 and 2, respectively; $R_{i,1}X$ and $R_{i,2}X$, dormant polymer chains with i (≥ 1) monomeric units long ended by monomer 1 and 2, respectively; P_n: dead polymer chains with i (≥ 1) monomeric units long; i or j: arbitrary numbers of monomeric units (≥ 1). [b] In this study it will be considered $k_{a0} = k_{a1} = k_{a2} = k_a$, $k_{da0} = k_{da1} = k_{da2} = k_{da}$, $k_{p01} = k_{p11}$ and $k_{p02} = k_{p22}$, that is a usual approximation in polymerization engineering. [c] See Section 4.1.4.1. for reference.

4.2.5. Model development (Part II)

4.2.5.1. General hypotheses (Part II)

The general hypotheses considered in the mathematical model developtment of solution random copolymerization via ARGET ATRP are: (i) isothermal batch operation; (ii) constant volume; (iii) perfect mixing is assumed; (iv) no side reactions (i.e., only initiation, propagation, termination, ATRP equilibrium, and ARGET mechanism are admitted); (v) monofunctional alkyl halides as initiators; (vi) diffusional effects neglected; (vii) both activator and deactivator are copper-based; (viii) copper transition metal salt is entirely complexed by ligand at the beginning of the polymerization, (ix) solvent is chemical inert; (x) steady-state approximation is valid for living chains; and (xi) the halogen-exchange mechanism [66] is not considered (i.e., different halide anions observed in both initiator and catalyst do not lead to the observation of side reactions).

4.2.5.2. Model equations for random solution copolymerization of two monomers via ARGET ATRP

Compared to homopolymerization, the mathematical modeling of a copolymerization process involves a much more complex populational balance, a fact evidenced by the higher number of elementary reactions considered in the kinetic mechanism admitted (see Table 14) and, consequently, by the sophistication of the representative system of equations obtained.

However, the mathematical treatment for a copolymerization can still be significantly simplified using the pseudo-kinetic rate constant method [77]. Applying it to this study, the method in question consider the model equations developed for homopolymerization via ARGET ATRP with the redefinition of some of the kinetic rate constants of the conventional ATRP (see Table 15), as well as the molar balance that represents the monomers consumption in the process should be rewritten (see Table 16).

Table 15. Pseudo-kinetic rated constants for a solution random copolymerization of two monomers via ATRP.[a,b]

Step	Pseudo-kinetic rate constant equation	
Propagation:	$k_{\mathrm{p}} = k_{\mathrm{p11}} f_{\mathrm{R1}} f_{\mathrm{M1}} + k_{\mathrm{p12}} f_{\mathrm{R1}} f_{\mathrm{M2}} + k_{\mathrm{p21}} f_{\mathrm{R2}} f_{\mathrm{M1}} + k_{\mathrm{p22}} f_{\mathrm{R2}} f_{\mathrm{M2}}$	(74)
Termination	$k_{\mathrm{tc}} = k_{\mathrm{tc11}} f_{\mathrm{R1}} f_{\mathrm{R1}} + k_{\mathrm{tc12}} f_{\mathrm{R1}} f_{\mathrm{R2}} + k_{\mathrm{tc21}} f_{\mathrm{R2}} f_{\mathrm{R1}} + k_{\mathrm{tc22}} f_{\mathrm{R2}} f_{\mathrm{R2}}$	(75)
	$k_{\mathrm{td}} = k_{\mathrm{td11}} f_{\mathrm{R1}} f_{\mathrm{R1}} + k_{\mathrm{td12}} f_{\mathrm{R1}} f_{\mathrm{R2}} + k_{\mathrm{td21}} f_{\mathrm{R2}} f_{\mathrm{R1}} + k_{\mathrm{td22}} f_{\mathrm{R2}} f_{\mathrm{R2}}$	(76)
ATRP equilibrium:	$k_{\mathrm{a}} = k_{\mathrm{a1}} f_{\mathrm{D1}} + k_{\mathrm{a2}} f_{\mathrm{D2}}$	(77)
	$k_{\mathrm{da}} = k_{\mathrm{da1}} f_{\mathrm{R1}} + k_{\mathrm{da2}} f_{\mathrm{R2}}$	(78)

[a] $f_{R,1}$ and $f_{R,2}$: molar fractions of living chains ended by monomers 1 and 2, respectively; $f_{M,1}$ and $f_{M,2}$: molar fractions of monomers 1 and 2 that not reacted, respectively; $f_{D,1}$ and $f_{D,2}$: molar fractions of dormant chains ended by monomers 1 and 2, respectively. [b] $f_{R,1}$, $f_{R,2}$, $f_{M,1}$, $f_{M,2}$, $f_{D,1}$ and $f_{D,2}$ expressions are available in Table 17.

These new kinetic rate constants presented in Table 15 are function of separating variables of the kinetic rate constants of the copolymerization process (i.e., k_{p11}, k_{p12}, k_{p21}, k_{p22}, k_{tc11}, k_{tc12}, k_{tc21}, k_{tc22}, k_{td11}, k_{td12}, k_{td21}, k_{td22}, k_{a1}, k_{a2}, k_{da1}, and k_{da2}) and of the molar fraction of the monomers, living and dormant chains (see Table 17). The steady-state approximation is used to obtain the molar fraction of living chains, (see Appendix B for details).

Table 16. The molar balance of monomers in solution random copolymerization of two monomers via ARGET ATRP.[a]

Monomer	Molar balance equation	
1:	$\frac{d[\mathrm{M}_1]}{dt} = -k_{\mathrm{p11}}\left([\mathrm{R}_0] + f_{\mathrm{R1}}\mu_{0,\mathrm{R}}\right)[\mathrm{M}_1] - k_{\mathrm{p21}} f_{\mathrm{R2}}\mu_{0,\mathrm{R}}[\mathrm{M}_1]$	(79)
2:	$\frac{d[\mathrm{M}_2]}{dt} = -k_{\mathrm{p22}}\left([\mathrm{R}_0] + f_{\mathrm{R2}}\mu_{0,\mathrm{R}}\right)[\mathrm{M}_2] - k_{\mathrm{p12}} f_{\mathrm{R1}}\mu_{0,\mathrm{R}}[\mathrm{M}_2]$	(80)
Total:	$\frac{d[\mathrm{M}]}{dt} = \frac{d[\mathrm{M}_1]}{dt} + \frac{d[\mathrm{M}_2]}{dt}$	(81)

[a] M_1: monomer 1; M_2: monomer 2; M: monomer total.

Hence, the model equations for solution copolymerization of two monomers via ARGET ATRP corresponds to the zeroth, first and second-order moments for dormant, living and dead chains molar balances (see Table 9 in Section 4.1.5.3.), as well as the molar balance of other relevant small chemical species considered in the kinetic model o solution ARGET ATRP (see Table 10 in Section 4.1.5.3.).

Note that the monomer consumption is now given by equations of Table 16 (i.e., Eq. (45) of Table 10 in Section 4.1.5.3. is now subdivided and represented by Eqs. (79), (80) and (81) presented in Table 16). The kinetic rate constants of the conventional ATRP mechanism (i.e., k_p, k_{tc}, k_{td}, k_a, and k_{da}) are now represented by the expressions shown in Table 15.

Table 17. The molar fraction of monomers, dormant and living chains in a solution random copolymerization of two monomers via ARGET ATRP.[a]

Molar fraction	Equation	
Monomer 1	$f_{M1} = \frac{[M_1]}{[M_1] + [M_2]}$	(82)
Monomer 2	$f_{M2} = \frac{[M_2]}{[M_1] + [M_2]}$	(83)
Dormant chains (ended by monomer 1)	$f_{D1} = \frac{\frac{k_{da1}}{k_{a1}} k_{p21} f_{M1}}{\frac{k_{da1}}{k_{a1}} k_{p21} f_{M1} + \frac{k_{da2}}{k_{a2}} k_{p12} f_{M2}}$	(84)
Dormant chains (ended by monomer 2)	$f_{D2} = \frac{\frac{k_{da2}}{k_{a2}} k_{p12} f_{M2}}{\frac{k_{da1}}{k_{a1}} k_{p21} f_{M1} + \frac{k_{da2}}{k_{a2}} k_{p12} f_{M2}}$	(85)
Living chains (ended by monomer 1)	$f_{R1} = \frac{k_{p21} f_{M1}}{k_{p21} f_{M1} + k_{p12} f_{M2}}$	(86)
Living chains (ended by monomer 2)	$f_{R2} = \frac{k_{p12} f_{M2}}{k_{p21} f_{M1} + k_{p12} f_{M2}}$	(87)

[a]The following mathematical relations are valid: $f_{M1} + f_{M2} = 1$, $f_{R1} + f_{R2} = 1$ and $f_{D1} + f_{D2} = 1$.

4.2.6. Kinetic modeling validation (Part II)

The experimental data of the synthesis of random poly[(styrene)-co-(acrylonitrile)] at 80°C via ARGET ATRP published by Pietrasik et al. [35] were considered in the model validation. In addition to styrene (St) and acrylonitrile (AN) as monomers, as well as tin(II) 2-ethylhexanoate (i.e., $Sn^{II}(eh)_2$) as reducing agent, it was considered ethyl 2-bromoisobutyrate (EBiB) as the alkyl halide initiator, copper(II) chloride/tris[2-(dimethylamino)ethyl]amine ($CuCl_2/Me_6TREN$) as deactivator and anisole as solvent. Table 18 presents the initial stoichiometry ratio of the reactants for the case study considered.

Table 18. Initial stoichiometry ratio of the concentrations used in the simulation for solution random copolymerization of St and AN via ARGET ATRP.[a]

$[M_1]_0:[M_2]_0:[R_0X]_0:[(Cu^{II}XL)X]_0:[A]_0$	Reference
600:390:1:0.03:0.5	[35]

[a] $[M_1]_0:[M_2]_0:[R_0X]_0:[(Cu^{II}XL)X]_0:[A]_0 = [St]_0:[AN]_0:[EBiB]_0:[CuCl_2/Me_6TREN]_0:[Sn^{II}(eh)_2]_0$, with $[St]_0 = 3.17$ $mol \cdot L^{-1}$.

Table 19 shows the kinetic rate constants for propagation and termination applied to the solution random copolymerization of St and AN via ARGET ATRP. Other additional parameters necessary to compute the value of the kinetic rate constants are shown in Table 20.

Concerning the experimental conditions of Table 18, in the literature, there are no reports of values for ATRP equilibrium kinetic rate constants (i.e., k_{a0}, k_{a1}, k_{a2}, k_{da0}, $k_{da1,}$ and k_{da2}), as well as for ARGET mechanism either (i.e., k_r). Therefore, such lacking kinetic rate constants were obtained via nonlinear regression by Levenberg–Marquardt algorithm as discussed in Section 3.2.2..

Table 19. Kinetic rate constants for solution random copolymerization of St and AN via ARGET ATRP.[a,b]

Description	Kinetic rate constant equation ($L \cdot mol^{-1} \cdot s^{-1}$)	Reference
Specific for St	$k_{p11} = 10^{7.630} \cdot \exp(-3908/T)$	[66]
	$k_{t11} = \begin{cases} F_1 \cdot DP_n^{-0,51} \cdot \exp(23.7 - 1117/T), & DP_n \leq 30 \\ F_1 \cdot DP_n^{-0,16} \cdot 0.3041 \cdot \exp(23.7 - 1117/T), & DP_n > 30 \end{cases}$	[67][c]
	$k_{tc11} = k_{t11}$	[68]
	$k_{td11} = 0$	[68]
Specific for AN	$k_{p22} = \exp(14.4 - 1855/T)$	[78]
	$k_{t22} = (7.762 \times 10^{13}) \cdot \exp(-4648/T)$	[79]
	$k_{tc22} = k_{t22}$	[79]
	$k_{td22} = 0$	[79]
Combined for St and AN	$k_{p12} = k_{p11}/r_1$	[80]
	$k_{p21} = k_{p22}/r_2$	[80]
	$k_{tc12} = 16 \cdot \frac{[0.0625 \cdot (1 - f_{M1,0}) + r_1 \cdot f_{M1,0}]}{[(1 - f_{M1,0}) + r_1 \cdot f_{M1,0}]} \cdot (2 \cdot k_{tc11} \cdot k_{tc22})^{0.5}$	[81]
	$k_{tc21} = k_{tc12}$	[81]
	$k_{td12} = 0$	[d]
	$k_{td21} = 0$	[d]

[a]Subscripts 1 and 2 are related to St and AN monomers, respectively. [b]r_1 and r_2: reactivity ratios; $f_{M1,0}$: initial molar fraction of monomer 1 (St); F_1: molar fraction of monomer 1 (St) that reacted. The expressions for r_1, r_2, $f_{M1,0}$, and F_1 are available in Table 20. [c]The dependence of the chain length in k_{t11} was adapted and, in this study, it is based on the number-average chain length (DP_n). [d]It was assumed $k_{td12} = k_{td21} = 0$, once $k_{td11} = k_{td22} = 0$.

Table 20. Additional parameters to compute the kinetic rate constants for solution random copolymerization of St and AN via ARGET ATRP.

Parameter description	Equation	Reference
Reactivity ratios	$r_1 = 0.36$	[80]
	$r_2 = 0.078$	[80]
Initial molar fraction of St	$f_{M1,0} = \frac{[M_1]_0}{[M_1]_0 + [M_2]_0}$	[80]
Molar fraction of St that reacted	$F_1 = \frac{(r_1 - 1)f_{M1}^2 + f_{M1}}{(r_1 + r_2 - 2)f_{M1}^2 + 2(1 - r_2)f_{M1} + r_2}$	[80]

4.2.7. Results and discussion (Part II)

4.2.7.1. Model validation (Part II)

Fig. 22 shows an adequate representativeness of the model for the experimental data of Pietrasik et al. [35] (see Table 18 for details). Linear profiles of both $\ln[M]_0/[M]$ vs. time and M_n vs. monomer conversion were obtained, characteristics of a successful ATRP running. Analogously to the Part I, the experimental data error bars were not represented since the values were extracted digitally with the WebPlotDigitizer software, where the measurement uncertainty can be neglected. Moreover, it was also obtained the profiles of predicted values and percent deviation (Eq. (51)) vs. experimental values for the same parameters presented in the Part I of this work (see Section 4.1.7.1.).

The effectiveness of the fitting was also obtained by a linear regression to correlate the predicted and experimental values. It was obtained R^2 values near 1 for $\ln[M_1]_0/[M]$, $\ln[M_2]_0/[M]$, monomer conversion, and number-average molecular weight (M_n), what indicates a strong relationship between the predicted and experimental values. The discrepancies noted for dispersity have already been discussed in Part I (see Section 4.1.7.1.) and it also apply to this case.

The estimated values of $\ln(k_r)$, $\ln(k_a)$, and $\ln(k_{da})$ obtained via nonlinear regression for the entries studied are presented in Table 21, considering a 95% confidence level. In the model validation process, it was assumed that k_{a0}, k_{a1} and k_{a2} have same value (i.e., $k_a = k_{a0} = k_{a1} = k_{a2}$), as well as k_{da0}, k_{da1} and k_{da2} are also equal (i.e., $k_{da} = k_{da0} = k_{da1} = k_{da2}$), there is a typical procedure considered in polymerization engineering (described in Table 14 footnotes).

Table 21. The estimated natural logarithm of the kinetic rate constants for solution random copolymerization of St and AN via ARGET ATRP.[a]

Step	Parameter	Estimated values[a]
		Mean ± error
ARGET mechanism	$\ln(k_r)$ ($L \cdot mol^{-1} \cdot s^{-1}$)	-5.68 ± 0.28
ATRP equilibrium	$\ln(k_a)$ ($L \cdot mol^{-1} \cdot s^{-1}$)	8.30 ± 0.29
	$\ln(k_{da})$ ($L \cdot mol^{-1} \cdot s^{-1}$)	15.39 ± 0.95

[a]The values presented lie within the estimated 95% confidence interval. [b]Solution copolymerization of St and AN via ARGET ATRP with EBiB, $CuCl_2$/Me_6TREN and $Sn^{II}(eh)_2$ carried out at 80 °C (see Table 18 for details)

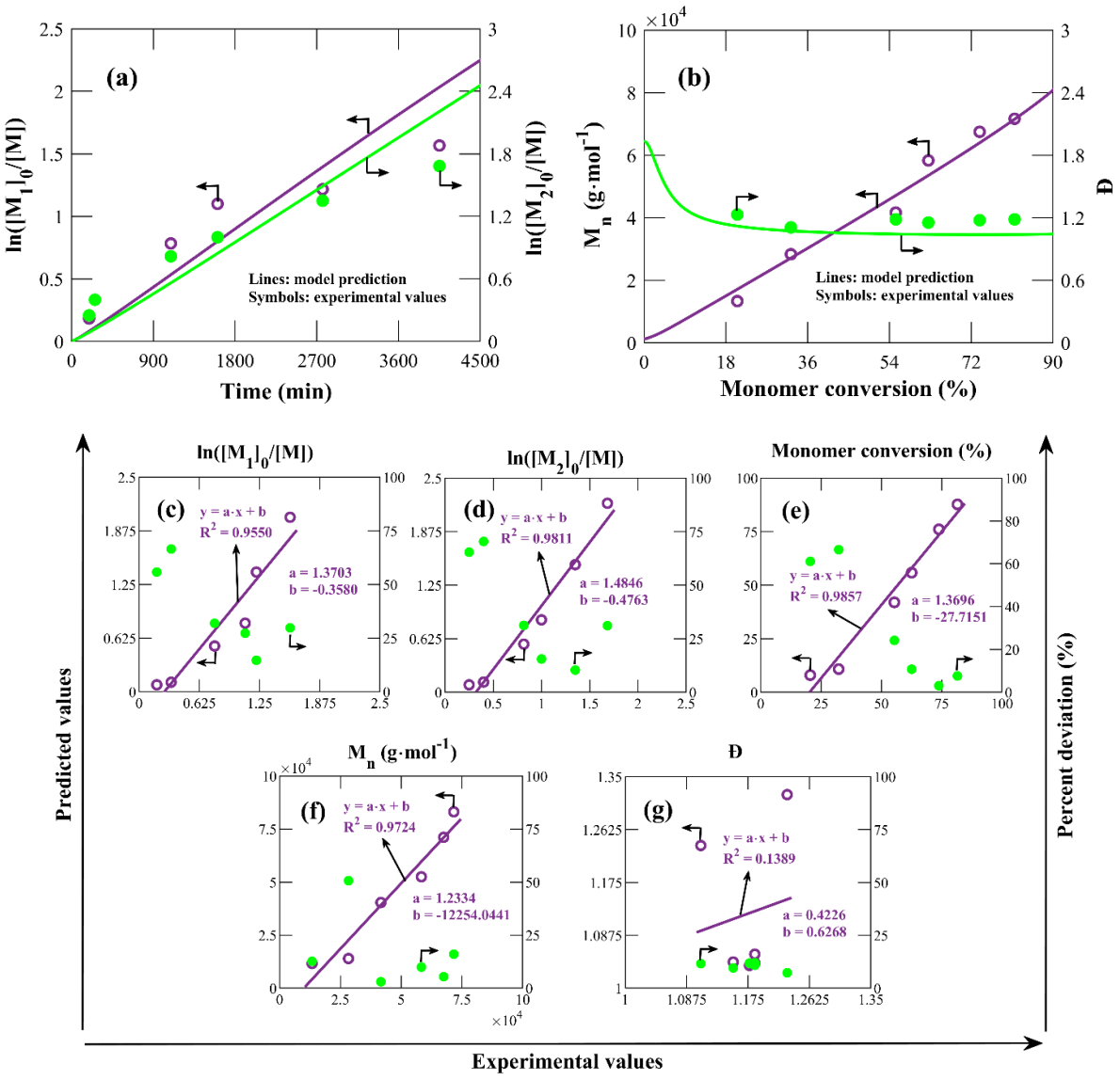

Fig. 22. Model validation for solution random copolymerization of St and AN via ARGET ATRP with $Sn^{II}(eh)_2$ and $CuCl_2$/Me_6TREN (see Table 18 for reference). (a) $\ln[M_1]_0/[M_1]$ (left) and $\ln[M_2]_0/[M_2]$ (right) vs. reaction time, (b) number-average molecular weight (M_n) (left) and dispersity (Đ) (right) vs. monomer conversion. Predicted values (left) and percent deviation (right) vs. experimental values of (c) $\ln[M_1]_0/[M]$, (d) $\ln[M_2]_0/[M]$, (e) monomer conversion, (f) number-average molecular weight (M_n), and (g) dispersity (Đ). Simulation at T = 80 °C, $[St]_0$ = 3.17 mol·L^{-1}, $[St]_0$:$[AN]_0$:$[EBiB]_0$:$[CuCl_2/Me_6TREN]_0$:$[Sn^{II}(eh)_2]_0$ = 600:390:1:0.03:0.5, based on kinetic parameters from Tables 19 and 21. Experimental values of [35].

By the Table 21, the best fit for the St/AN/EBiB/$CuBr_2$/Me_6TREN/$Sn^{II}(eh)_2$ system at 80°C was k_r = 0.0034 L·mol^{-1}·s^{-1}, k_a = 4023.9 L·mol^{-1}·s^{-1} and k_{da} = 4.8×10^6 L·mol^{-1}·s^{-1}, wherein $K_{ATRP} = k_a/k_{da}$ = 8.4×10^{-4}. If compared to the parameters experimentally obtained by Tang et al. [10] for the ATRP EBiB/Cu^I/Me_6TREN system (i.e., k_a = 227.8 L·mol^{-1}·s^{-1} at 22 °C and $K_{ATRP} = k_a/k_{da}$ = 1.5×10^{-4} at 35 °C), previously presented in Section 4.1.7.1., the adjusted values of k_a and K_{ATRP} are consistent, since the higher temperature for the case study (i.e., 80 °C) the higher kinetic rate constant would be expected.

Considering the ARGET mechanism kinetic rate constant for $Sn^{II}(eh)_2$ as reducing agent, in Part I of this work (see Section 4.1.7.1.), it was reported k_r = 0.04 L·mol^{-1}·s^{-1} for the St/EBiB/$CuBr_2$/Me_6TREN/$Sn^{II}(eh)_2$ system at 110 °C (Table 11, entry 1). Hence, the value reported in this study (i.e., Part II) for the St/AN/EBiB/$CuCl_2$/Me_6TREN/$Sn^{II}(eh)_2$ system at 80°C is also compatible, due to the temperature effect (i.e., the lower temperature, the lower kinetic rate constant), neglecting a possible effect of the halide anion in the transition metal salt.

4.2.7.2. Model prediction (Part II)

Analogously to the Part I of this work, Fig. 23 shows the concentration profiles of the reactants consumption and products formation (other than polymer chains) throughout the polymerization for the solution random copolymerization of St and AN via ARGET ATRP with $Sn^{II}(eh)_2$ as reducing agent and $CuCl_2$/TPMA as deactivator at 80 °C.

Comparing the results provided by this study (i.e., Part II) with the ones presented for the St/EBiB/$CuBr_2$/Me_6TREN/$Sn^{II}(eh)_2$ system at 110 °C (Table 11, entry 1) analyzed in the Part I of this work (see Section 4.1.7.2.), a lower k_r obtained (i.e., k_r = 0.0034 L·mol^{-1}·s^{-1} vs. k_r = 0.04 L·mol^{-1}·s^{-1}) leads to slower decay in the concentration profile of $Sn^{II}(eh)_2$ species than that observed for entry 1 (c.f., A and A_{oxi} profiles in Figs. 10 and 23).

Even with a value of K_{ATRP} higher than for entry 1 (i.e., K_{ATRP} = 8.4×10^{-4} vs. K_{ATRP} = 5×10^{-6}), the [Cu^I]/[Cu^{II}] ratio through monomer conversion obtained in this study is lower, since the formation of Cu^I species is limited by the ARGET mechanism (i.e., ARGET mechanism is the kinetic rate-determining step for the ARGET ATRP processes), which a lower k_r is also observed (i.e., k_r = 0.0034 L·mol^{-1}·s^{-1} vs. k_r = 0.04 L·mol^{-1}·s^{-1}) by the St/AN/EBiB/$CuBr_2$/Me_6TREN/$Sn^{II}(eh)_2$ system at 80°C (c.f., (Cu^{II}XL)X and (Cu^IL)X profiles in Figs. 10 and 23).

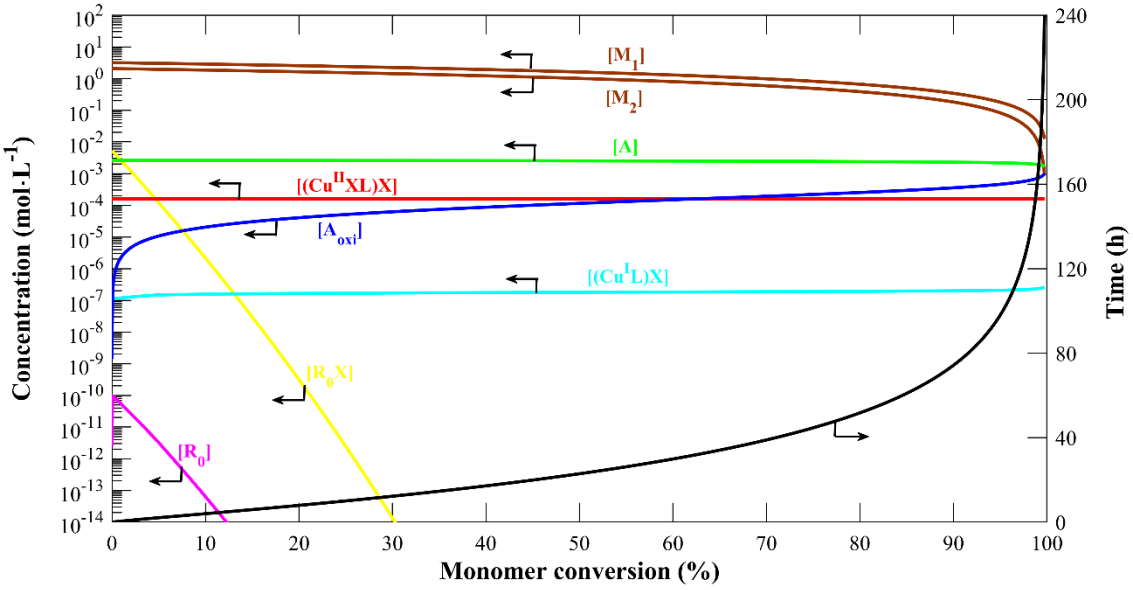

Fig. 23. Concentration profiles of the main chemical species considered in the kinetic model (other than polymer chains) (left) and reaction time (right) vs. monomer conversion for solution random copolymerization of St and AN via ARGET ATRP with $Sn^{II}(eh)_2$ and $CuCl_2$/Me_6TREN (see Table 18 for reference). Simulation at T = 80 °C, $[St]_0$ = 3.17 mol·L^{-1}, $[St]_0$:$[AN]_0$:$[EBiB]_0$:$[CuCl_2/Me_6TREN]_0$:$[Sn^{II}(eh)_2]_0$ = 600:390:1:0.03:0.5, based on kinetic parameters from Tables 19 and 21.

Fig. 24 presents zeroth and first-order moments profiles for the St/AN/EBiB/$CuBr_2$/Me_6TREN/$Sn^{II}(eh)_2$ system at 80°C. In this study, the mathematical modeling is based on the pseudo-kinetic rate constant method. Thus, the moments related to the dormant and living chains are subdivided according to the description given by the terminal model (i.e., ended by monomers 1 and 2), as shown in Table 22.

Table 22. Redefinition of the m^{th} order moments in a solution random copolymerization of two monomers via ARGET ATRP.[a]

m^{th} order moment	Equation			
	Ended by monomer 1		Ended by monomer 2	
Living chains	$\mu_{m,R,1} = f_{R1}\mu_{m,R}$	(86)	$\mu_{m,R,2} = f_{R2}\mu_{m,RX}$	(88)
Dormant chains	$\mu_{m,RX,1} = f_{D1}\mu_{m,RX}$	(87)	$\mu_{m,RX,2} = f_{D2}\mu_{m,RX}$	(89)

[a] $\mu_{m,R,1}$ and $\mu_{m,R,2}$: m^{th} order moments for living chains ended by monomer 1 and 2, respectively; $\mu_{m,RX,1}$ and $\mu_{m,RX,2}$: m^{th} order moments for dormant chains ended by monomer 1 and 2, respectively.

Note that in the model validation it was assumed $k_a = k_{a0} = k_{a1} = k_{a2}$ and $k_{da} = k_{da0} = k_{da1} = k_{da2}$. Consequently, the molar concentration of dormant chains is equal to the living chains (i.e., $f_{D1} = f_{R1}$ and $f_{D2} = f_{R2}$) according by Eqs. (84)–(87) presented in Table 17, which is a reasonable approximation.

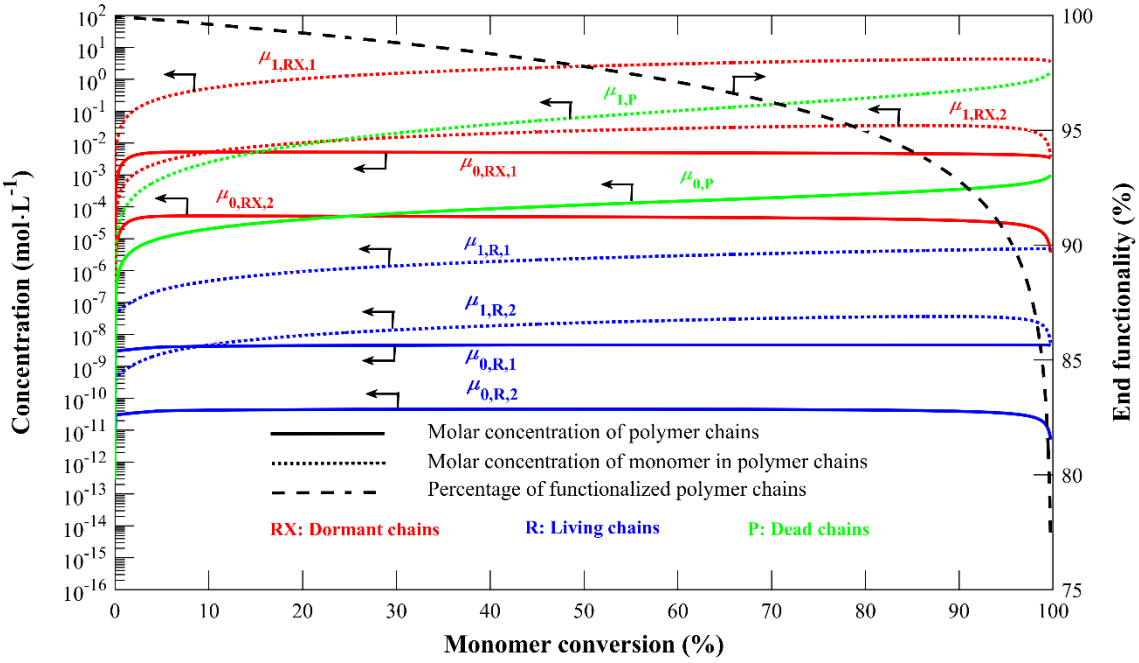

Fig. 24. Prediction of zeroth and first-order moments for dormant, living, and dead chains (left) and percentage of functionalized polymer chains (right) vs. monomer conversion for solution random copolymerization of St and AN via ARGET ATRP with $Sn^{II}(eh)_2$ and $CuCl_2/Me_6TREN$ (see Table 18 for reference). Simulation at T = 80 °C, $[St]_0$ = 3.17 mol·L^{-1}, $[St]_0$:$[AN]_0$:$[EBiB]_0$:$[CuCl_2/Me_6TREN]_0$:$[Sn^{II}(eh)_2]_0$ = 600:390:1:0.03:0.5, based on kinetic parameters from Tables 19 and 21.

Similarly to the results obtained in Part I (Section 4.1.7.2.) of this work (see Figs. 13, 14 and 15), the concentration of dormant species is higher than those of radical and dead polymer chains, a characteristic observed in ATRP systems (see Fig. 24). Such results lead to a high percentage of functionalized polymer chains, as obtained in Part I (Section 4.1.7.2.) of this work (c.f., Fig. 24 with Figs. 13, 14 and 15), which is related to the good control of the systems studied.

4.2.7.3. Analysis of critical parameters for solution ARGET ATRP (Part II)

4.2.7.3.1. Effects of k_r, k_a, and k_{da} kinetic rate constants in solution random copolymerization of two monomers via ARGET ATRP

A sensitivity analysis was done around the adjusted kinetic rate constants (i.e., k_r, k_a, and k_{da}) varying one at a time from 0.1 to 10 times relative to the values referenced in Table 21. Fig. 25 depicts the effects of such parameters on the prediction of the monomer conversion, number-average molecular weight, and dispersity for the St/AN/EBiB/$CuCl_2$/Me_6TREN/$Sn^{II}(eh)_2$ system at 80 °C.

According to the results presented, k_r influences significantly all the variables analyzed. Figs. 25a, 25d, and 25g show the higher k_r values, the higher rate of polymerization and the higher number-average molecular weight obtained of the random poly[(styrene)-co-(acrylonitrile)] and the lower dispersity, respectively.

However, although the trends previously described are maintained for the ATRP equilibrium constants (i.e., k_a and k_{da}), they are visibly less sensitive (i.e., more robust) than verified for k_r (see Figs. 25b, 25c, 25e, 25f, 25h, and 25i), except when analyzed the influence of k_{da} on the dispersity (see Fig. 25i).

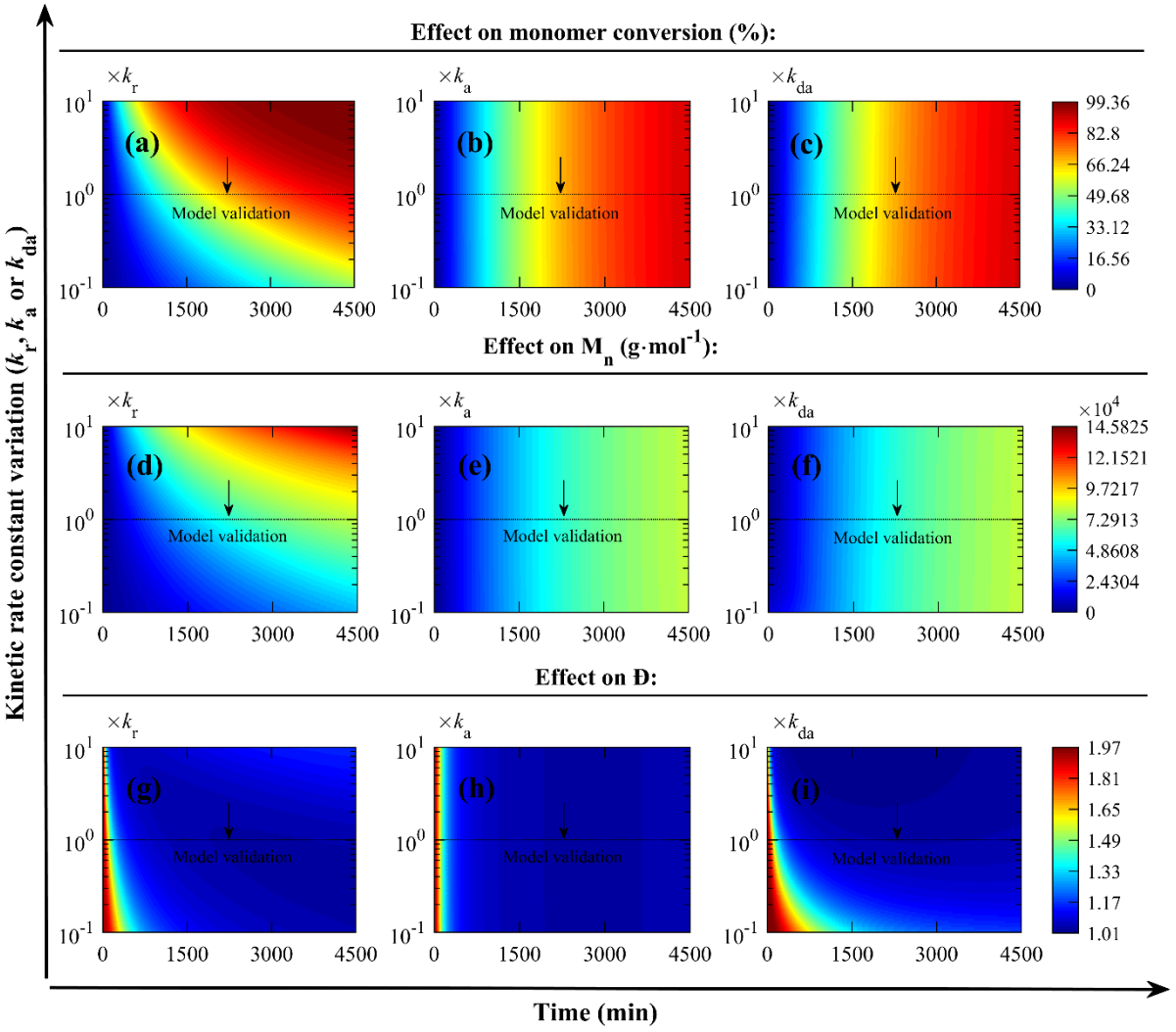

Fig. 25. Influence of k_r, k_a, and k_{da} kinetic rate constants on the model prediction in solution random copolymerization of St and AN via ARGET ATRP with $Sn^{II}(eh)_2$ and $CuCl_2$/Me_6TREN (see Table 18 for reference). Effects of (a) k_r, (b) k_a, and (c) k_{da} values on the profile monomer conversion vs. reaction time. Effects of (d) k_r, (e) k_a, and (f) k_{da} values on the profile number-average molecular weight (M_n) vs. reaction time. Effects of (g) k_r, (h) k_a, and (i) k_{da} values on the profile dispersity (Đ) vs. reaction time. Simulation at T = 80 °C, $[St]_0$ = 3.17 mol·L^{-1}, $[St]_0$:$[AN]_0$:$[EBiB]_0$:$[CuCl_2/Me_6TREN]_0$:$[Sn^{II}(eh)_2]_0$ = 600:390:1:0.03:0.5, based on kinetic parameters from Table 19 and 21.

4.2.7.3.2. Effects of $[R_0X]_0/[(Cu^{II}XL)X]_0$ and $[(Cu^{II}XL)X]_0/[A]_0$ ratios in solution random copolymerization of two monomers via ARGET ATRP

The $[R_0X]_0/[(Cu^{II}XL)X]_0$ and $[(Cu^{II}XL)X]_0/[A]_0$ ratios are important stoichiometric parameters in ARGET ATRP systems. Hence, keeping constant the referenced $[R_0X]_0$ value (see Table 18), the $[R_0X]_0/[(Cu^{II}XL)X]_0$ ratios were varied from 10 to 1000. In a uniform procedure, the referenced $[(Cu^{II}XL)X]_0$ values (see Table 18) were fixed and $[(Cu^{II}XL)X]_0/[A]_0$ ratios were modified from 0.01 to 1.

Fig. 26 presents the simulation results of a sensitivity analysis around the $[R_0X]_0/[(Cu^{II}XL)X]_0$ and $[(Cu^{II}XL)X]_0/[A]_0$ ratios on the monomer conversion, number-average molecular weight and dispersity for the St/AN/EBiB/$CuBr_2$/Me_6TREN/$Sn^{II}(eh)_2$ system at 80 °C. The trends obtained in this case study are consistent with those presented in Part I (Section 4.1.7.3.2.) of this work.

Both rate of polymerization (see Figs. 26a and 26b) and number-average molecular weight (see Figs. 26c and 26d) are positively impacted by the reduction of both $[R_0X]_0/[(Cu^{II}XL)X]_0$ and $[(Cu^{II}XL)X]_0/[A]_0$ ratios. An opposite tendency is noted by the dispersibility, which reduces (see Figs. 26e and 26f).

According to the simulations done, the prediction of both rate of polymerization and number-average molecular weight is more sensitive to the variations of $[(Cu^{II}XL)X]_0/[A]_0$ than $[R_0X]_0/[(Cu^{II}XL)X]_0$, differently from which occurs with the dispersity. Therefore, from such behavior produced by the proposed model, the $[(Cu^{II}XL)X]_0$ is a critical parameter with higher sensitivity than $[A]_0$ in the solution random copolymerization of St and AN via ARGET ATRP with $Sn^{II}(eh)_2$ and $CuCl_2$/Me_6TREN (see Table 18 for reference).

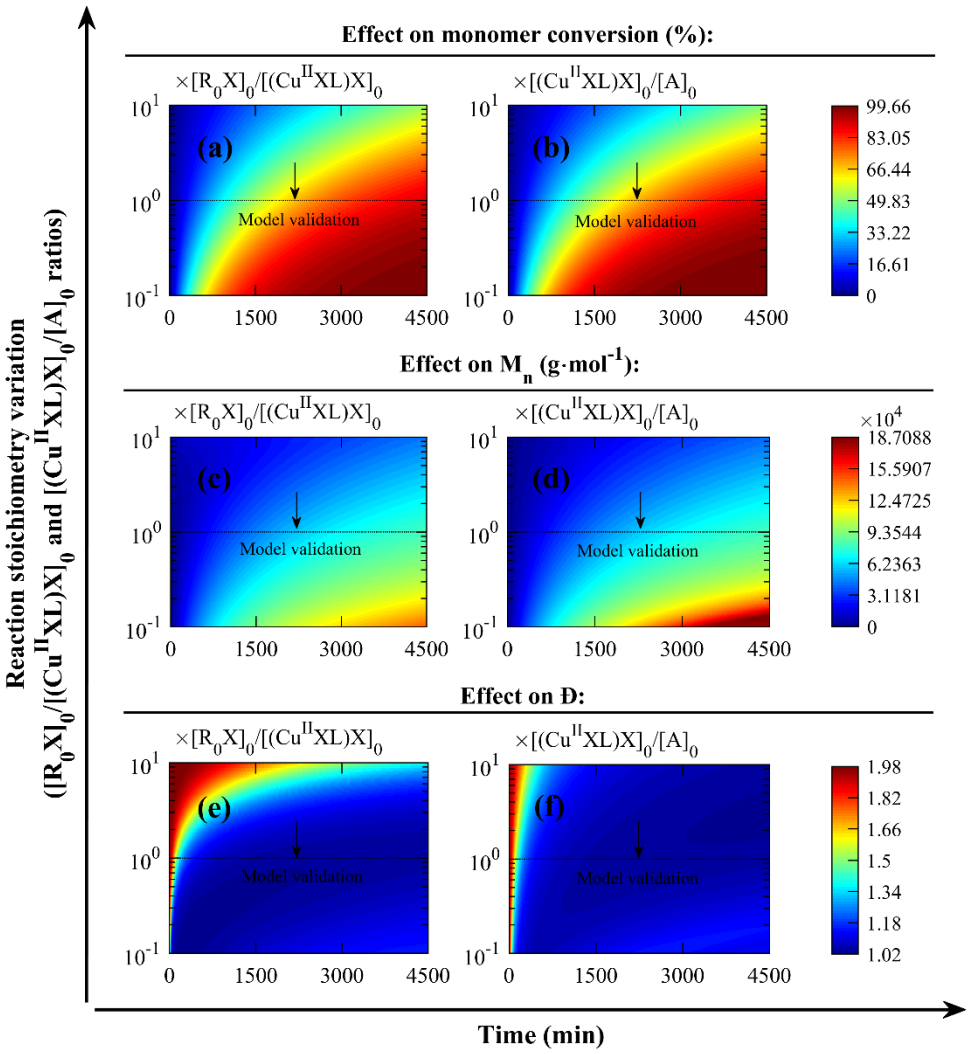

Fig. 26. Influence of $[R_0X]_0/[(Cu^{II}XL)X]_0$ and $[(Cu^{II}XL)X]_0/[A]_0$ ratios on the model prediction in solution random copolymerization of St and AN via ARGET ATRP with $Sn^{II}(eh)_2$ and $CuCl_2/Me_6TREN$ (see Table 18 for reference). Effects of (a) $[R_0X]_0/[(Cu^{II}XL)X]_0$ and (b) $[(Cu^{II}XL)X]_0/[A]_0$ ratios values on the profile monomer conversion vs. reaction time. Effects of (c) $[R_0X]_0/[(Cu^{II}XL)X]_0$ and (d) $[(Cu^{II}XL)X]_0/[A]_0$ ratios values on the profile number-average molecular weight (M_n) vs. reaction time. Effects of (e) $[R_0X]_0/[(Cu^{II}XL)X]_0$ and (f) $[(Cu^{II}XL)X]_0/[A]_0$ ratios values on the profile dispersity (Đ) vs. reaction time. Simulation at T = 80 °C, $[St]_0$ = 3.17 mol·L^{-1}, $[St]_0$:$[AN]_0$:$[EBiB]_0$:$[CuCl_2/Me_6TREN]_0$:$[Sn^{II}(eh)_2]_0$ = 600:390:1:0.03:0.5, based on kinetic parameters from Tables 19 and 21.

4.2.8. Conclusion (Part II)

A comprehensive mathematical model for the solution random copolymerization of two monomers via ARGET ATRP considering tin(II) 2-ethylhexanoate and copper-based catalysts was proposed and validated with experimental data available in the literature. The model presented was proposed based on the pseudo-kinetic rate constant method and developed from a solution homopolymerization model via ARGET ATRP.

The synthesis of random poly[(styrene)-co-(acrylonitrile)] via ARGET ATRP at 80°C with ethyl 2-bromoisobutyrate as the alkyl halide initiator, copper(II) chloride/tris[2-(dimethylamino)ethyl]amine as deactivator, anisole as solvent, as well as tin(II) 2-ethylhexanoate as reducing agent was studied. The kinetic rate constants were obtained for both ARGET mechanism (i.e., k_r = 0.0034 $L \cdot mol^{-1} \cdot s^{-1}$) and ATRP equilibrium (i.e., k_a = 4023.9 $L \cdot mol^{-1} \cdot s^{-1}$ and k_{da} = 4.8×10^6 $L \cdot mol^{-1} \cdot s^{-1}$, wherein $K_{ATRP} = k_a/k_{da} = 8.4 \times 10^{-4}$), which are consistent with results generated in Part I of this work as well as in the literature.

Simulations were carried out varying k_r or K_{ATRP} around the values obtained for the case study validated and same conclusions obtained in Part I were reported, wherein the increase of such parameters also increases both monomer conversion and number-average molecular weight but reduces dispersity. Analogously to the Part I, in this study it was also proved that copper(II) halide complex (i.e., deactivator) initial concentration is a critical parameter with higher sensitivity than reducing agent.

CHAPTER 5. CONTRIBUTIONS AND FUTURE PERSPECTIVES

Among the most relevant contributions provided by this research, the following stand out: (i) the understanding of the mechanics of the use of some reducing agents (e.g., tin(II) 2-ethylhexanoate, ascorbic acid, and hydrazine) to reduce the concentration of (copper-based) catalysts in the polymerization via ARGET ATRP, and (ii) the presentation of mathematical tools (i.e., kinetic-based models for homo and random copolymerization processes) able to describe experimental trends observed in the polymerization via ARGET ATRP.

The studies carried out in this work also allowed to understand the influence of the reduction kinetic rate constant (k_r) of the ARGET mechanism. An increase on k_r leads to an increase on both polymerization rate and number-average molecular weight, however, with a reduction on the dispersity. The challenge is, then, to think about which approaches could be taken to modify such kinetic rate constant in order to optimize the monomer conversion and reduce dispersity for an interest number-average molecular weight. Among the possibilities, reaction temperature, chemical nature of the reducing agent, and configuration of the catalyst (i.e., the pair transition metal salt plus ligand) can be mentioned and were presented in this work.

Another point is that a simultaneous increase in k_r values and reducing agent concentration should not be indiscriminately performed, because the polymerization control could be not achieved. Although there are many experimental works of ARGET ATRP available in the literature, they do not emphasize the discussion of the polymerization controllability limits, which would be also interesting for the application of technique in the industrial scale, as discussed in this research.

Over the past few years, researches on ATRP have been expanded by the study of strategies to diminish the concentration of catalysts using reducing agents. Techniques such as ARGET, ICAR, and SARA ATRP were designed. Although these polymerization methods allowed to reduce the catalyst concentrations at parts per million levels, they still lead to the formation of unwanted by-products (i.e., unreacted reducing agent and its oxidized form) that needs to be separated from the system at the end of the reaction. Even so, the development of such methods on an industrial scale tends to be promising, due to the simpler reaction apparatus and the costs reduction compared to the normal ATRP. As the polymerization techniques previously described are more advanced in terms of research, it is expected that over the next few years the literature will report more studies to make feasible photoATRP, eATRP and mechanoATRP processes, even scarce in literature.

Regarding mathematical modeling, ICAR ATRP is well discussed in the literature. However, in relation to the other techniques previous described, there are still some points to be elucidated, such as the effects of copper(0) area in SARA ATRP, potential applied in eATRP, light intensity in photoATRP and sonication power in mechanoATRP.

The truth is that the complete elimination of contamination of the final polymer by metal catalysts has not yet been achieved and it will hardly be with the techniques previously described. In this panorama, more recently, in the literature it has been reported the use of photoredox catalysts in a mechanism called organocatalysed ATRP. Although such a systems are still not as efficient as those of metal based catalysts, studies in this field will also tend to rise in the next years, where predictive mathematical models still need to be developed too.

REFERENCES

[1] D.A. Ship, Reversible-deactivation radical polymerizations, Polymer Reviews 51 (2) (2011) 99–103.

[2] P. Krys, K. Matyjaszewski, Kinetics of atom transfer radical polymerization, European Polymer Journal 89 (2017) 482–523.

[3] M. Kato, M. Kamigaito, M. Sawamoto, T. Higashimura, Polymerization of methyl methacrylate with the carbon tetrachloride/dichlorotris-(triphenylphosphine)ruthenium(II)/Methylaluminum bis(2,6-di-tert-butylphenoxide) initiating system: possibility of living radical polymerization, Macromolecules 28 (5) (1995) 1721–1723.

[4] J.-S. Wang, K. Matyjaszewski, Controlled/“living” radical polymerization. atom transfer radical polymerization in the presence of transition-metal complexes, J. Am. Chem. Soc. 117 (20) (1995) 5614–5615.

[5] F. Minisci, Free-radical additions to olefins in the presence of redox systems, Acc. Chem. Res. 8 (5) (1975) 165–171.

[6] F. Seeliger, K. Matyjaszewski, Temperature effect on activation rate constants in ATRP: new mechanistic insights into the activations process, Macromolecules 42 (16) (2009) 6050–6055.

[7] J. Morick, M. Buback, K. Matyjaszewski, Effect of pressure on activation-deactivation equilibrium constants for ATRP of methyl methacrylate, Macromol. Chem. Phys. 213 (21) (2012) 2287–2292.

[8] M.B. Gillies, K. Matyjaszewski, P-O. Norrby, T. Pintauer, R. Poli, P. Richard. A DFT study of R-X bond dissociation enthalpies of relevance to the initiation process of atom transfer radical polymerization, Macromolecules 36 (22) (2003) 8551–8559.

[9] W. Tang, K. Matyjaszewski, Effects of initiator structure on activation rate constants in ATRP, Macromolecules 40 (6) (2007) 1858–1868.

[10] W. Tang, Y. Kwak, W. Braunecker, N.V. Tsarevsky, M.L. Coote, K. Matyjaszewski, Understanding atom transfer radical polymerization: effects of ligand and initiator structures on the equilibrium constants, J. Am. Chem. Soc. 130 (32) (2008) 10702–10713.

[11] M. Horn, K. Matyjaszewski, Solvent effects on the activation rate constant in atom transfer radical polymerization, Macromolecules 46 (9) (2013) 3350–3357.

[12] W.A. Braunecker, N.V. Tsarevsky, A. Gennaro, K. Matyjaszewski, Thermodynamic components of the atom transfer radical polymerization equilibrium: quantifying solvent effects, Macromolecules 42 (17) (2009) 6348–6360.

[13] X. Pan, M. Fantin, F. Yuan, K. Matyjaszewski, Externally controlled atom transfer radical polymerization, Chem. Soc. Rev. 47 (2018) 5457–5490.

[14] E. Mastan, X. Li, S. Zhu, Modeling and theoretical development in controlled radical polymerization, Progress in Polymer Science 45 (2015) 71–101.

[15] E. Mastan, S. Zhu, S., Method of moments: a versatile tool for deterministic modeling of polymerization kinetics, European Polymer Journal 68 (2015) 139–160.

[16] E. P. Lyra, C. L. Petzhold, L. M. F. Lona, Tin(II) 2-ethylhexanoate and ascorbic acid as reducing agents in solution ARGET ATRP: a kinetic study approach by mathematical modeling and simulation, Chemical Engineering Journal 364 (2019) 186–200.

[17] C.W. Gear, The numerical integration of ordinary differential equations, Math. Comp. 21 (1967) 146–156.

[18] K. Levenberg, A method for the solution of certain non-linear problems in least squares, Quart. Appl. Math. 2 (2) (1944) 164–168.

[19] D.W. Marquardt, An algorithm for least-squares estimation of nonlinear parameters, J. Soc. Indust. Appl. Math. 11 (2) (1963) 431–441.

[20] K. Matyjaszewski, N.V. Tsarevsky, Macromolecular engineering by atom transfer radical polymerization, J. Am. Chem. Soc. 136 (18) (2014) 6513–6533.

[21] K. Matyjaszewski, W. Jakubowski, K. Min, W. Tang, J. Huang, W.A. Braunecker, N.V. Tsarevsky, Diminishing catalyst concentration in atom transfer radical polymerization with reducing agents, Proc. Natl. Acad. Sci. USA 103 (42) (2006) 15309–15314.

[22] W. Jakubowski, K. Min., K. Matyjaszewski, Activators regenerated by electron transfer for atom transfer radical polymerization of styrene, Macromolecules 39 (1) (2006) 39–45.

[23] W. Jakubowski, K. Matyjaszewski, Activators regenerated by electron transfer for atom-transfer radical polymerization of (meth)acrylates and related block copolymers, Angew. Chem. In. Ed. 45 (27) (2006) 4482–4486.

[24] A. Simakova, S.E. Averick, D. Konkolewicz, K. Matyjaszewski, Aqueous ARGET ATRP, Macromolecules 45 (16) (2012) 6371–6379.

[25] Y. Kwak, K. Matyjaszewski, ARGET ATRP of methyl methacrylate in the presence of nitrogen-based ligands as reducing agents, Polym. Int. 58 (2009) 242–247.

[26] X. Li, W. Wang, B. Li, S. Zhu, Kinetics and modeling of solution ARGET ATRP of styrene, butyl acrylate and methyl methacrylate, Macromol. React. Eng. 5 (9–10) (2011) 467–478.

[27] S.K. Fierens, D.R. D'Hooge, P.H.M. Van Steenberge, M-F. Reyniers, G.B. Marin, Exploring the full potential of reversible deactivation radical polymerization using pareto-optimal fronts, Polymers 7 (4) (2015), 655–679.

[28] J.G. Preturlan, R.P. Vieira, L.M.F. Lona, Numerical simulation and parametric study of solution ARGET ATRP of styrene, Computational Materials Science 124 (2016) 211–219.

[29] J.C. Hernández-Ortiz, E. Vivaldo-Lima, M.A. Dubé, A. Penlidis, Modeling of network formation in the atom transfer radical co-polymerization (ATRP) of vinyl/divinyl monomers using a multifunctional polymer molecule approach, Macromol. Theory Simul. 23 (7) (2014) 429–441.

[30] J.J. Keating, A. Lee, G. Belfort, Predictive tool for design and analysis of ARGET ATRP grafting reactions, Macromolecules 50 (20) (2017) 7930–7939.

[31] K.A. Payne, D.R. D'Hooge, P.H.M. Van Steenberge, M.F. Reyniers, M.F. Cunningham, R.A. Hutchinson, G.B. Marin, ARGET ATRP of butyl methacrylate: utilizing kinetic modeling to understand experimental trends, Macromolecules 46 (10) (2013) 3828–3840.

[32] K.A. Payne, P.H.M. Van Steenberg, D.R. D'Hooge, M-F. Reyniers, G.B. Marin, R.A. Hutchinson, M.F. Cunningham, Controlled synthesis of poly[(butyl methacrylate)-co-(butyl acrylate)] via activator regenerated by electron transfer atom transfer radical polymerization: insights and improvement, Polym. Int. 63 (5) (2014) 848–857.

[33] I. Zapata-González, R.A. Hutchinson, K.A. Payne, E. Saldívar-Guerra, Mathematical modeling of the full molecular weight distribution in ATRP Techniques, AIChe Journal 62 (8) (2016) 2762–2777.

[34] P. Leophairatana, S. Samanta, C. C. De Silva, J. T. Koberstein, Preventing alkyne-alkyne (i.e., glaser) coupling associated with the ATRP synthesis of alkyne-functional polymers/macromonomers and for alkynes under click (i.e., CuAAC) reaction conditions, J. Am. Chem. Soc. 139 (10) (2017) 3756–3766.

[35] J. Pietrasik, H. Dong, K. Matyjaszewski, Synthesis of high molecular weight poly(styrene-co-acrylonitrile) copolymers with controlled architecture, Macromolecules 39 (19) (2006) 6384–6390.

[36] L. Mueller, W. Jakubowski, W. Tang, K. Matyjaszewski, Successful chain extension of polyacrylate and polystyrene macroinitiators with methacrylates in an ARGET and ICAR ATRP, Macromolecules 40 (18) (2007) 6464–6472.

[37] H. Dong, W. Tang, K. Matyjaszewski, Well-defined high-molecular-weight polyacrylonitrile via activators regenerated by electron transfer ATRP, Macromolecules 40 (9) (2007) 2974–2977.

[38] K. Tanaka, K. Matyjaszewski, Copolymerization of (meth)acrylates with olefins using activators regenerated by electron transfer for atom transfer radical polymerization (ARGET ATRP), Macromol. Symp. 261 (1) (2008) 1–9.

[39] W. Jakubowski, B. Kirci-Denizli, R.R. Gil, K. Matyjaszewski, Polystyrene with improved chain-end functionality and higher molecular weight by ARGET ATRP, Macromol. Chem. Phys. 209 (1) (2008) 32–39.

[40] T. J. Aitchison, M. Ginic-Markovic, S. Clarke, S. Valiyaveettil, Polystyrene-block-poly(methyl methacrylate): initiation issues with block copolymer formation using ARGET ATRP, Macromol. Chem. Phys. 213 (1) (2012) 79–86.

[41] W.C.E. Higginson, R.T. Leigh, R. Nightingale, Reducing reactions of tin(II) in aqueous solution. Part I. A method for the detection of tin(III), J. Chem. Soc. 0 (0) (1962) 435–439.

[42] D.J. Drye, W.C.E. Higginson, P. Knowles, Reducing reactions of tin(II) in aqueous solution. Part II. The reaction between tin(II) and vanadium(V) in dilute hydrochloric acid, J. Chem. Soc. 0 (0) (1962) 1137–1143.

[43] E.A.M. Wetton, W.C.E. Higginson, Reducing reactions of tin(II) in aqueous solution. Part III. The reduction of various common oxidizing agents, J. Chem. Soc. 0 (0) (1965), 5890–5906.

[44] T.L. Nunes, A kinetic study of the reduction of copper(II) by tin(II) chloride, Inorg. Chem. 9 (6) (1970) 1325–1329.

[45] N. Shinohara, K. Mori, M. Inoue, Aqueous chemistry of tin(III). A flash photolysis study, Chemistry Letters 15 (5) (1986) 661–664.

[46] N. Shinohara, M. Inoue, Photochemical generation of Sn(III) in hydrochloric acid solutions, Bull. Chem. Soc. Jpn. 62 (3) (1989) 730–733.

[47] W.P. Jensen, G.J. Palenik, E.R.T. Tiekink, Bond valence sums in coordination chemistry. Sn(II), Sn(III), and Sn(IV) complexes containing Sn-S and/or Sn-N bonds, Polyhedron 20 (17) (2001) 2137–2143.

[48] J. Chang, A. Bard, Detection of the Sn(III) intermediate and the mechanism of the Sn(IV)/Sn(II) electroreduction reaction in bromide media by cyclic voltammetry and scanning electrochemical microscopy, J. Am. Chem. Soc. 136 (1) (2014) 311–320.

[49] M.B. Davies, J. Austin, D.A. Partridge, Vitamin C - its chemistry and biochemistry, Royal Society of Chemistry, Cambridge, 1991.

[50] S.B. Nimse, D. Pal, Free radicals, natural antioxidants, and their reaction mechanisms, RSC Adv. 5 (35) (2015) 27986–28006.

[51] C. Creutz, Complexities of ascorbate as a reducing agent, Inorg. Chem. 20 (12) (1981) 4449–4452.

[52] M.B. Davies, Reactions of L-ascorbic acid with transition metal complexes, Polyhedron 11 (3) (1992) 285–321.

[53] K. Min, H. Gao, K. Matyjaszewski, Use of ascorbic acid as reducing agent for synthesis of well-defined polymers by ARGET ATRP, Macromolecules 40 (6) (2007) 1789–1791.

[54] S. Hansson, E. Östmark, A. Carlmark, E. Malmström, ARGET ATRP for versatile grafting of cellulose using various monomers, ACS Appl. Mater. Interfaces 1 (11) (2009) 2651–2659.

[55] J.J. Ruiz, A. Aldaz, M. Domínguez, Mechanism of L-ascorbic acid oxidation and dehydro-L-ascorbic acid reduction on a mercury electrode. I. Acid medium, Can. J. Chem 55 (15) (1977) 2799–2806.

[56] B.H.J. Bielski, A.O. Allen, H.A. Schwarz, Mechanism of disproportionation of ascorbate radicals, J. Am. Chem. Soc. 103 (12) (1981) 3516–3518.

[57] D.E. Cabelli, B.H.J. Bielski, Kinetics and mechanism for the oxidation of ascorbic/ascorbate by HO2/O2- (hydroperoxyl/superoxide) radicals. A pulse radiolysis and stopped-flow photolysis study, J. Phys. Chem. 87 (10) (1983) 1809–1812.

[58] E.V. Shtamm, A.P. Purmal, Y.I. Skurlatov, Mechanism of catalytic ascorbic acid oxidation system Cu^{2+}-ascorbic acid-O_2, International Journal of Chemical Kinetics 11 (5) (1979) 461–494.

[59] J. Xu, R.B. Jordan, Kinetics and mechanism of the reaction of aqueous copper(II) with ascorbic acid, Inorg. Chem. 29 (16) (1990) 2933–2936.

[60] M.J. Sysley, R.B. Jordan, Kinetic study of the oxidation of ascorbic acid by aqueous copper(II) catalyzed by chloride ion, J. Chem. Soc. Dalton Trans. 0 (20) (1997) 3883–3888.

[61] A.A. Isse, A. Gennaro, C.Y. Lin, J.L. Hodgson, M.L. Coote, T. Guliashvili, Mechanism of carbon-halogen bond reductive cleavage in activated halide initiators relevant to living radical polymerization: theoretical and experimental study, J. Am. Chem. Soc. 133 (16) 2011 6254–6264.

[62] J.P. Desmarquest, O. Bloch, Électrode redox à hydrazine: Étude de la reduction du chlorure cuivrique, Electrochimica Acta 13 (5) 1968 1109–1118.

[63] F. Bottomley, The reactions of hydrazine with transition-metal complexes, Q. Rev. Chem. Soc. 24 (4) 1970 617–638.

[64] T. Varea, M.E. González-Núñez, J. Rodrigo-Chiner, G. Asensio, Aryl radicals by copper(II) oxidation of hydrazines: a new method for the oxidative and reductive arylation of alkenes, Tetrahedron Letters 30 (35) 1989 4709–4712.

[65] C.-H. Peng, J. Kong, F. Seeliger, K. Matyjaszewski, Mechanism of halogen exchange in ATRP, Macromolecules 44 (19) (2011) 7546–7557.

[66] M. Buback, R.G. Gilbert, R.A. Hutchinson, B. Klumperman, F-D. Kuchta, B.G. Manders, K.F O'Driscoll, G.T. Russel, J. Schweer, Critically evaluated rate coefficients for free-radical polymerization, 1. Propagation rate coefficient for styrene, Macromol. Chem. Phys. 196 (1995) 3267–3280.

[67] H. Kattner, M. Buback, Chain-length-dependent termination of styrene bulk homopolymerization studied by SP-PLP-EPR, Macromolecules 48 (2) (2015) 309–315.

[68] C.H. Bamford, R.W. Dyson, G.C. Eastmond, Network formation IV. The nature of termination reaction in free-radical polymerization, Polymer 10 (1969) 885–899.

[69] C. Barner-Kowolik, S. Beuermann, M. Buback, P. Castignolles, B. Charleux, M.L. Coote, R.A. Hutchinson, T. Junkers, I. Lacik, G.T. Russel, M. Stach, A.M. van Herk, Critically evaluated rate coefficients in radical polymerization – 7. Secondary-radical propagation rate coefficients for methyl acrylate in the bulk, Polym. Chem. 5 (1) (2014) 204–212.

[70] M. Buback, A. Kuelpmann, C. Kurz, Termination kinetics of methyl acrylate and dodecyl acrylate free-radical homopolymerizations up to high pressure, Macromol. Chem. Phys. 203 (8) (2002) 1065–1070.

[71] A.N.F. Peck, R.A. Hutchinson, Secondary reactions in the high-temperature free radical polymerization of butyl acrylate, Macromolecules 37 (16) (2004) 5944–5951.

[72] J.M. Asua, S. Buermann, M. Buback, P. Castignolles, B. Charleux, R.G. Gilbert, R.A. Hutchinson, J.R. Leiza, A.N. Nikitin, J.-P. Vairon, A.M. van Herk, Critically evaluated rate coefficients for free-radical polymerization, 5. Propagation rate coefficient for butyl acrylate, Macromol. Chem. Phys. 205 (2004) 2151–2160.

[73] J. Barth, M. Buback, P. Hesse, T. Sergeeva, Termination and transfer kinetics of butyl acrylate radical polymerization studied via SP-PLP-EPR, Macromolecules 43 (9) (2010) 4023–4031.

[74] T. Gruendling, T. Junkers, M. Guilhaus, C. Barner-Kowollik, Mark–Houwink parameters for the universal calibration of acrylate, methacrylate and vinyl acetate polymers determined by online size-exclusion chromatography–mass spectrometry, Macromol. Chem. Phys 211 (5) (2010) 520–528.

[75] H.K. Mahabadi, L. Alexandru, Molecular weight – viscosity relationships for a broad molecular weight distribution polymer, Canadian Journal of Chemistry 63 (1) (1984) 221–222.

[76] T.P. Davis, K.F. O'Driscoll, M.C. Pinton, M.A. Winnik, Copolymerization propagation kinetics of styrene with alkyl acrylates, Polymer International 24 (2) (1991) 65–70.

[77] A.E. Hamielec, J.F. MacGregor, A. Penlidis, Multicomponent free-radical polymerization in batch, semi-batch and continuous reactors, Makromol. Chem., Macromol. Symp. 10–11 (1) (1987) 521–570.

[78] T. Junkers, M. Schneider-Baumann, S.S.P. Koo, P. Castignolles, C. Barner-Kowollik, Determination of the propagation rate coefficient of acrylonitrile, Polym. Chem. 1 (4) (2010) 438–441.

[79] M. Tirrell, K. Gromley, Composition control of batch copolymerization reactors, Chemical Engineering Science 36 (2) (1981) 367–375.

[80] L.H. Garcia-Rubio, M.G. Lord, J.F. MacGregor, A.E. Hamielec, Bulk copolymerization of styrene and acrylonitrile: experimental kinetics and mathematical modelling, Polymer 26 (13) (1985) 2001–2013.

[81] A. Keramopoulos, C. Kiparissides, Development of a comprehensive model for diffusion-controlled free-radical copolymerization reactions, Macromolecules 35 (10) (2002) 4155–4166.

APPENDIX A

ARGET mechanism reaction order analysis

The ARGET mechanism for the reducing agents studied are proposed to be of first order in relation to the copper(II) halide complex (i.e., deactivator) based on the following considerations: (i) it is known that in ARGET ATRP the excess of reducing agent ($Sn^{II}(eh)_2$, H_2asc, and N_2H_4) is verified, due to this fact the equilibriums represented by Eqs. (20), (23), (26) are displaced to the products formation and, therefore, they can be simplified as irreversible reactions; (ii) in those systems, unstable species ($Sn^{III}(eh)_2X$, asc^{*-}, N_2H_3*, and N_2H_2) are present, so considering the steady-state hypothesis, their concentrations are too low compared to the copper(II) halide complex and, therefore, the equilibriums represented by Eqs. (21), (24), (27), and (28) are also displaced to the products formation and irreversible reactions.

Supposing the abovementioned considerations are valid, exemplifying when $Sn^{II}(eh)_2$ is used as a reducing agent, it is verified that:

$$Sn^{II}(eh)_2 + (Cu^{II}XL)X \xrightarrow{k_{r1}} Sn^{III}(eh)_2X + (Cu^{I}L)X \tag{A.1}$$

$$Sn^{III}(eh)_2X + (Cu^{II}XL)X \xrightarrow{k_{r2}} Sn^{IV}(eh)_2X_2 + (Cu^{I}L)X \tag{A.2}$$

By the previous reactions, applying the steady-state hypothesis for the unstable intermediate, the molar balance for Sn^{III} is:

$$\frac{d[Sn^{III}(eh)_2X]}{dt} = k_{r1}[Sn^{II}(eh)_2][(Cu^{II}XL)X] - k_{r2}[Sn^{III}(eh)_2X][(Cu^{II}XL)X] = 0 \tag{A.3}$$

Thus:

$$[Sn^{III}(eh)_2X] = \frac{k_{r1}[Sn^{II}(eh)_2][(Cu^{II}XL)X]}{k_{r2}[(Cu^{II}XL)X]} = \frac{k_{r1}}{k_{r2}}[Sn^{II}(eh)_2] \tag{A.4}$$

The molar balance for the $(Cu^{II}XL)X$ is:

$$\begin{aligned}\frac{d[(Cu^{II}XL)X]}{dt} &= k_a[(Cu^{I}L)X]\left([R_0X] + \mu_{0,RX}\right) - k_{da}[(Cu^{II}XL)X]\left([R_0] + \mu_{0,R}\right) \\ &- k_{r1}[Sn^{II}(eh)_2][(Cu^{II}XL)X] - k_{r2}[Sn^{III}(eh)_2X][(Cu^{II}XL)X]\end{aligned} \tag{A.5}$$

Substituting Eq. (A.4) expression in Eq. (A.5), hence:

$$\begin{aligned}\frac{d[(Cu^{II}XL)X]}{dt} &= k_a[(Cu^{I}L)X]\left([R_0X] + \mu_{0,RX}\right) - k_{da}[(Cu^{II}XL)X]\left([R_0] + \mu_{0,R}\right) \\ &- 2k_{r1}[Sn^{II}(eh)_2][(Cu^{II}XL)X]\end{aligned} \tag{A.6}$$

It can be noted the equivalence of k_{r1} and k_r comparing Eqs. (A.6) and (46). According to the considerations that have been done, it can be inferred that the reaction represented by Eq. (A.1) is the rate-determining step.

Analogous interpretations can be applied when both H_2asc and N_2H_4 are employed as reducing agent, considering Eqs. (23), (24), (26), (27), and (28) as irreversible reactions, allowing to obtain similar results.

APPENDIX B

Molar fraction of living and dormant chains

The pseudo-kinetic rate constant method is based on the equation of the molar fractions of monomer (Eqs. (82) and (83), herein Eqs. (B.1) and (B.2)), living (Eqs. (B.3) and (B.4)) and dormant (Eqs. (B.5) and (B.6)) chains as follows (for the random copolymerization of two monomers):

$$f_{\mathrm{M1}} = \frac{[\mathrm{M}_1]}{[\mathrm{M}_1] + [\mathrm{M}_2]} \tag{B.1}$$

$$f_{\mathrm{M2}} = \frac{[\mathrm{M}_2]}{[\mathrm{M}_1] + [\mathrm{M}_2]} \tag{B.2}$$

$$f_{\mathrm{R1}} = \frac{\sum_{i=1}^{\infty}[\mathrm{R}_{i,1}]}{\sum_{i=1}^{\infty}[\mathrm{R}_{i,1}] + \sum_{i=1}^{\infty}[\mathrm{R}_{i,2}]} \tag{B.3}$$

$$f_{\mathrm{R2}} = \frac{\sum_{i=1}^{\infty}[\mathrm{R}_{i,2}]}{\sum_{i=1}^{\infty}[\mathrm{R}_{i,1}] + \sum_{i=1}^{\infty}[\mathrm{R}_{i,2}]} \tag{B.4}$$

$$f_{\mathrm{D1}} = \frac{\sum_{i=1}^{\infty}[\mathrm{R}_{i,1}\mathrm{X}]}{\sum_{i=1}^{\infty}[\mathrm{R}_{i,1}\mathrm{X}] + \sum_{i=1}^{\infty}[\mathrm{R}_{i,2}\mathrm{X}]} \tag{B.5}$$

$$f_{\mathrm{D2}} = \frac{\sum_{i=1}^{\infty}[\mathrm{R}_{i,2}\mathrm{X}]}{\sum_{i=1}^{\infty}[\mathrm{R}_{i,1}\mathrm{X}] + \sum_{i=1}^{\infty}[\mathrm{R}_{i,2}\mathrm{X}]} \tag{B.6}$$

If it is assumed that the steady-state hypothesis is valid for living chains and the number of times that monomer 1 follows monomer 2 is reciprocally the same, the relation represented by Eq. (B.7) is valid. Hence, Eqs. (B.3) and (B.4) can be rewritten in the form of Eqs. (86) and (87) (herein Eqs. (B.8) and (B.9), respectively).

$$k_{\mathrm{p12}}\left(\sum_{i=1}^{\infty}[\mathrm{R}_{i,1}]\right)[\mathrm{M}_2] = k_{\mathrm{p21}}\left(\sum_{i=1}^{\infty}[\mathrm{R}_{i,2}]\right)[\mathrm{M}_1] \tag{B.7}$$

$$f_{\mathrm{R1}} = \frac{k_{\mathrm{p21}} f_{\mathrm{M1}}}{k_{\mathrm{p21}} f_{\mathrm{M1}} + k_{\mathrm{p12}} f_{\mathrm{M2}}} \tag{B.8}$$

$$f_{\mathrm{R2}} = \frac{k_{\mathrm{p12}} f_{\mathrm{M2}}}{k_{\mathrm{p21}} f_{\mathrm{M1}} + k_{\mathrm{p12}} f_{\mathrm{M2}}} \tag{B.9}$$

If it is postulated that the concentration of dormant polymer chains do not vary significantly by the time (a reasonable assumption by the high percentage of functionalized polymer chains observed in ATRP systems, proved by Figs. 13, 14 and 15 in Section 4.1.7.2.), Eqs. (B.10) and (B.11) are valid. With this consideration, Eqs. (B.5) and (B.6) can be rewritten as Eqs. (84) and (85) (herein Eqs. (B.12) and (B.13), respectively).

$$k_{a1}\sum_{i=1}^{\infty}\left[\mathrm{R}_{i,1}\mathrm{X}\right]\left[(\mathrm{Cu^{I}L})\mathrm{X}\right] = k_{da1}\sum_{i=1}^{\infty}\left[\mathrm{R}_{i,1}\right]\left[(\mathrm{Cu^{II}XL})\mathrm{X}\right] \tag{B.10}$$

$$k_{a2}\sum_{i=1}^{\infty}\left[\mathrm{R}_{i,2}\mathrm{X}\right]\left[(\mathrm{Cu^{I}L})\mathrm{X}\right] = k_{da2}\sum_{i=1}^{\infty}\left[\mathrm{R}_{i,2}\right]\left[(\mathrm{Cu^{II}XL})\mathrm{X}\right] \tag{B.11}$$

$$f_{D1} = \frac{\frac{k_{da1}}{k_{a1}}k_{p21}f_{M1}}{\frac{k_{da1}}{k_{a1}}k_{p21}f_{M1} + \frac{k_{da2}}{k_{a2}}k_{p12}f_{M2}} \tag{B.12}$$

$$f_{D2} = \frac{\frac{k_{da2}}{k_{a2}}k_{p12}f_{M2}}{\frac{k_{da1}}{k_{a1}}k_{p21}f_{M1} + \frac{k_{da2}}{k_{a2}}k_{p12}f_{M2}} \tag{B.13}$$